Endo : Press®

ENDOSCOPIC PITUITARY AND SKULL BASE SURGERY

Anatomy and Surgery of the Endoscopic Endonasal Approach

3rd Edition

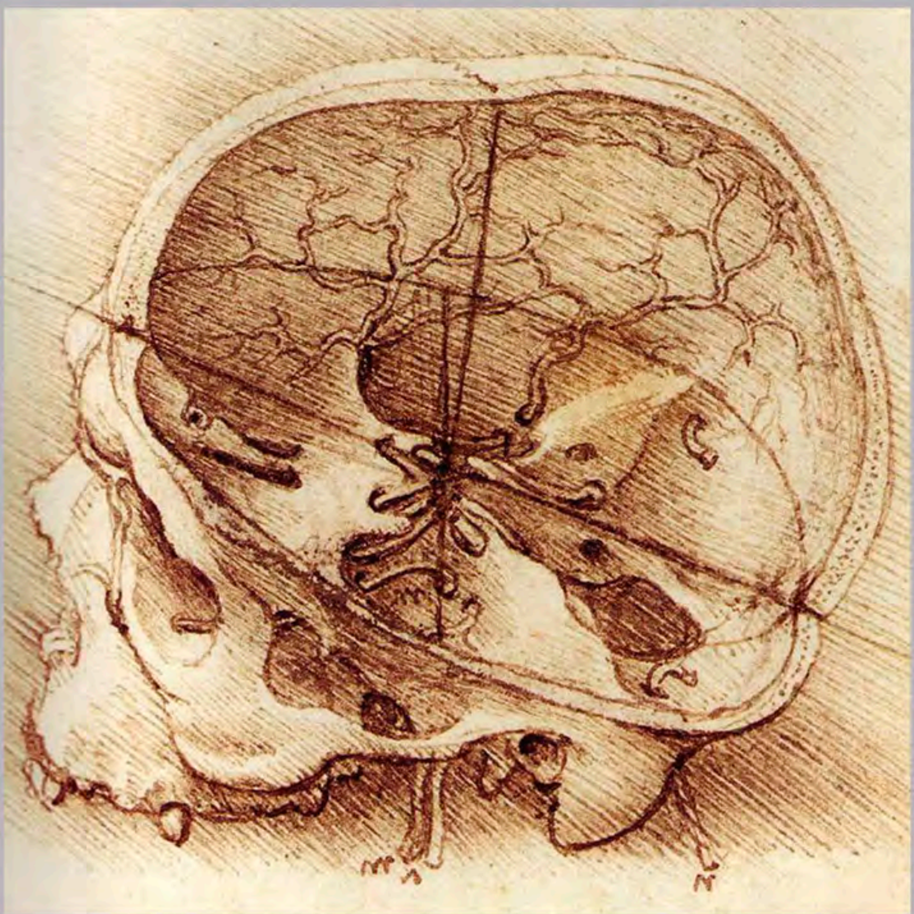

Paolo CAPPABIANCA
Luigi Maria CAVALLO

Endo : Press®

Third Edition

ENDOSCOPIC PITUITARY AND SKULL BASE SURGERY

Anatomy and Surgery of the Endoscopic Endonasal Approach

Prof. Paolo CAPPABIANCA, M.D.
Luigi Maria CAVALLO, M.D., Ph.D.

Department of Neurosciences,
Reproductive and Odontostomatological Sciences,
Division of Neurosurgery,
Università degli Studi di Napoli "Federico II" Naples, Italy

Academic collaborators:

Oreste de DIVITIIS, M.D.[1]
Felice ESPOSITO, M.D., Ph.D.[2]
Domenico SOLARI, M.D., Ph.D.[1]
Matteo DE NOTARIS, M.D., Ph.D [3]
Michelangelo DE ANGELIS, M.D.[1]
Alessandro VILLA, M.D.[1]
Teresa SOMMA, M.D.[1]
Alberto DI SOMMA, M.D.[1]
Carmela CHIARAMONTE, M.D.[1]
Chiara CAGGIANO, M.D.[1]
Salih AYDIN, M.D.[4]
Manfred TSCHABITSCHER, M.D.[5]

[1] | Department of Neurosciences, Reproductive and Odontostomatological Sciences, Division of Neurosurgery, Università degli Studi di Napoli Federico II Naples, Italy

[2] | Department of Neurosurgery, University of Messina, Italy

[3] | Department of Neuroscience, "G. Rummo" Hospital, Neurosurgery Operative Unit, Benevento, Italy

[4] | Department of Neurosurgery, Emsey Hospital, Pendik, Istanbul, Turkey

[5] | Centre for Anatomy and Cell Biology, Department of Systematic Anatomy, Medical University of Vienna, Austria

Cover image:
Anatomical drawing of the skull base (*Leonardo Da Vinci,* 1452–1519).

Anatomical-surgical drawings,
except for Figs. 26, 67, 73 and 124c, by Mr. **Harald Konopatzki,**
Grünewaldstraße 3a,
69126 Heidelberg, Germany
Email: konillu@t-online.de

Fig. 124c by **Carmela Chiaramonte,** Department of Neurosciences and Reproductive and Odontostomatological Sciences, Division of Neurosurgery, Università degli Studi di Napoli "Federico II" Naples, Italy

Endoscopic Pituitary and Skull Base Surgery
Anatomy and Surgery of the Endoscopic Endonasal Approach
3rd Edition

Prof. **Paolo Cappabianca,** M.D., **Luigi Maria Cavallo,** M.D., Ph.D.
Department of Neurosciences, Reproductive and Odontostomatological Sciences, Division of Neurosurgery, Università degli Studi di Napoli "Federico II" Naples, Italy

Correspondence address of the first author:
Prof. **Paolo Cappabianca,** M.D.
Professor and Chairman of Neurosurgery, Department of Neurosciences, Reproductive and Odontostomatological Sciences, Division of Neurosurgery, Università degli Studi di Napoli "Federico II" Naples, Italy
Via Sergio Pansini, 5
80131 Napoli, Italy
Phone: +39 081 7 46 25 59
Telefax: +39 081 7 46 25 94
E-mail: paolo.cappabianca@unina.it
Internet: www.neurochirurgia.unina.it

3rd edition | 1st edition 2005

P.O. Box, 78503 Tuttlingen, Germany
Phone: +49 (0) 74 61/1 45 90
Fax: +49 (0) 74 61/708–529
E-mail: endopress@t-online.de

Editions in languages other than English and German are in preparation. For up-to-date information, please contact Endo:Press® GmbH at the address shown above.

Design and Composing:
Endo:Press® GmbH, Germany

Printing and Binding:
Straub Druck + Medien AG
Max-Planck-Straße 17, 78713 Schramberg, Germany

04.16–2.0

ISBN 978-3-89756-059-8

Table of Contents

1 Introduction

The endoscopic endonasal approach to the sellar region is an evolution of the conventional transsphenoidal technique performed with the operating microscope. For more than 40 years, our school has focused its study and efforts on this technique and has contributed to the recent success of the endoscopic transsphenoidal procedure, which has been employed extensively since 1997. It is a surgical approach through both nostrils, using the endoscope as a pure visualization tool bringing the eye of the surgeon and of the entire OR staff close to the relevant surgical target site. In the nasal step of this procedure, the first surgeon holds the endoscope with the non-dominant hand, while during the subsequent phases two surgeons are jointly working together using a four-hand technique. Accordingly, the first surgeon is enabled to proceed bimanually just as with the microsurgical technique. On the other hand, the second surgeon takes the task of dynamically guiding the endoscope by actively moving it backward and foreward, thus allowing adequate depth perception.

More recently, the evolution of the endoscopic surgical techniques and the technological advancements have prompted the development of a variety of modifications of the standard transsphenoidal approach to the sellar region. It was Prof. *Kassam's* team in Pittsburgh (PA, USA) that introduced the concept of a systematic anterior endonasal approach to the skull base on the sagittal and coronal planes. Teamwork proficiency and adherence to strict anatomical principles is of paramount importance in this concept, which is continuously evolving. As a matter of fact, today, such approaches are targeted mainly on the midline skull base from the frontal sinus to the lower clivus.

The present brochure provides a step-by-step guide to the surgical pathway defined by the natural splanchnocranial cavities, shown here in an anatomic dissection study that was performed on cadaver specimens. In addition, the same steps are described on the basis of *in vivo* endoscopic neurosurgical procedures.

The text concludes with a detailed description of the instruments and videoendoscopic equipment required for the various stages of surgery. Some of these instruments were developed by the authors in close collaboration with KARL STORZ Tuttlingen, Germany.

Neurosurgical Clinic, Università degli studi di Napoli Federico II, Naples, Italy
Chairman:
Prof. *Paolo Cappabianca,* M.D.

2 General Aspects of the Procedure

The first attempts to use the endoscope in sellar region surgery dates back to 1963 when the French neurosurgeon *Gérard Guiot* proposed the use of endoscopy to supplement the transsphenoid transseptal approach for exploration of the sellar cavity. The recent progress achieved at several schools of otorhinolaryngology in endoscopic surgery of the nasal and paranasal sinuses has caused *Guiot's* idea to be reconsidered, but with a more up-to-date slant this time. No longer is it considered a complement to microscopic surgery; rather it has now become "fully" endoscopic pituitary surgery – the term "fully" being appropriate because the procedure is performed with the endoscope as the only optical device used to visualize the surgical target area (Fig. 1).

The endoscope has opened the eyes of the surgeon to structures like the planum sphenoidale, the clivus, the carotid and optic bony protuberances, from upside down the common surgical sellar view. Nevertheless, the present frontier is represented by the extended or expanded endoscopic endonasal skull base approaches.

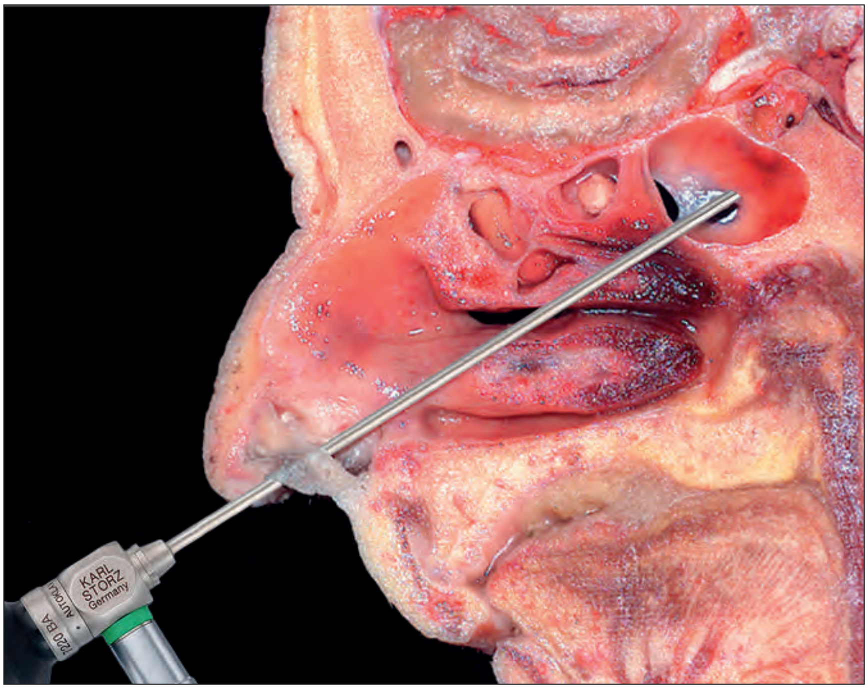

Fig. 1 Transsphenoidal endonasal endoscopic approach.

This approach has several benefits:

- it avoids the need for the oral and the rhinoseptal submucosal nasal route;
- the special features of the telescopes used in this approach allow for a wider exposure of the operating field including the options of advancing toward the anatomical target area or inspecting the sphenoid sinus, sellar, supraparasellar and retroclival regions via wide-angle panoramic view (Figs. 2, 3);
- the high-resolution close-up view of the anatomical structures allows a lesion arising from or involving such areas to be removed more safely, which, in turn, contributes to a reduced incidence of overall complications;
- an improved postoperative course provides greater comfort for the patient: since there is no need to distend the nasal speculum the risk of inadvertent trauma to naso-facial structures is reduced;
- it avoids the need for postoperative nasal packing, thus minimizing breathing difficulties and discomfort for the patient, particularly beneficial for elderly patients;
- it reduces the duration of hospitalization and, therefore, the costs.

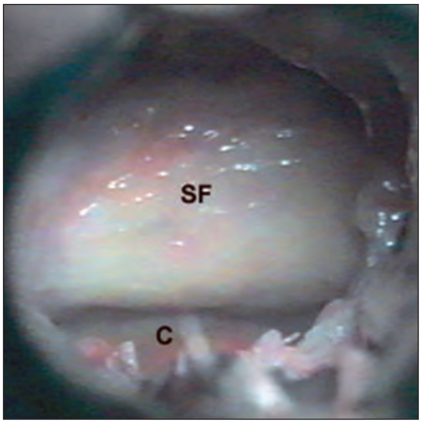

Fig. 2 Microscopic view. Clivus (**C**); sellar floor (**SF**).

This approach:

- requires the physician to go through a learning curve. In-depth hands-on training, virtual reality-based simulation training, and specific endoscopic skills are needed, in order to be able to recognize multiple anatomic landmarks that are used during surgery. Last but not least, the use of specific instrumentation facilitates the procedure.

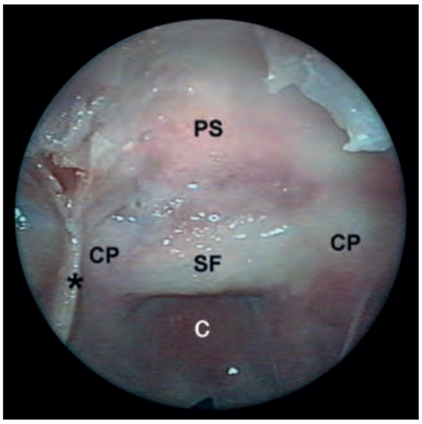

Fig. 3 Endoscopic view of the same case as shown in Fig. 2. Planum sphenoidale (**PS**); sellar floor (**SF**); sphenoid septum (✱); carotid protuberance (**CP**); clivus (**C**).

3

Bone Anatomy of the Nasal Cavities and the Sphenoid Sinus

3.1. Nasal Cavities

Each of the *nasal cavities* can be compared to a transversely flattened channel, larger at the bottom and narrowing as it proceeds upward. It has four walls and two openings.

The inferior wall comprises, the maxillary palatine process at the front, and, the horizontal lamella of the palatine bone at the back. From anterior to posterior, the superior wall is made up of the nasal bone, frontal bone, cribriform plate of the ethmoid, and anterior surface of the sphenoid bone.

The *medial nasal wall* (Fig. 4) is made up of the perpendicular plate of the ethmoid above, and, of the vomer below. These two bones articulate with each other describing a broad inward angle filled with cartilage – the septal cartilage – which plays a crucial role in the formation of the nasal septum. The latter only rarely follows the median plane; most often it deviates somewhat to either the left or right.

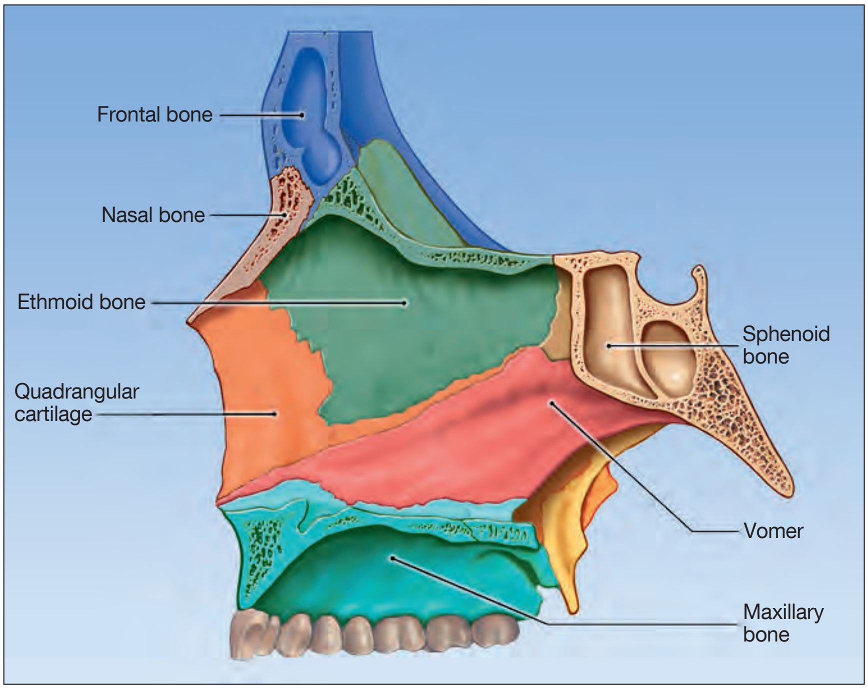

Fig. 4 Nasal cavity, medial wall.

The *lateral nasal wall* (Fig. 5) is tilted downward in a mediolateral direction and is made up of six bones: the maxillary, lacrimal, ethmoid and sphenoid bone, the vertical portion of the palatine bone and the inferior nasal turbinate. The surface is highly irregular and is covered with depressions and orifices that place the nasal cavities in communication with the various facial and cranial bone sinuses. The superior and middle turbinates form a single body with the ethmoid while the inferior turbinate is a separate, totally independent bone. At times, just above the superior turbinate, there is a small extra turbinate, called the supreme turbinate. Each of these has a convex medial surface, a concave upper surface, an upper adherent edge and a lower free edge facing the nasal cavity. The spaces lying between the turbinates and the corresponding portion of the lateral nasal fossa wall constitute the three meati (upper, middle, lower). The medial portion of the middle nasal meatus has a small rounded protrusion – the ethmoid bulla – which is always present, although its volume varies greatly.

The posterior opening of the nasal cavities is made up of the choanae, formed by the sphenoid at the top, the horizontal portion of the palatine bone at the bottom, the medial plate of the pterygoid process laterally, and by the posterior margin of the vomer medially.

The anterior opening of the nasal cavities is called the apertura piriformis and made up of the two maxillary bones and the nasal bones.

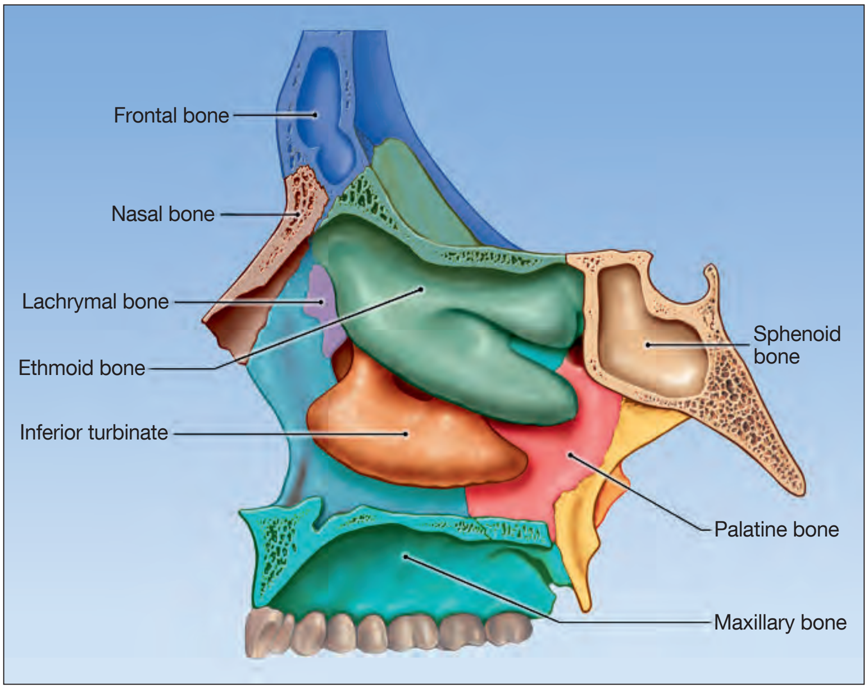

Fig. 5 Nasal cavity, lateral wall.

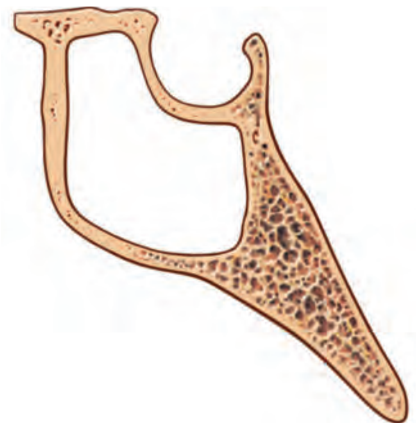

Fig. 6 Sellar-type sphenoid sinus.

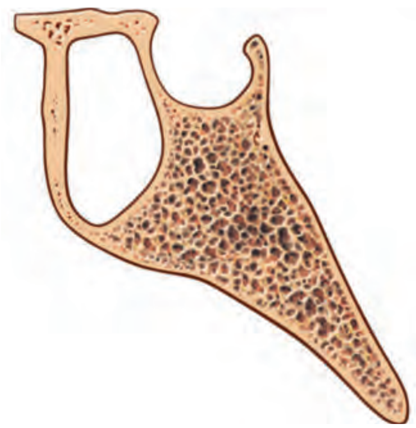

Fig. 7 Presellar-type sphenoid sinus.

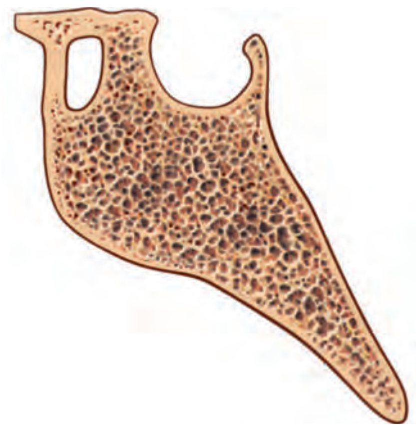

Fig. 8 Conchal-type sphenoid sinus.

3.2. Sphenoid Sinus

The sphenoid sinus – a cavity in the sphenoid bone – is the posteriormost paranasal cavity. A median septum, most often veering laterally, divides it into two completely independent parts, right and left. Frequently, numerous minor septa are also present and vary in shape, thickness, location, orientation and extension. Most often, these septa divide the cavity into a series of small compartments that are lined with nasal mucosa.

In the adult, the sphenoid sinus can have one of three variations depending on the extent to which the sphenoid bone is pneumatized: sellar, presellar and conchal. The sellar-type sinus (Fig. 6) is the most common (approx. 75%) and, in this case, the air cell extends under the sella turcica, passing the clivus plane; in the presellar-type sinus (approx. 24%) (Fig. 7) the cavity does not pass the vertical plane parallel to the anterior sella wall; the conchal-type sinus (Fig. 8), where the thickness of the bone separating the sella from the sphenoid sinus exceeds 10 mm, is highly uncommon in adults.

The natural sphenoid ostium, the entrance to the sphenoid sinus, is located in the spheno-ethmoid recess, medial to the superior and/or supreme turbinate. The anatomic landmark used to identify the ostium is the upper margin of the choana: from here, moving vertically approximately 1.5 cm upward within the sphenoethmoid recess, the sphenoid ostium can be found; the latter provides access to the sphenoid sinus. With age, as bone is resorbed and the walls progressively thin, the volume of the sinus cavity often increases and, at times, the sphenoid mucosa can come into direct contact with the sellar dura mater. The sellar floor comes into view at the posterior sphenoid sinus wall and continues above with the planum sphenoidale and below with the clivus. Two bulges in the lateral wall of the sphenoid cavity are of utmost importance: the optic nerve prominences, above, caused by the bony covering of the optic nerves, and the carotid prominences, below, encasing the internal carotid arteries. On each side, between the two prominences, there is a recess: the opto-carotid recess. It varies in depth and is made up of the pneumatization of the anterior clinoid process. The inferolateral portion of a well-pneumatized sphenoid sinus presents additional small prominences, formed by the second and third branches of the trigeminal nerve.

4 Anatomical Structures Involved in the Endonasal Approach to the Sella

In correspondence with the anatomical structures subjected to anatomical dissection, the procedure can be subdivided into three stages: *nasal, sphenoid and sellar.*

4.1. Endoscopic Nasal Exploration

When the scope is introduced parallel to the floor of the nasal cavity, the first structure to come into view is the inferior turbinate (Fig. 9). Lateral to this structure we see the lower meatus, where the nasolacrimal duct opens. The scope is advanced in an anteroposterior direction along the floor of the nasal cavity, passing between the posterior end of the inferior turbinate and the nasal septum (Fig. 10), to reach the choana where the Eustachian tube opens (Fig. 11).

Above and posterior to the head of the inferior turbinate we find the middle turbinate (Fig. 12). In some cases, its head may be pneumatized to some degree; in this case the term “concha bullosa” is used (Fig. 13).

Moving the endoscope forward between the middle turbinate and nasal septum, at a 30° upward angle relative to the floor of the nasal cavity, we reach the sphenoethmoid recess extending between the roof of the choana and the natural sphenoid ostium (Figs. 14–16).

This ostium varies in size and cannot always be viewed as it may be covered by the tail of the superior or the supreme turbinate. At this point, it is not necessary to visualize the sphenoid ostium since the access to the sphenoid cavity can be gained as well by proceeding from the choana slightly upward for approx. 1.5 cm along the spheno-ethmoid recess.

If the ostium is particularly wide, as may be the case in older patients, introduction of the endoscope through the ostium may allow the sellar region to be viewed (Fig. 17).

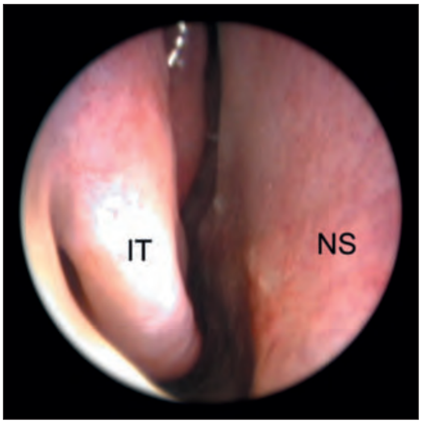

Fig. 9

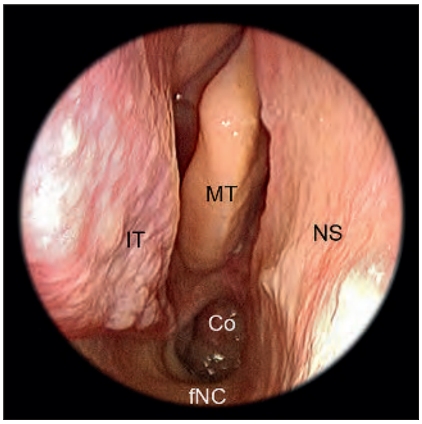

Fig. 10

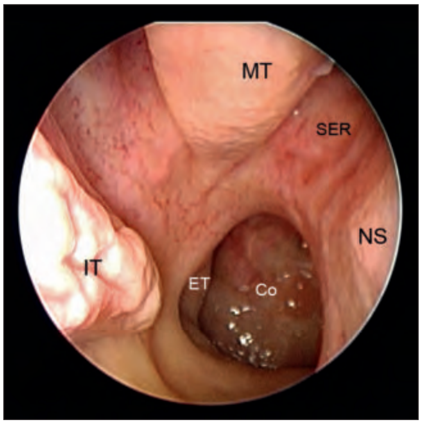

Fig. 11

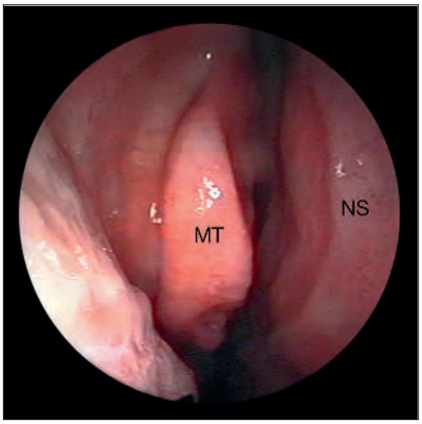

Fig. 12

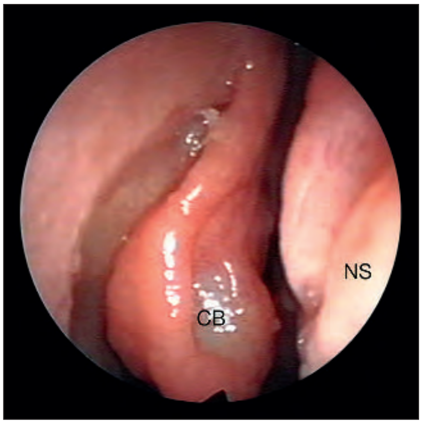

Fig. 13

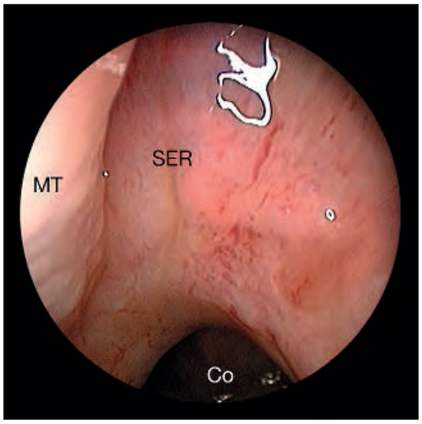

Fig. 14

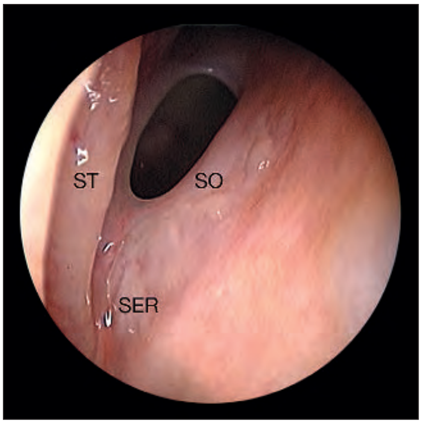

Fig. 15

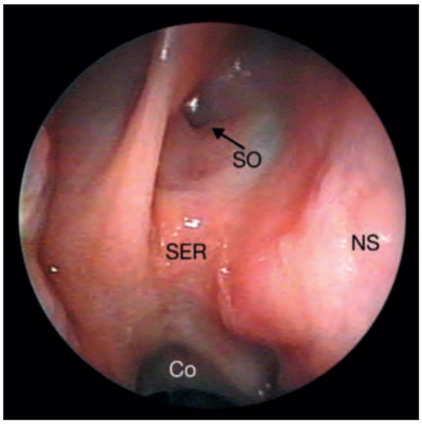

Fig. 16

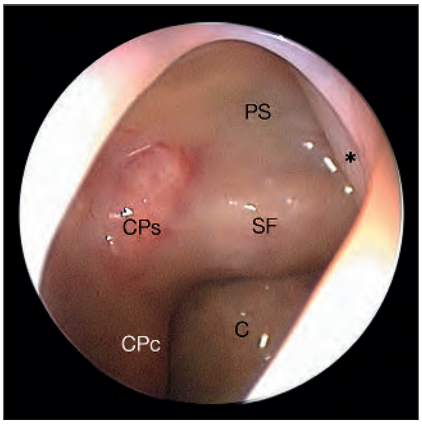

Fig. 17

Figs. 9–13 Right nasal cavity.
Inferior turbinate (**IT**); middle turbinate (**MT**); nasal septum (**NS**); choana (**Co**); Eustachian tube (**ET**); floor of the nasal cavity (**fNC**); floor of the nasal cavity (**fNC**); concha bullosa (**CB**); spheno-ethmoid recess (**SER**).

Figs. 14–17 Right nasal cavity, nasal stage.
Clivus (**C**); concha bullosa (**CB**); paraclival segment of the carotid protuberance (**CPc**); parasellar segment of the carotid protuberance (**CPs**); choana (**Co**); floor of the nasal cavity (**fNC**); middle turbinate (**MT**); nasal septum (**NS**); planum sphenoidale (**PS**); spheno-ethmoid recess (**SER**); sellar floor (**SF**); sphenoid ostium (**SO**); superior turbinate (**ST**); sphenoid septum (**✱**).

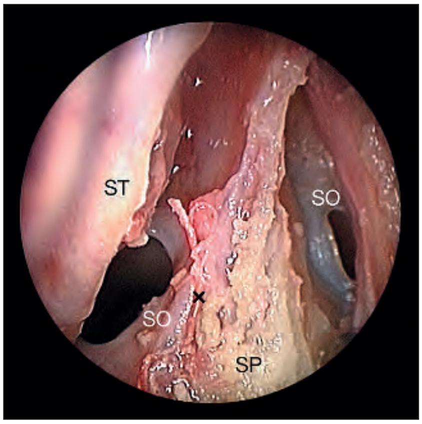

Fig. 18 Sphenoid stage. Right nasal cavity. Exposure of the sphenoid prow. Superior turbinate (**ST**); sphenoid prow (**SP**); sphenoid ostium (**SO**); spheno-palatine artery (✱).

4.2. Endoscopic Sphenoid Sinus Exploration

After having identified the sphenoid cavity, the nasal septum is detached from the anterior wall of the sphenoid sinus with a high-speed microdrill using a diamond burr of 5 mm in diameter. Fig. 18 shows the anterior sphenoid sinus wall, which is removed from the KERRISON rongeurs) and the microdrill. During this step it is possible to view into the infero-lateral aspect and identify the sphenopalatine artery.

This artery is the terminal branch of the internal maxillary artery, which in turn is a branch of the external carotid artery. The sphenopalatine artery enters the nasal cavity through the sphenopalatine foramen (Fig. 20) which is located topographically behind the tail of the middle turbinate.

Within the nasal cavity the artery ramifies into two branches, the medial of which forms the naso-palatine artery and, passing above the choana, it vascularizes the nasal septum. The other branch, the posterior nasal artery, joins the lateral nasal wall to vascularize the turbinates (Fig. 21).

Within the sphenoid cavity, one or several septa are identified and may be removed, as needed, to expose all accessible anatomical landmarks on the posterior sphenoid sinus wall. The sphenoid septa can be removed with through-cutting nasal forceps to avoid any elevation of the sphenoid mucosa. The posterior wall of the sphenoid sinus presents depressions and bony prominences that cover vulnerable neurovascular structures.

The major anatomical landmarks for proper identification of the sellar floor are as follows (Figs. 22, 23):

- the planum sphenoidale, above;
- the clivus, below;
- the carotid protuberances, laterally;
- the optic nerve prominences;
- the opto-carotid recesses.

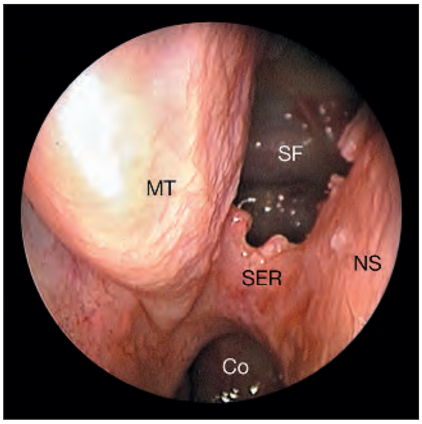

Fig. 19 Sphenoid stage. Right nasal cavity. Anterior sphenoidectomy. Choana (**Co**), spheno-ethmoid recess (**SER**); middle turbinate (**MT**); nasal septum (**NS**); sellar floor (**SF**).

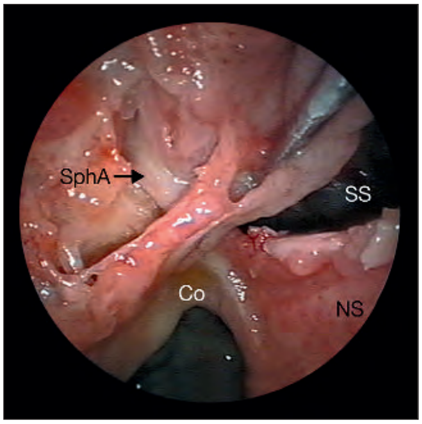

Fig. 20 Right nasal cavity. Exposure of the spheno-palatine artery. Choana (**Co**); sphenoid sinus (**SS**); nasal septum (**NS**); spheno-palatine artery (**SphA**).

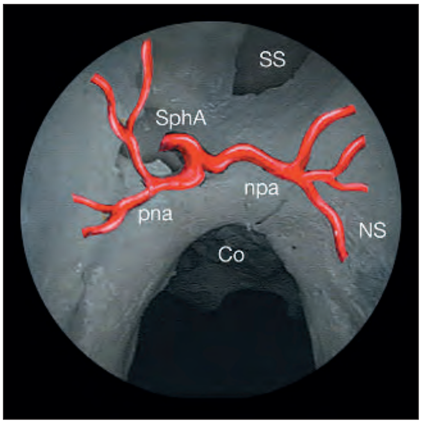

Fig. 21 Right nasal cavity. Course of the main branches of the spheno-palatine artery. Sphenoid sinus (**SS**); choana (**Co**); nasal septum (**NS**); spheno-palatine artery (**SphA**); naso-palatine artery (**npa**); posterior nasal artery (**pna**).

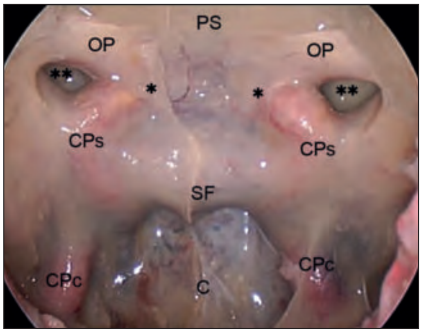

Fig. 22 Sphenoid stage. Major landmarks of the posterior wall of the sphenoid sinus. Planum sphenoidale (**PS**); optic protuberance (**OP**); parasellar segment of the carotid protuberance (**CPs**); sellar floor (**SF**); paraclival segment of the carotid protuberance (**CPc**); clivus (**C**); medial opto-carotid recess (✱); lateral opto-carotid recess (✱✱).

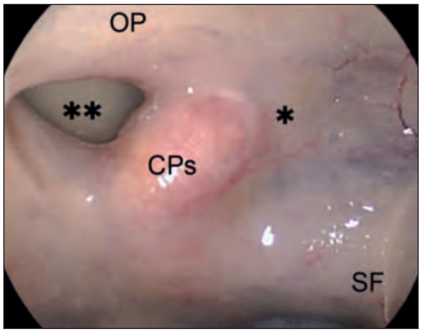

Fig. 23 Sphenoid stage. Close-up view of the medial and lateral opto-carotid recesses. Optic protuberance (**OP**); parasellar segment of the carotid protuberance (**CPs**); sellar floor (**SF**); medial opto-carotid recess (✱); lateral opto-carotid recess (✱✱).

4.3. Endoscopic Sella Opening

A microdrill with diamond burr is used to create an opening in the sellar floor. With the help of a KERRISON bone punch and/or a STAMMBERGER circular cutting punch the fenestration is enlarged step-by-step to such an extent, that the carotid prominences laterally, the planum sphenoidale above, and the clivus below, come into view (Fig. 24).

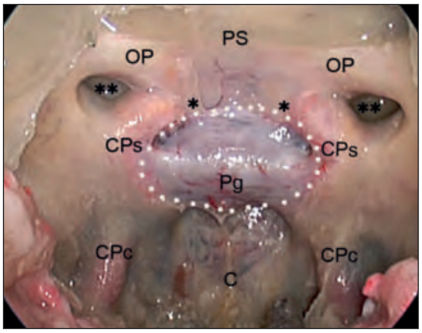

Fig. 24 Sphenoid stage. Sella opening. Pituitary gland (**Pg**); planum sphenoidale (**PS**); optic protuberance (**OP**); parasellar segment of the carotid protuberance (**CPs**); sellar floor (**SF**); paraclival segment of the carotid protuberance (**CPc**); clivus (**C**); medial opto-carotid recess (**✱**); lateral opto-carotid recess (**✱✱**).

5 Endoscopic Endonasal Approach to the Sella

5.1. Operating Room Set-up

The design of the operating theatre is by its own a surgical instrument. An integrated operating room helps to optimize teamwork and improve patient care. In the operating room, all of the equipment, i.e, cold light source, video camera, monitor, and video recording system, are placed ergonomically behind the head of the patient and in front of the first surgeon, who is at the right side of the patient. The anesthesiologist is positioned with his/her equipment at the left side of the patient at the level of the head. The second surgeon is at the left side of the patient, and the scrub nurse is positioned at the level of the patient's legs (Figs. 25–26).

Fig. 25 Integrated operating theater (KARL STORZ OR1™).

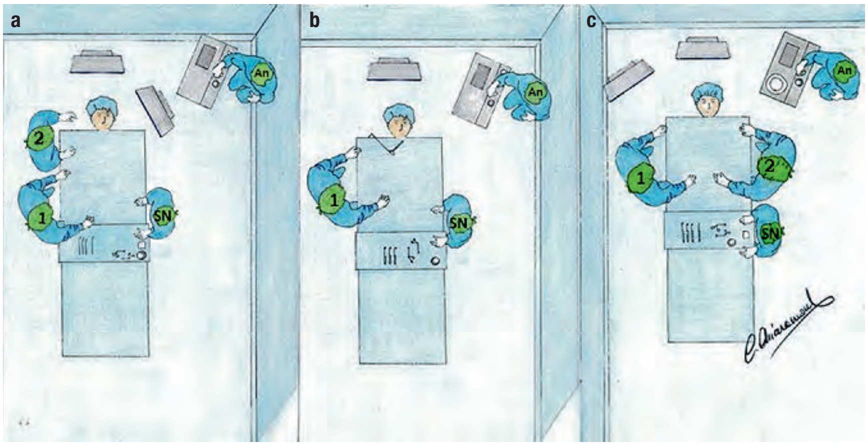

Fig. 26 Schematic drawings showing the three alternative options of operating room set-up (**a–c**) that can be chosen according to surgeons' preferences.
Right-handed surgeon (**a**); surgeon operating with a holder (**b**); left-handed surgeon (**c**).
First surgeon (**1**); assisting surgeon (**2**); scrub nurse (**SN**); anesthesiologist (**An**).

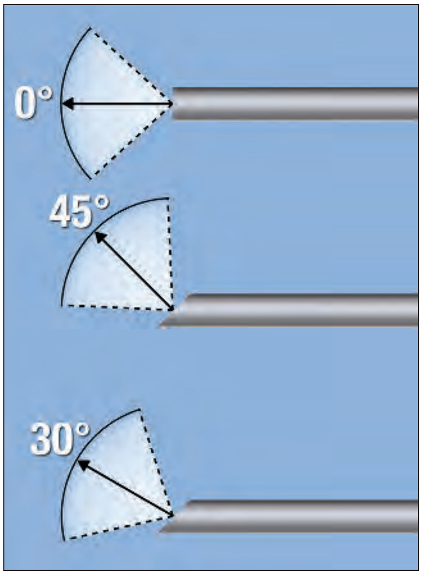

Fig. 27 HOPKINS® rod lens telescopes, directions of view 0°, 45° and 30°, without a working channel.

During a fully endoscopic endonasal transsphenoidal approach, rigid diagnostic HOPKINS® telescopes – *without* a working channel – are used. There are three types of telescopes available, that vary in length, diameter and direction of view:

0°, 30°, 45° telescopes, length 18 cm, diameter 4 mm; 0° and 30° telescopes; length 18 cm, diameter 2.7 mm; 0° and 30° telescopes, length 30 cm, diameter 4 mm. The 0° scope, length 18 cm, diameter 4 mm, is the one most frequently used (Figs. 27–30).

In view of the fact, that the scope is mainly an optical device, it is usually not equipped with an operating channel. Accordingly, the surgical instruments are introduced alongside the scope.

A special outer sheath and irrigation system (CLEARVISION® II, KARL STORZ Tuttlingen, Germany) are used to rinse the distal objective lens, obviating the need for repeated withdrawal and reinsertion of the scope into the nasal cavity during surgery.

The most commonly used 0° scope (diameter 4 mm, length 18 cm) (Fig. 28) is usually *operated freehand throughout the entire surgical procedure.* During the sellar step of the procedure, the endoscope is held dynamically by a second surgeon, allowing the first surgeon to work bimanually with two instruments. 30° or 45° telescopes are used in selected cases or in specific phases of the surgical procedure, e.g., the exploration of the sellar cavity after tumor removal (Figs. 29, 30). Usually, the surgical approach is performed through both nostrils.

Fig. 28 Straight ahead view offered by a 0° telescope.

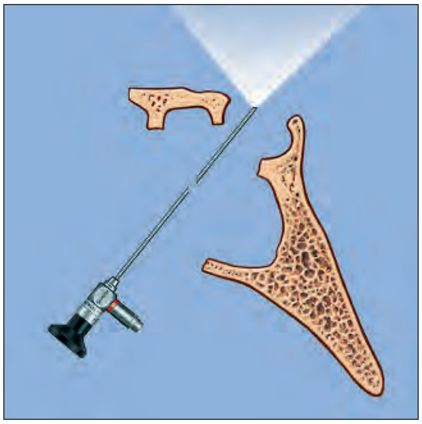

Fig. 29 The 30° and/or 45° telescope directed toward the suprasellar region.

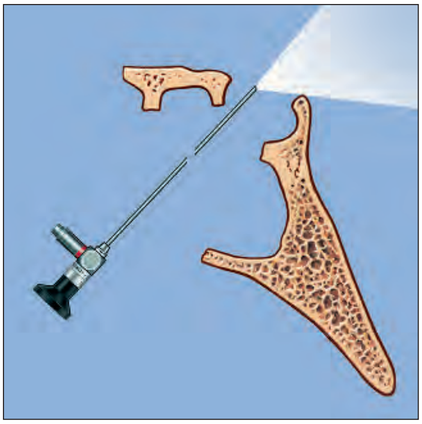

Fig. 30 The 30° and/or 45° telescope directed toward the retrosellar region.

Fig. 31 Patient positioning.

Two or three operating instruments – depending on the specific needs and circumstances – plus the endoscope can be inserted through both nostrils, thus providing increased working space and improved maneuverability.

The use of neuronavigation during a standard endoscopic approach is currently reserved for selected cases only, e.g, in the presence of a conchal-type sphenoid sinus, and/or in certain cases of recurrences with a previous history of trans-sphenoidal surgery, or in patients with large lesions involving the para-suprasellar areas. Furthermore, the use of a micro-doppler probe can be useful to localize the course of the ICA during removal of pituitary adenomas with lateral extension into the cavernous sinus.

5.2. Patient Positioning

During the endoscopic approach to the sellar area, the patient is positioned supine on the operating table, with the trunk raised 10° and the head in neutral position, rotated 10° towards the surgeon. The head is adequately secured in a horse-shoe headrest without rigid three-pin fixation (Fig. 31).

5.3. Disinfection and Decongestion of the Nasal Cavities

Using a small KILLIAN-type nasal speculum, cotton pledgets soaked in 50% povidone-iodine are placed along the floor of the nasal cavities and in the space between the nasal septum and the middle turbinates. They are allowed to take effect for approximately five minutes. The cotton pledgets soaked with povidone-iodine are then removed and disinfection of the nasal skin is performed. Using the same procedure as described above, eight cotton pledgets (four per nostril) soaked in a decongestant solution (1 mg of adrenaline, 5 ml of 20% diluited lidocaine and 4 ml of saline solution) are placed between the nasal septum and the middle turbinate to achieve a vasoconstrictive effect particularly at the relevant, richly vascularized areas involved in the subsequent procedure. They are allowed to take effect for approximately 15 minutes during which the patient is draped.

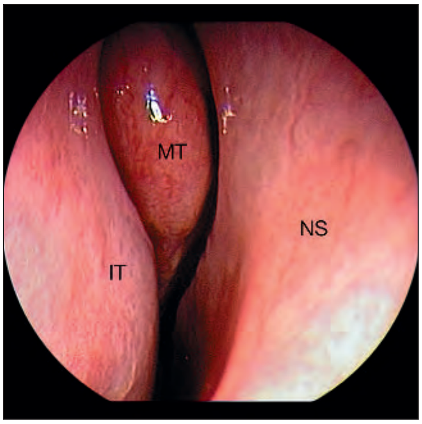

Fig. 32 Nasal stage. Right nasal cavity. Middle turbinate (**MT**); nasal septum (**NS**); inferior turbinate (**IT**).

5.4. Surgical Procedure

The procedure consists of three main aspects: exposure of the lesion, removal of the relevant pathology and reconstruction of the sella. It involves three phases, the nasal, the sphenoid, and the sellar stages.

5.4.1. Nasal Stage

During this stage, a 0°-scope (4 mm in diameter, 18 cm in length) is used freehand. Once the scope has been inserted into the right nostril, the inferior and middle turbinates, and the nasal septum are identified (Figs. 32, 33). The scope is moved along the floor of the nasal cavity, following the inferior turbinate to reach the choana, which is the key anatomical landmark of this step of the procedure (Fig. 34).

The middle turbinate is gently lateralized to make sure that the surgical pathway, that passes between the nasal septum and the turbinate itself (Figs. 35–36), is wide enough.

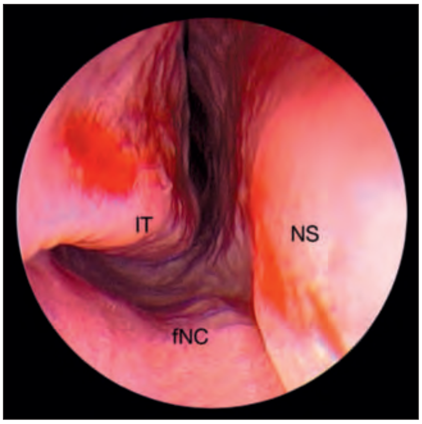

Fig. 33 Nasal stage. Right nasal cavity. Nasal septum (**NS**); floor of the nasal cavity (**fNC**); inferior turbinate (**IT**).

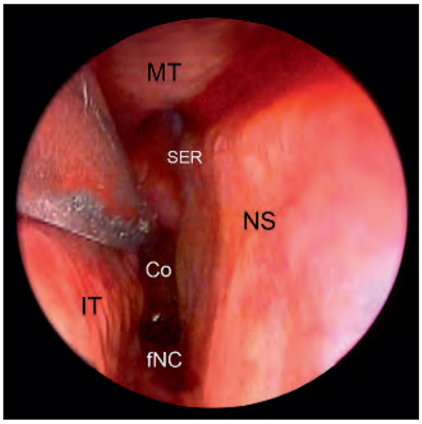

Fig. 34 Nasal stage. Right nasal cavity. Middle turbinate **(MT)**; nasal septum (**NS**); inferior turbinate (**IT**); choana (**Co**); spheno-ethmoid recess (**SER**); floor of the nasal cavity (**fNC**).

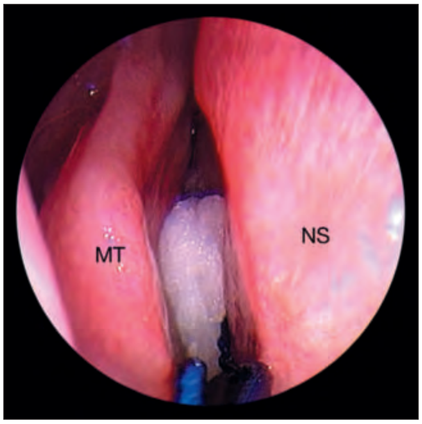

Fig. 35 Nasal stage. Right nasal cavity. A cotton pledget is placed between the nasal septum and the middle turbinate. Middle turbinate (**MT**); nasal septum (**NS**).

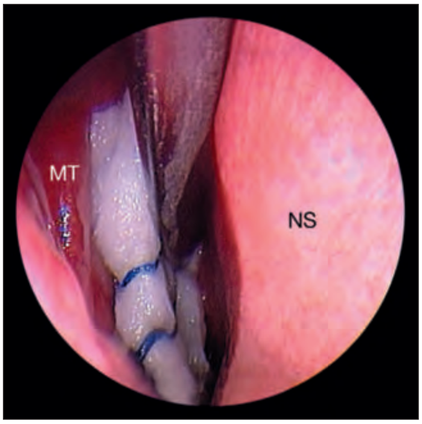

Fig. 36 Nasal stage. Right nasal cavity. The middle turbinate is pushed laterally. Middle turbinate (**MT**); nasal septum (**NS**).

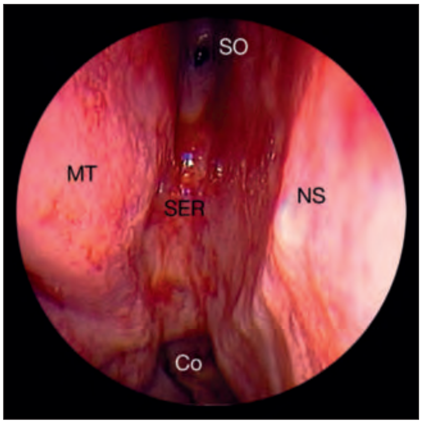

Fig. 37 Nasal stage. Right nasal cavity. Main anatomical landmarks of the posterior nasal cavity. Middle turbinate (**MT**); nasal septum (**NS**); spheno-ethmoid recess (**SER**); sphenoid ostium (**SO**); choana (**Co**).

Once the cotton pledgets have been removed, there will be a noticeable increase in space between the nasal septum and the middle turbinate allowing for adequate inspection of the posterior portion of the nasal cavity, where the choana, the sphenoethmoid recess and the sphenoid ostium are identified (Fig. 37).

5.4.2 Sphenoid Stage

The sphenoid stage of the procedure begins after decongestion or coagulation of the sphenoetmoidal recess with the dissection of the mucosa to expose the anterior face of the sphenoid (Figs. 38–41).

This part of the procedure is usually performed through both nostrils. The unilateral route may be used in some selected cases, provided the nasal cavity offers adequate space for passage of instruments, in the presence of a well-pneumatized sphenoid sinus, and, if the lesion to be treated is of small to medium size.

Subsequently, the bone of the anterior sphenoid sinus wall is widely opened with a microdrill and/or bone punches (Fig. 42), proceeding circumferentially, taking care not to oversize the opening in the inferolateral direction, where the sphenopalatine artery and its major branches traverse.

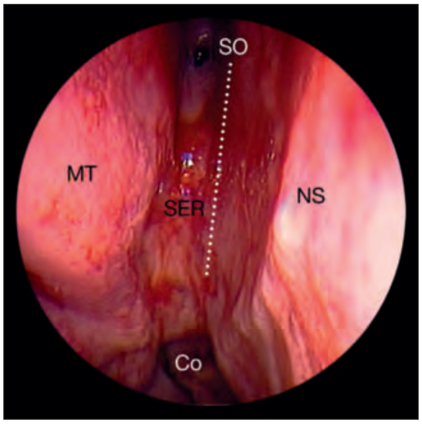

Fig. 38 Sphenoid stage. Right nasal cavity. Middle turbinate (**MT**); nasal septum (**NS**); spheno-ethmoid recess (**SER**); sphenoid ostium (**SO**); choana (**Co**); boundary of the area that is carefully coagulated (**white dotted line**).

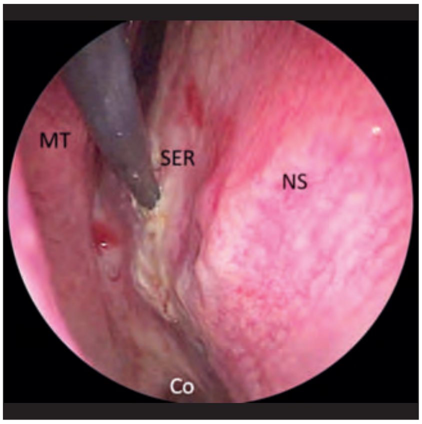

Fig. 39 Sphenoid stage. Right nasal cavity. Coagulation of the spheno-ethmoid recess. spheno-ethmoid recess (**SER**); middle turbinate (**MT**); nasal septum (**NS**); choana (**Co**).

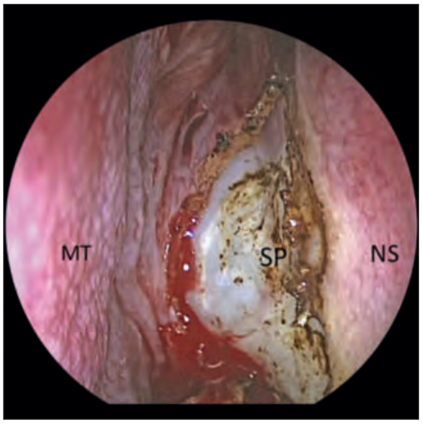

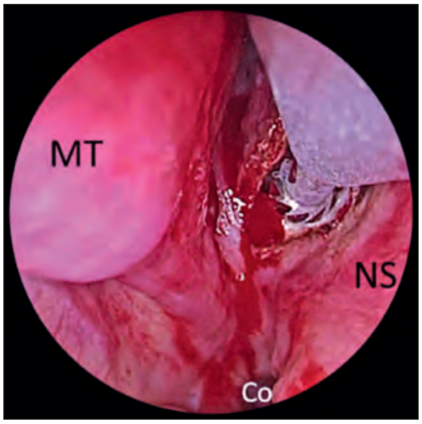

Figs. 40, 41 Sphenoid stage. Submucosal dissection of the sphenoid sinus anterior wall. Middle turbinate (**MT**); nasal septum (**NS**); sphenoid prow (**SP**); choana (**Co**).

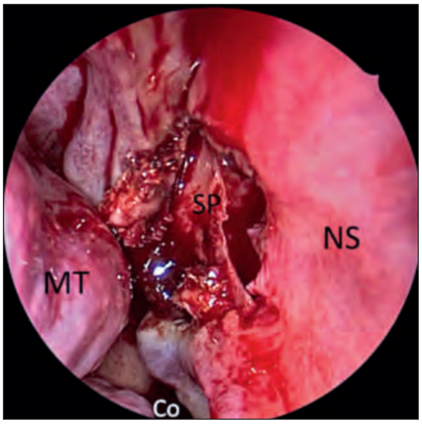

Fig. 42 Sphenoid stage. Removal of the anterior wall of the sphenoid. Middle turbinate (**MT**); nasal septum (**NS**); choana (**Co**); sphenoid prow (**SP**).

In case of arterial bleeding from a branch of the sphenopalatine artery, it is worth using bipolar coagulation, in order to prevent postoperative early or delayed epistaxis.

Once the anterior wall of the sphenoid sinus becomes visible, it is removed in a circumferential manner using a microdrill with a diamond burr, 5 mm in diameter (Figs. 43–44). Care must be taken not to remove too much bone and mucosa in the infero-lateral direction, where the sphenopalatine artery enters the nasal cavity while crossing the sphenopalatine foramen.

In some cases, a median or paramedian septum is present inside the sphenoid cavity (Fig. 45), while in others multiple septa are found. Particularly in the latter case, the septa may be located at the site of the optic or carotid prominence, a condition which requires the surgeon to pay particular attention during removal of these structures. At this point, the field of vision must encompass the entire sellar region. The endoscopic technique thus provides a panoramic view of the entire sphenoid cavity and allows identification of all anatomical landmarks which is mandatory for obtaining access to the sellar floor (optic and carotid protuberances, clivus, planum sphenoidale and opto-carotid recess) (Fig. 46).

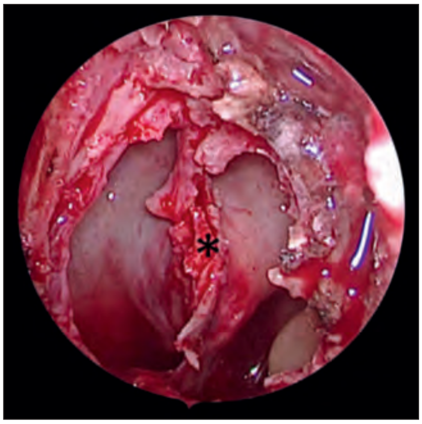

Fig. 43 Sphenoid stage. Anterior sphenoidotomy. Sphenoid septum (✱).

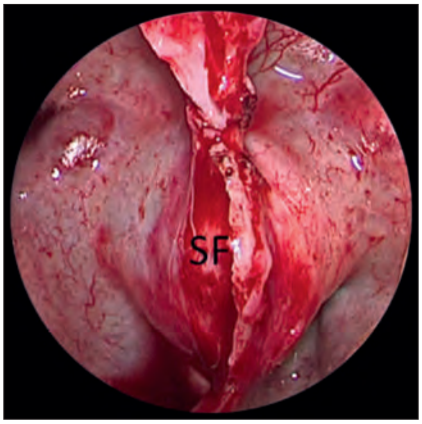

Fig. 44 Sphenoid stage. Close-up view of the sellar floor bulging into the sphenoid sinus cavity. Sellar floor (**SF**).

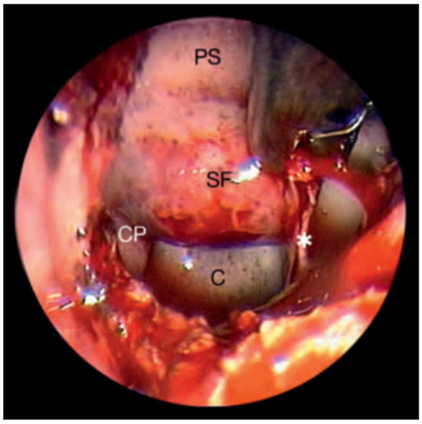

Fig. 45 Sphenoid stage. Removal of a left paramedian sphenoid septum. Planum sphenoidale (**PS**); sellar floor (**SF**); clivus (**C**); carotid protuberance (**CP**); sphenoid septum (✱).

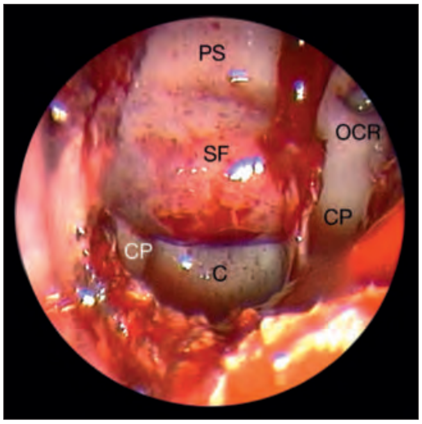

Fig. 46 Sphenoid stage. Exposure of the main anatomical landmarks of the posterior sphenoid sinus wall. Planum sphenoidale (**PS**); sellar floor (**SF**); clivus (**C**); carotid protuberance (**CP**); opto-carotid recess (**ocr**).

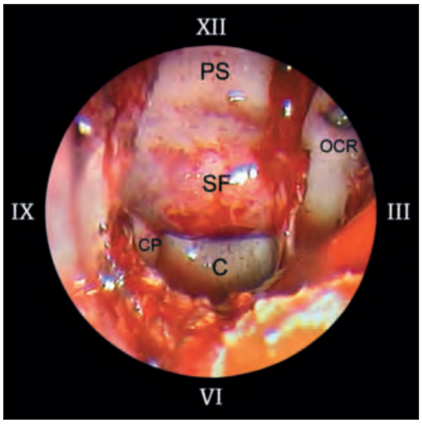

Fig. 47 Sellar stage. **Correct** orientation of the anatomical landmarks inside the sphenoid cavity. Planum sphenoidale (**PS**); sellar floor (**SF**); clivus (**C**); carotid protuberance (**CP**); opto-carotid recess (**ocr**).

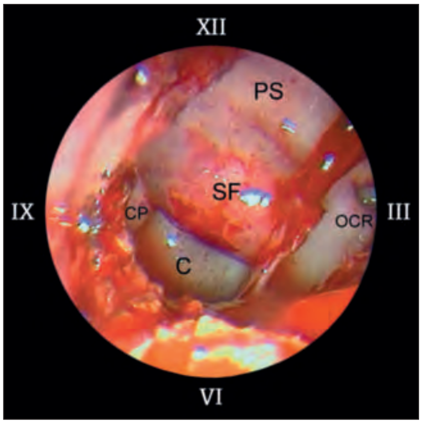

Fig. 48 Sellar stage. **Incorrect** orientation caused by misalignment of the videocamera. The left opto-carotid recess is at 3 o'clock. Planum sphenoidale (**PS**); sellar floor (**SF**); clivus (**C**); carotid protuberance (**CP**); opto-carotid recess (**ocr**).

5.4.3. Sellar Stage

In order to free both hands of the first surgeon and allow for comfortable introduction of two instruments, from this stage onwards, the endoscope is guided dynamically by the assisting second surgeon.

Prior to opening the sellar floor, the assisting surgeon must take care that the endoscope has the proper initial orientation to ensure that all anatomical landmarks inside the sphenoid cavity are displayed in their appropriate positions (Figs. 47–48).

Creation of an opening in the sellar floor may be accomplished by several methods and use of various instruments, depending on the individual anatomical situation (intact, thinned-out, eroded sellar floor). Consistency of the sellar floor depends on the type of lesion present in the sellar cavity. It is nearly always intact in many types of craniopharyngiomas, in Rathke's cleft cysts, and in microadenomas, while it is frequently thinned-out and/or eroded in pituitary macroadenomas.

Therefore, depending on its thickness, the sellar floor may be initially opened with a microdrill when intact (Fig. 49), or by means of a dissector, when thinned out or eroded. The opening may be then enlarged with KERRISON bone punches, if thickness is reduced or if there are signs of erosion.

The opening of the sellar floor should be enlarged as required by each individual case and, if necessary, as far as the planum sphenoidale above, the inferior clivus below, and the cavernous sinuses, laterally.

Once the opening of the floor has been completed, the dura mater may appear intact, thinned-out or infiltrated by the lesion (Fig. 50).

An ultrasound doppler probe can be helpful for identifying the carotid arteries, thus allowing a safer dura opening.

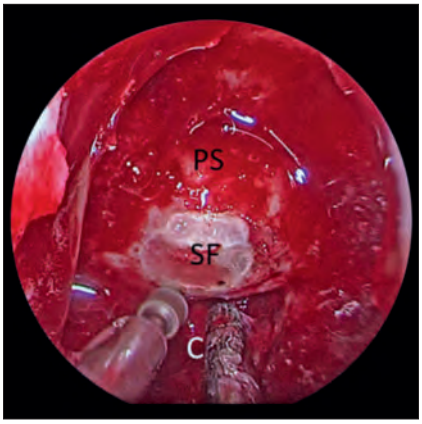

Fig. 49 Sellar stage. Opening of the sellar floor with a microdrill. Sellar floor (**SF**); planum sphenoidale (**PS**); clivus (**C**).

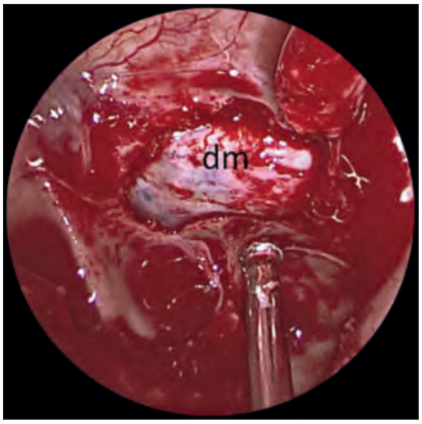

Fig. 50 Sellar stage. After opening the sellar floor, the dura mater is exposed. Dura mater (**dm**).

Taking into account that the distal portions of the surgical field are located in the focal plane of the scope, the surgical knife is not always under direct visual control during this stage of surgery, particularly during its advancement. For this reason, the use of a scalpel with telescopic blade is highly recommended. The blade of this dedicated instrument is retracted before the tip enters the endoscope's field of vision, where the blade is extended. In this way, iatrogenic trauma to the mucosa during insertion of the instrument can be prevented.

Once the dural incision has been made (Fig. 51), the intrasellar lesion is removed by curettage and aspiration, using curettes and suction tubes of varying diameters and angulations (Figs. 52–57).

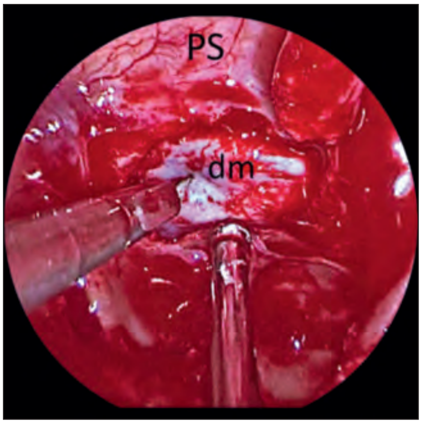

Fig. 51 Sellar stage. Incision of the dura mater using a surgical knife with telescopic blade. Dura mater (**dm**); planum sphenoidale (**PS**).

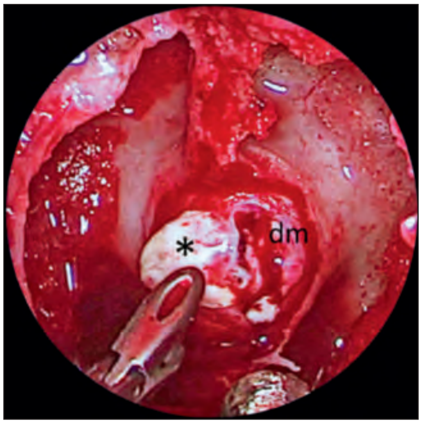

Figs. 52, 53 Sellar stage. The tumor is dissected with a curette and removed in a piecemeal fashion.

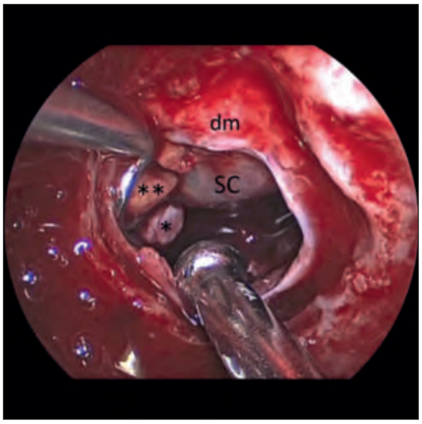

Fig. 54 Sellar stage. View of the sellar cavity after tumor removal; residual gland (**✱✱**); neurohypophysis (**✱**); suprasellar cistern (**SC**); dura mater (**dm**).

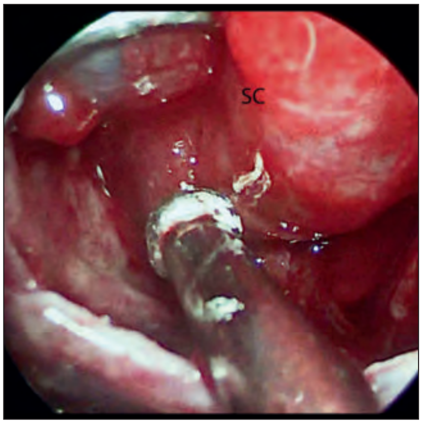

Fig. 55 Sellar stage. Exploration of sellar cavity after tumor removal. Suprasellar cistern (**SC**).

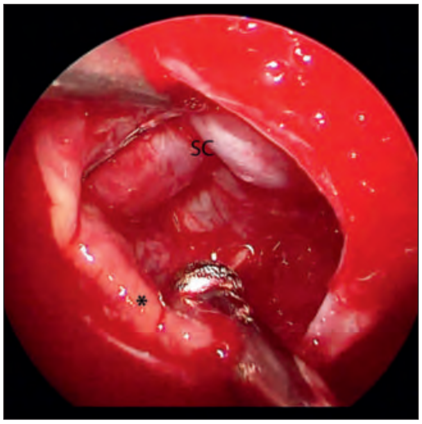

Fig. 56 Sellar stage. The suprasellar cistern has been pushed upward and the residual gland is identified. Suprasellar cistern (**SC**); residual gland (**✱**).

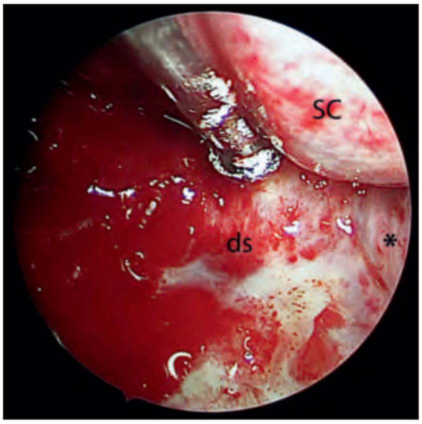

Fig. 57 Close-up view of the dorsum sellae, suprasellar cistern and the left cavernous sinus medial wall after adenoma removal. Suprasellar cistern (**SC**); dorsum sellae (**ds**); cavernous sinus medial wall (**✱**).

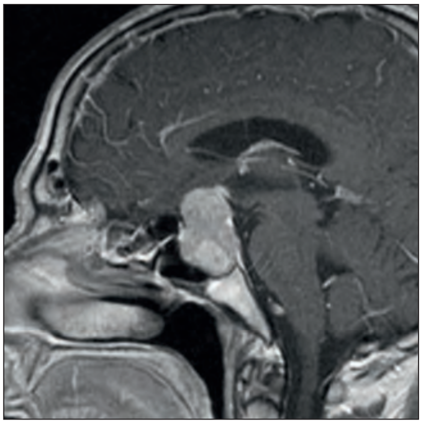

Fig. 58 Sagittal MRI scan showing an intra- and suprasellar macroadenoma.

In the case of a macroadenoma (Fig. 58), the inferior and lateral components of the lesion should be removed before addressing the superior aspect (Figs. 59–62). Indeed, removal of the superior part first will cause the suprasellar cistern and the redundant diaphragma sellae to prematurely descend into the operative field, thus reducing the chance to expose and remove the lateral portions of the lesion.

Conversely, in case of a microadenoma, one should attempt to identify a leavage plane of the tumor pseudocapsule for “en bloc” excision which, if possible, should be accomplished without compromising the residual pituitary gland tissue.

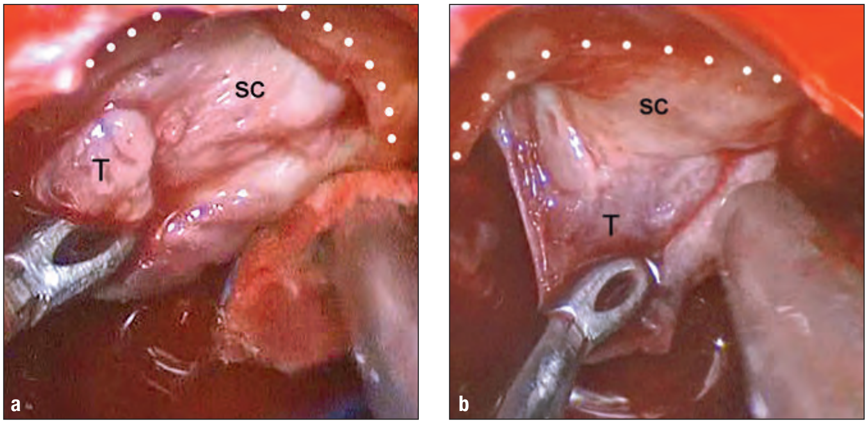

Fig. 59 Intraoperative images (**a, b**) showing progressive dissection of the tumor from the suprasellar cistern. Suprasellar cistern (**SC**); tumor (**T**).

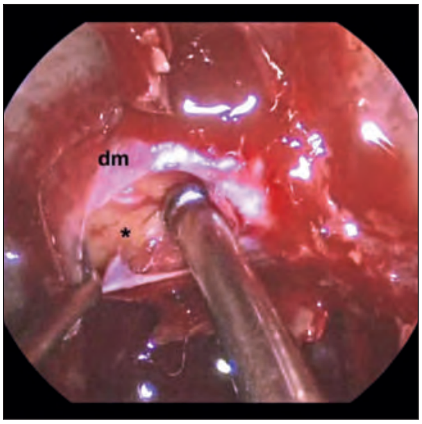

Fig. 60 Case of intrasellar adenoma located in the right portion of the sella. Dura mater (**dm**); tumor (**✱**).

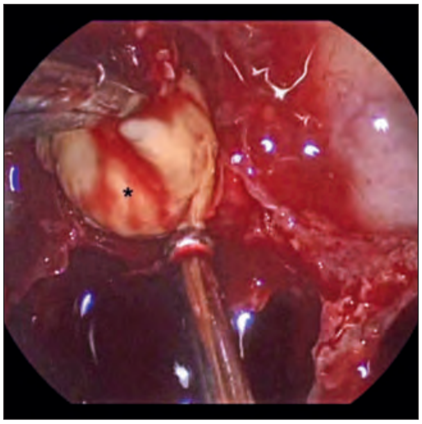

Fig. 61 The adenoma is removed “en bloc”. Tumor (**✱**)

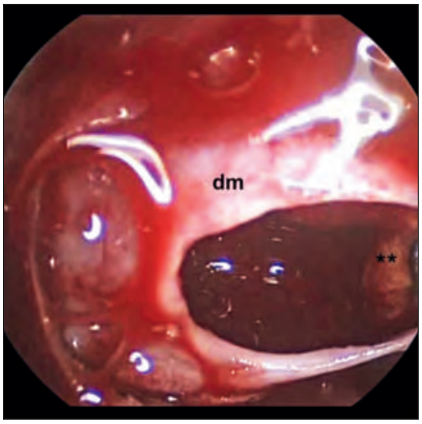

Fig. 62 Panoramic view after the removal of the adenoma. Dura mater (**dm**); residual gland (**✱✱**).

Tumor removal is usually performed with a 0°-scope. In addition, 30°- or 45°-scopes can be helpful for inspecting the sellar cavity after tumor removal, evaluating the presence of some remnant or identifying the site of cerebrospinal fluid leakage (CSF) over the cistern surface (Figs. 63, 64).

5.4.4. Sellar Repair

Upon completion of the endoscopic procedure, sellar reconstruction is required, mainly when an intraoperative CSF leak has occurred. Autologous or heterologous materials, either resorbable or not, are used, if necessary, to achieve a safe and effective sellar reconstruction.

The aim of the repair is to guarantee a watertight closure, reduce the dead space, and prevent the descent of the chiasm into the sellar cavity (Figs. 65, 66). This must be performed with care to avoid overpacking, which carries the risk of subsequent damage to the optic chiasm.

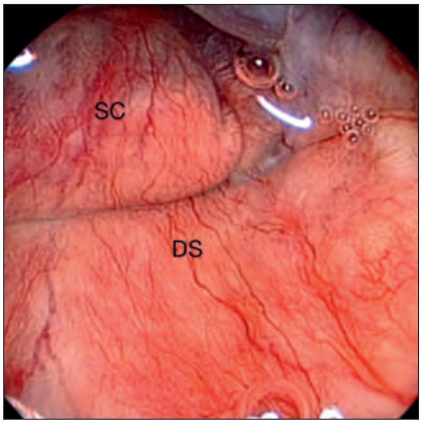

Fig. 63 Case of an intraoperative CSF leak after evacuation of an intrasellar and suprasellar arachnoid cyst. The 0°-scope allows the dorsum sellae and parts of the suprasellar cistern to be inspected. Suprasellar cistern (**SC**); dorsum sellae (**DS**).

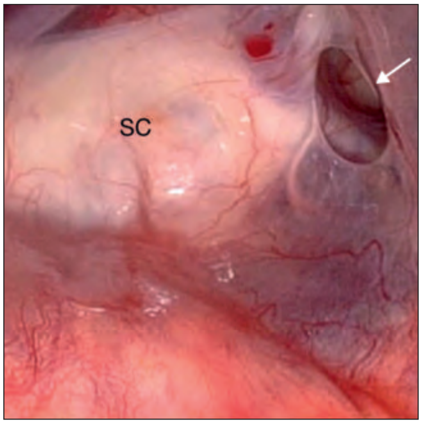

Fig. 64 With the direction of view pointing upward, the 30°-scope allows to detect the arachnoid tearing (**arrowhead**). Suprasellar cistern (**SC**).

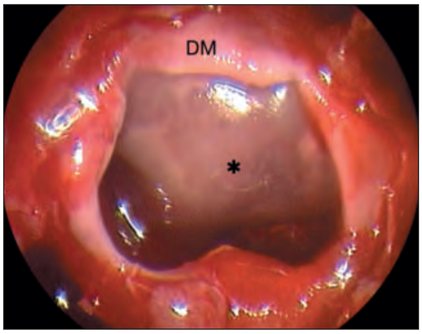

Fig. 65 Sellar packing. Placement of a single-layer dural substitute for protection of the suprasellar cistern. Dura mater (**dm**); dural substitute (**✱**).

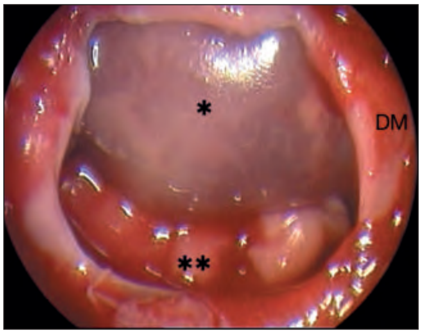

Fig. 66 Sellar packing. The sellar cavity is filled with pieces of collagen sponge. Dura mater (**dm**); dural substitute (**✱**); collagen sponge (**✱✱**).

If a CSF leak becomes evident during the operation, it is necessary to accurately seal the sellar cavity. Different techniques are used (intra- and/or extradural closure of the sella, and packing of the sella with or without packing of the sphenoid sinus), depending on the size of the osteo-dural defect and of the "dead space" inside the sella.

According to *Esposito-Kelly's* paradigm, intraoperative CSF leaks are managed as follows:

- **Grade 1** (small weeping leak): collagen sponge placed over the exposed suprasellar cistern, followed by filling of the sellar cavity with fibrin glue and intra- or extradural closure of the sellar floor.
- **Grade 2** (moderate CSF leak): in this case, reconstruction starts with the management of the arachnoid defect. A small amount of fibrin glue is injected though the arachnoid defect and, if possible, the redundant arachnoid is used to cover the defect. Different layers of collagen sponge are then placed over the cisternal surface, whilst autologous abdominal fat or fibrin glue is used to fill the sellar cavity. Thereafter, the sellar floor is closed intra- or better extradurally with a dural substitute, and other layers of collagen sponge are positioned to cover the posterior wall of the sphenoid sinus. These layers are kept in place by means of fibrin glue (Tisseel®, Baxter AG, Vienna, Austria), see also Fig. 123.
- **Grade 3** (profuse CSF leak): this condition more often concerns the case of an extended approach for suprasellar lesions rather than standard pituitary surgery. Whichever approach is used, reconstruction proceeds in the same way as for Grade 2 up to the closure of the sellar floor, which in this case is performed with a single large layer of dural substitute in the extradural space. In addition, a sheet of resorbable solid material, tailored to conform to the size and grade of the defect, is then placed over the dural substitute and embedded in the extradural space dragging the dural substitute into overlay position (Fig. 124). The dural substitute is positioned and the bone substitute is embedded in the extradural space dragging the dural substitute. Other layers of dural substitute or mucoperichondrium are overlapped. Eventually, a vascularized nasoseptal flap according to *Hadad-Bassagasteguy's* technique can be used.

Once sellar reconstruction has been finished, the surgical procedure is completed by medializing the middle turbinate previously displaced to avoid maxillary sinusitis.

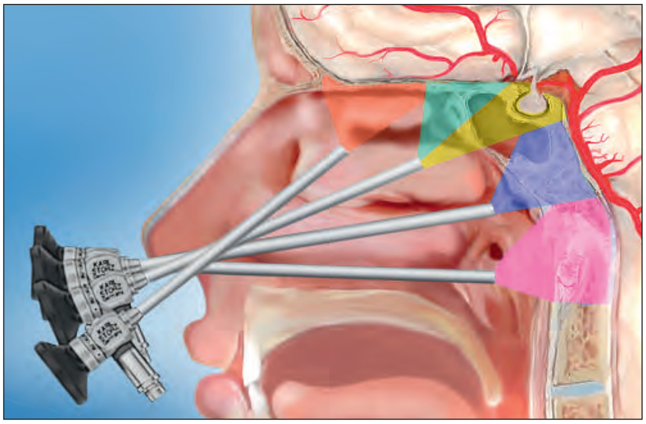

Fig. 67 Schematic drawing showing the different trajectories that are followed to expose the olfactory groove (**red**), the planum sphenoidale (**turquoise**), the sella (**yellow**), the clivus (**blue**) and the cranio-vertebral junction (**purple**).

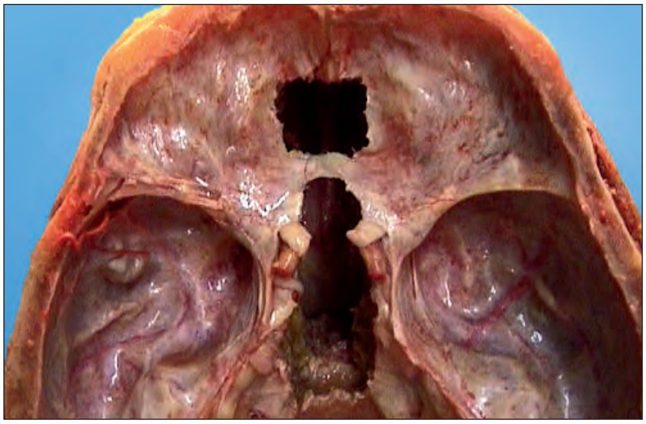

Fig. 68 Anatomic view of the cranial surface of the skull base showing the boundaries of bone removal obtained through the endoscopic endonasal route.

6 Anatomical Structures Involved in Extended Endonasal Approaches to the Skull Base

In order to achieve a wider working space that facilitates maneuvering of instruments while exploring areas around the sella, or even in selected sellar lesions, the basic rules for extended approaches to the skull base (Figs. 67, 68), according to *Kassam's* indications, have to be applied.

The following basic steps are therefore required:

- unilateral removal of the middle turbinate;
- lateralization of the middle turbinate in the other nostril;
- removal of the posterior portion of the nasal septum;
- removal of the superior turbinate and of the posterior ethmoid air cells (on the same side where the middle turbinate has been removed).

6.1. Anterior Skull Base Approaches

6.1.1. Endoscopic Anatomy of the Planum Sphenoidale

Immediately above the sellar floor, the angle formed by the convergence of the sphenoid planum with the sellar floor, represented by the tuberculum sellae, can be observed. The sphenoid planum is slightly anterior to it, bounded on both sides by the protuberances of the optic nerves, that diverge towards the apices of the orbits (Fig. 69).

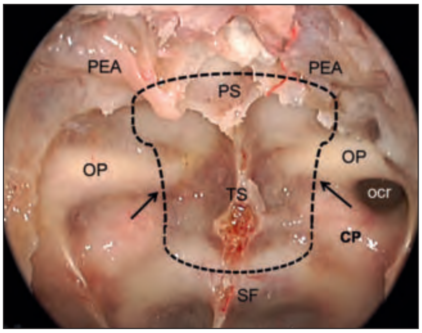

Fig. 69 Wide exposure of the planum sphenoidale. The **broken line** demarcates the boundary of bone removal to gain access to the suprasellar area; the pointers indicate the medial opto-carotid recess. Planum sphenoidale (**PS**); tuberculum sellae (**TS**); carotid protuberance (**CP**); sellar floor (**SF**); opto-carotid recess (**ocr**); optic protuberance (**OP**); posterior ethmoidal artery (**PEA**).

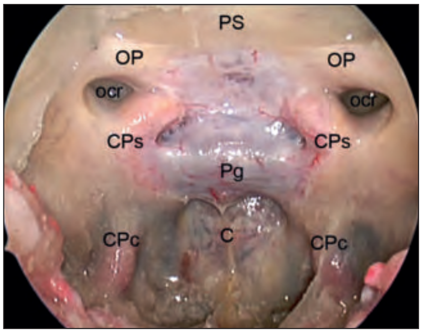

Fig. 70 Opening of the planum sphenoidale. Bone removal. Planum sphenoidale (**PS**); sellar floor (**SF**); clivus (**C**); parasellar segment of the carotid protuberance (**CPs**); optic protuberance (**OP**); paraclival segment of the carotid protuberance opto-carotid recess (**CPc**); pituitary gland (**Pg**).

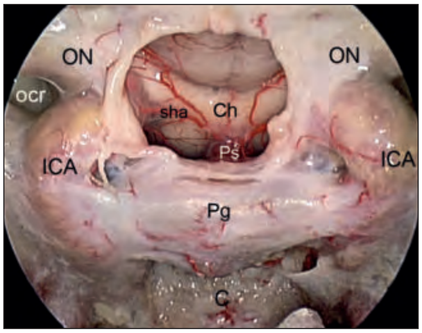

Fig. 71 Opening of the planum sphenoidale. Exposure of the neurovascular structures. Optic nerve (**ON**); optic chiasm (**Ch**); superior hypophyseal artery (**sha**); pituitary stalk (**Ps**); opto-carotid recess (**ocr**); internal carotid artery (**ICA**); pituitary gland (**Pg**); clivus (**C**).

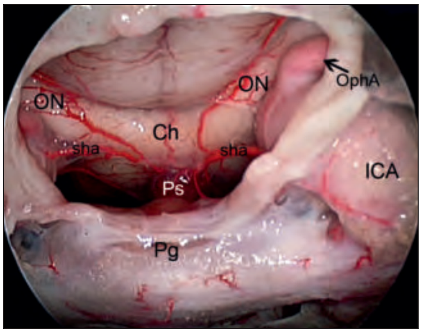

Fig. 72 Opening of the planum sphenoidale. The close-up view highlights the origin of the left ophthalmic artery. Optic nerve (**ON**); optic chiasm (**Ch**); superior hypophyseal artery (**sha**); pituitary stalk (**Ps**); pituitary gland (**Pg**); internal carotid artery (**ICA**); ophthalmic artery (**OphA**).

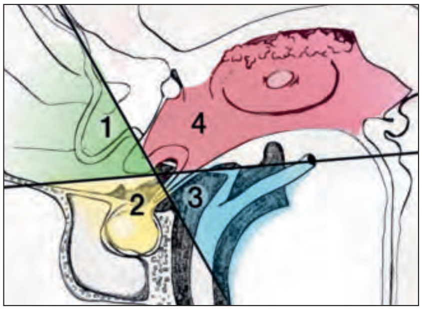

Fig. 73 Schematic drawing illustrating the areas explorable with the endoscope through the transtuberculum-transplanum approach. They can be divided into four areas: suprachiasmatic (**1**); subchiasmatic (**2**); retrosellar (**3**); intraventricular (**4**).

After the bone has been removed, the dura over the sellar floor, the tuberculum sella and planum sphenoidale is opened gaining access to the main suprasellar neurovascular structures (Figs. 70–72). The entire suprasellar region can be divided into four areas by two ideal planes, one passing through the inferior surface of the chiasm and mammillary bodies, and another passing through the posterior margin of the chiasm and dorsum sellae: the *suprachiasmatic, subchiasmatic, retrosellar* and *intraventricular* area (Fig. 73).

In the *suprachiasmatic* area, the anterior margin of the chiasm, the medial portion of both optic nerves, the anterior portion of the circle of Willis, and the gyri recti of the frontal lobes are exposed (Figs. 74, 75).

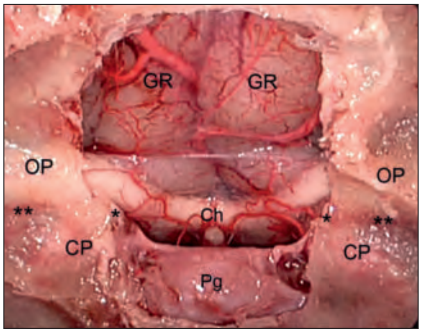

Fig. 74 Suprachiasmatic area. Medial opto-carotid recess (✱); lateral opto-carotid recess (✱✱). Optic chiasm (**Ch**); optic protuberance (**OP**); carotid protuberance (**CP**); pituitary gland (**Pg**); gyrus rectus (**GR**).

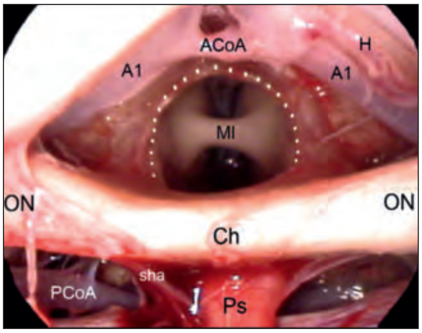

Fig. 75 Suprachiasmatic area after fenestration of the lamina terminalis. The dotted line demarcates the boundary of the fenestration. Massa intermedia (**MI**); anterior communicating artery (**ACoA**); pre-communicating segment of the anterior cerebral artery (**A1**); Heubner's artery (**H**); optic nerve (**ON**); optic chiasm (**Ch**); superior hypophyseal artery (**sha**); pituitary stalk (**Ps**); posterior communicating artery (**PCoA**).

In the *subchiasmatic* space, the pituitary stalk is encountered first, surrounded by the superior hypophyseal artery coming from the ICA with its branches; the internal carotid artery, its bifurcation and the A1 segment, as the superior aspect of the pituitary gland and the dorsum sellae can be seen laterally and deeply (Fig. 76).

In the retrosellar area, above the dorsum sellae, the upper third of the basilar artery, the pons, the superior cerebellar arteries, the oculomotor nerves, the posterior cerebral arteries and, lastly, the mammillary bodies and the floor of the third ventricle are visualized (Figs. 77, 78).

Opening the floor of the third ventricle at the level of tuber cinereum, a panoramic view of the intraventricular area is obtained (Figs. 79, 80).

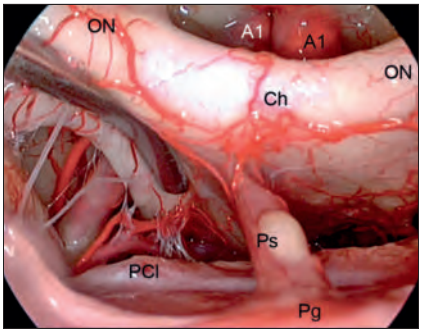

Fig. 76 Subchiasmatic area. Optic nerve (**ON**); optic chiasm (**Ch**); pituitary stalk (**Ps**); pituitary gland (**Pg**); Pre-communicating segment of the anterior cerebral artery (**A1**); posterior clinoid (**PC**).

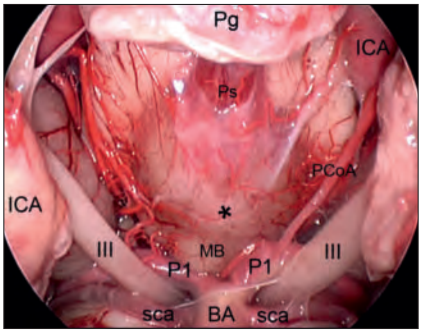

Fig. 77 Retrosellar area after pituitary elevation. Floor of the third ventricle (✱); pituitary stalk (**Ps**); pituitary gland (**Pg**); internal carotid artery (**ICA**); posterior communicating artery (**PCoA**); oculomotor nerve (**III**); mammillary body (**MB**); pre-communicating segment of the posterior cerebral artery **(P1**); basilar artery (**BA**); superior cerebellar artery (**sca**).

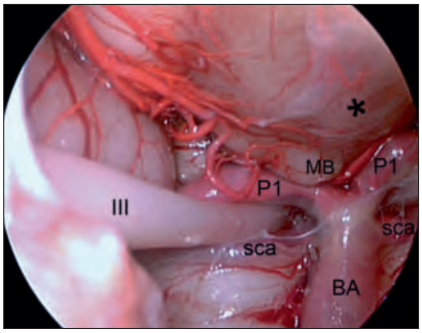

Fig. 78 Lateral aspect of the retrosellar area. Floor of the third ventricle (✱); oculomotor nerve (**III**); mammillary body (**MB**); pre-communicating segment of the posterior cerebral artery (**P1**); basilar artery (**BA**); superior cerebellar artery (**sca**).

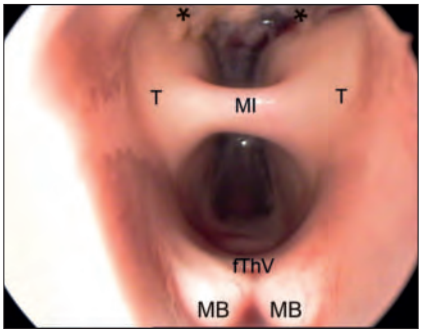

Fig. 79 Anterior part of the third ventricle area. Choroid plexus (✱); massa intermedia (**MI**); mammillary body (**MB**); thalamus (**T**); floor of the third ventricle (**fThV**).

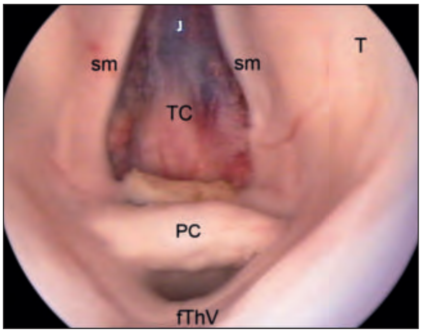

Fig. 80 Posterior part of the third ventricle area. Striae medullaris (**sm**); tela choroidea (**TC**); posterior commissure (**PC**); thalamus (**T**); floor of the third ventricle (**fThV**).

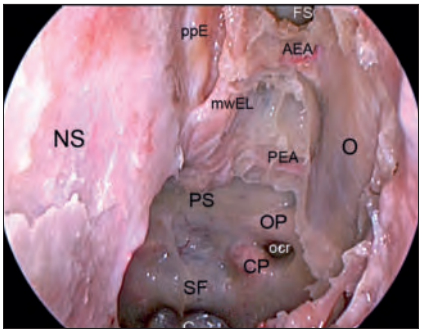

Fig. 81 Exposure of the anterior skull base. Anterior and posterior ethmoidectomy have been completed. Nasal septum (**NS**); clivus (**C**); sellar floor (**SF**); carotid protuberance (**CP**); opto-carotid recess (**ocr**); optic protuberance (**OP**); planum sphenoidale (**PS**); posterior ethmoidal artery (**PEA**); orbit (**O**); anterior ethmoidal artery (**AEA**); frontal sinus (**FS**); medial wall of the ethmoidal labyrinth (**mwEL**); perpendicular plate of the ethmoid (**ppE**).

6.1.2. Endoscopic Anatomy of the Olfactory Groove

In order to gain access to this area of the skull base, middle turbinates of both nostrils, anterior and posterior ethmoid cells and the superior half of the nasal septum are completely removed. When explored through the endonasal route, the olfactory groove is a rectangular area of the cranial base demarcated by the lamina papyracea (orbital walls) laterally, the planum sphenoidale posteriorly, and the frontal sinus anteriorly. Such an area is composed of two symmetrical parts divided by the perpendicular plate of the ethmoid, the lamina cribrosa medially and the ethmoidal labyrinth laterally (Figs. 81–83).

The anterior and posterior ethmoidal arteries, which both are branches of the ophthalmic artery, reach the cribriform plate emerging from the anterior and posterior ethmoidal canals respectively (Fig. 84). The anterior ethmoidal artery (AEA) traverses the ethmoidal planum horizontally between the second and third ethmoidal lamellae. The course of the AEA inside the homonymous canal is an important anatomical reference used to locate the frontal sinus. Furthermore, the posterior ethmoidal artery can be considered a sort of anatomical boundary between the sphenoid and the ethmoid planum. These arteries represent critical landmarks in the endoscopic endonasal approach to the anterior skull base and, if necessary, should be coagulated with bipolar forceps and then cut. Extreme care must be taken so as not to expose the anterior and/or posterior ethmoidal arteries to any traction, which can lead to retraction inside the orbit, where bleeding can cause a retrobulbar hematoma, with loss of vision.

Once the anterior skull base has been exposed in the area between the orbits and the dura opening has been completed, the intracranial contents become visible (Fig. 85).

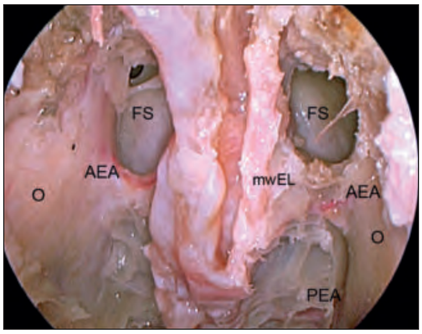

Fig. 82 Exposure of the anterior skull base. The superior part of the nasal septum has been removed, thus allowing a bilateral median exposure.
Medial wall of the ethmoidal labyrinth (**mwEL**); posterior ethmoidal artery (**PEA**); orbit (**O**); anterior ethmoidal artery (**AEA**); frontal sinus (**FS**).

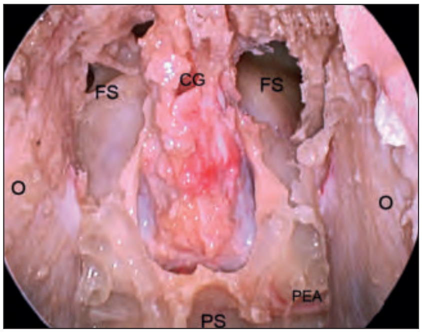

Fig. 83 Exposure of the anterior skull base. The cribriform plate has been removed. Planum sphenoidale (**PS**); posterior ethmoidal artery (**PEA**); orbit (**O**); frontal sinus (**FS**); inferior aspect of the crista galli (**CG**).

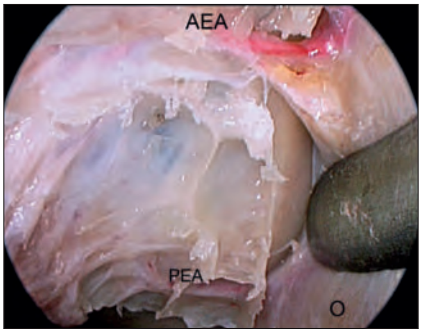

Fig. 84 Exposure of the anterior skull base. Isolation of the ethmoidal arteries. Posterior ethmoidal artery (**PEA**); orbit (**O**); anterior ethmoidal artery (**AEA**).

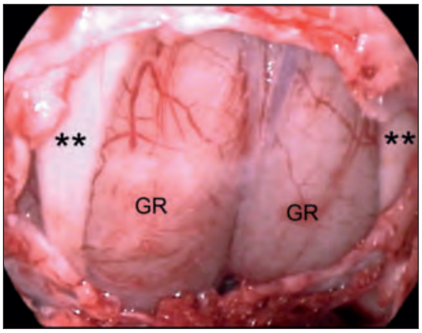

Fig. 85 Exposure of the anterior skull base. Intradural view of the olfactory nerves and the gyri recta (**GR**); olphactory nerve (**✱✱**).

6.2. Posterior Skull Base Approaches

6.2.1. Endoscopic Anatomy of the Clivus

The clivus is divided by the inferior wall (floor) of the sphenoid sinus in two portions, the upper, i.e. the sphenoid and the lower, i.e. the rhinopharyngeal segment. Therefore, the vomer and the floor of the sphenoid sinus have to be completely removed to allow exposure of both parts of the clivus. The lateral boundary is the vidian nerve, which can be identified at the exit from its canal, lateral to the vomer-sphenoid junction (Fig. 86). This nerve leads to the anterior genu of the horizontal segment of the internal carotid artery (ICA) and should be followed during bone removal, thus reducing the risk of iatrogenic injury to the ICA. It also represents a key landmark to unlock the lateral aspect of the middle cranial fossa.

The lateral boundary of the sphenoid portion of the clivus is demarcated by the paraclival tracts of the intracavernous carotid arteries (Fig. 87). Nevertheless, one should bear in mind that particular attention must be paid when extending the bone removal laterally. As a matter of fact, the abducent nerve enters the cavernous sinus by traversing the basilar sinus in close proximity to the paraclival tract of the intracavernous carotid artery. Once the dura mater has been opened, the basilar artery and its branches, as well as the upper cranial nerves, are well visualized along their courses in the posterior cranial fossa (Figs. 88 , 89).

The removal of the inferior part of the clival bone exposes the anterior surface of the craniovertebral junction. The lower third of the clivus can be removed up to the occipital condyles (Fig. 90).

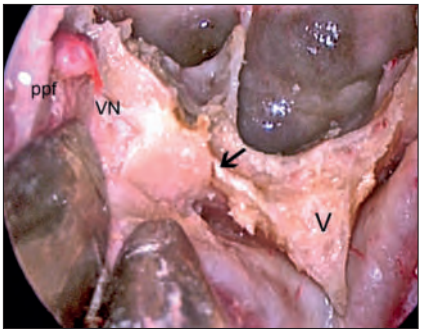

Fig. 86 Exposure of the vomer-sphenoid junction and identification of the vidian nerve. Vomer-sphenoid junction (**pointer**); vomer (**V**); vidian nerve (**VN**); pterygo-palatine fossa (**ppf**).

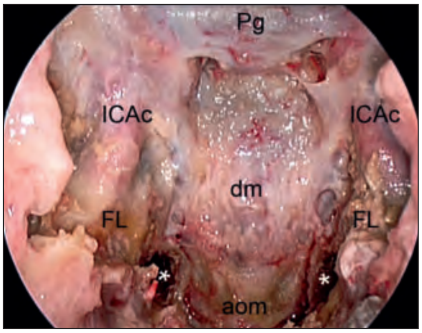

Fig. 87 Exposure of the clival region from the sella to the foramen magnum. Occipital condyle (✱); pituitary gland (**Pg**); clival portion of the internal carotid artery (**ICAc**); foramen lacerum (**FL**); anterior atlanto-occipital membrane (**aom**); dura mater (**dm**).

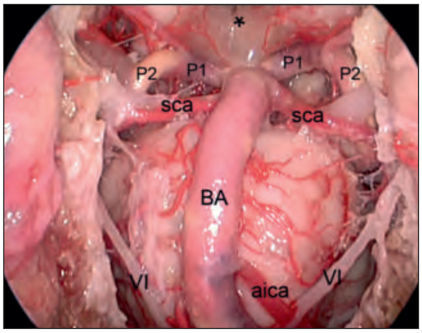

Fig. 88 After bone removal and opening of the dura mater, the neurovascular structures can be visualized. Floor of the third ventricle (✱); basilar artery (**BA**); superior cerebellar artery (**sca**); pre-communicating segment of the posterior cerebral artery (**P1**); post-communicating segment of the posterior cerebral artery (**P2**); anterior inferior cerebellar artery (**aica**); abducent nerve (**VI**).

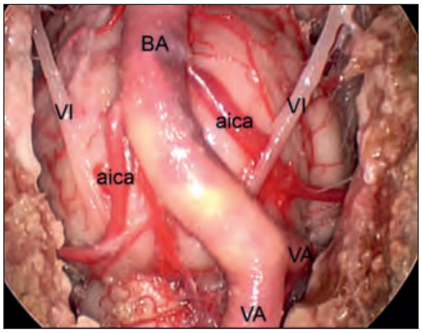

Fig. 89 Retroclival exploration. Note the oblique course of the sixth cranial nerve. Basilar artery (**BA**); anterior inferior cerebellar artery (**aica**); abducent nerve (**VI**); vertebral artery (**VA**).

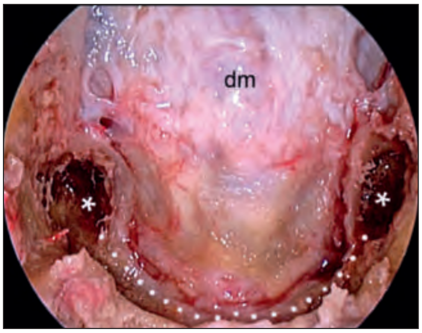

Fig. 90 Drilling of the inner third of the occipital condyles to expose the anterior part of the foramen magnum. Occipital condyle (✱); anterior part of the foramen magnum (**dotted line**); dura mater (**dm**).

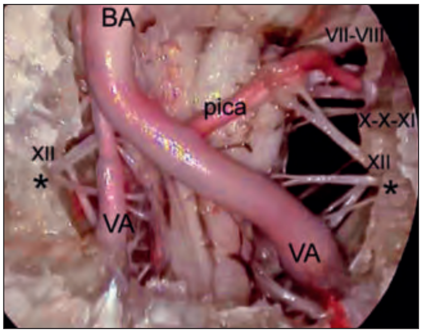

Fig. 91 Intradural exploration. Note the lateral boundaries of the osteodural opening at the level of the hypoglossal canals. Hypoglossal canal (**✱**); basilar artery (**BA**); posterior inferior cerebellar artery (**pica**); acustico-facial bundle (**VII-VIII**); glossopharyngeal, vagus and accessory nerves nerve (**IX-X-XI**); hypoglossal nerve (**XII**); vertebral artery (**VA**).

The lateral boundaries of the bone removal at the level of the floor of the sphenoid sinus are defined by the *foramina lacera* with the intrapetrous carotid artery, while at the level of the craniovertebral junction they are defined by the hypoglossal canals, which course into the occipital condyles between their anterior and middle third (Fig. 91). As a matter of fact, the articular surface of the condyles lies on its lateral portion. Therefore, removal of the inner surface of the anterior third of the condyles can be performed without affecting the functional integrity of the joints. Upon dural opening, the vertebral arteries can be explored up to the basilar artery (see Fig. 91). The posterior inferior cerebellar artery (PICA), the lower cranial nerves and the acoustic-facial bundle (VII–VIII) with the anterior inferior cerebellar artery (AICA) can be visualized as well.

6.2.2. Endoscopic Anatomy of the Craniovertebral Junction

Extending the clival bone opening downward, the anterior surface of the cranio-vertebral junction can be exposed as well. Once the mucosa of the rhinopharynx has been removed, the atlantooccipital membrane, the *longus capitis* and *longus colli muscles,* and the atlas and axis are exposed (Fig. 92). Dissection of the muscular structures together with removal of the anterior arch of the atlas are required to visualize the dens (Fig. 93). The dens is then thinned, separated from the apical and alar ligaments, dissected from the transverse ligament, and finally removed. Once the dura mater has been opened, all the neurovascular structures running through the anterior part of the foramen magnum can be visualized; particularly, the intradural tract of the vertebral artery and the C1 and C2 ventral rootlets should be clearly visible (Fig. 94).

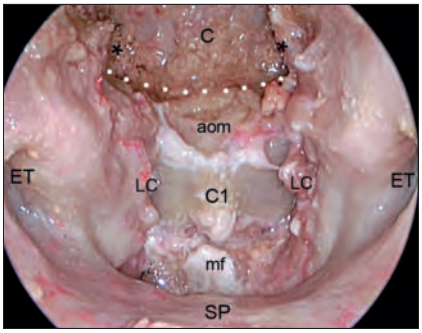

Fig. 92 Exposure of the anterior arch of the atlas. Occipital condyle (**✱**); anterior atlantooccipital membrane (**aom**); anterior part of the foramen magnum (**dotted line**); atlas (**C1**); Eustachian tube (**ET**); longus capitis muscle (**LC**); mucosal flap (**mf**); soft palate (**SP**).

6.3. Cavernous Sinus Approach – Endoscopic Anatomy

This approach involves removal of the bone that covers the intracavernous carotid artery (carotid protuberance) and allows both the medial and lateral compartments of the cavernous sinus to be exposed. Viewing the intracavernous carotid artery within the sphenoid sinus, resembling a shrimp, permits to identify the various segments by their topographical relationship to the surrounding structures. Therefore, we are able to distinguish a parasellar and a paraclival segment. The latter forms the shape of a “C” with medial concavity and can be subdivided into three segments: upper horizontal, vertical and inferior horizontal. The paraclival segment can be divided into an extracavernous lacerum portion, which is caudal, and an intracavernous trigeminal portion, which is cranial (Fig. 95).

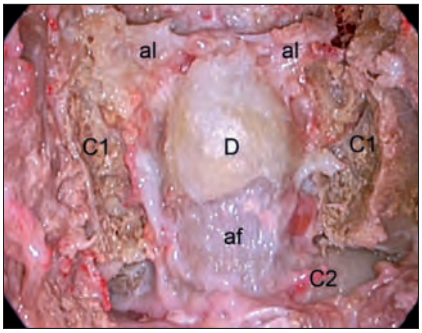

Fig. 93 Exposure of the dens after removal of the anterior arch of the atlas. Atlas (**C1**); alar ligaments (**al**); dens (**D**); articular facet of the dens (**af**); body of the axis (**C2**).

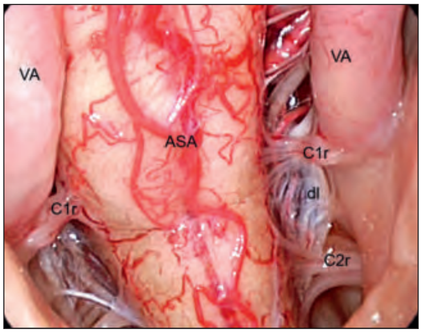

Fig. 94 Intradural exploration at the level of the craniovertebral junction. Vertebral artery (**VA**); anterior spinal artery (**ASA**); ventral rootles (**C1r – C1**); ventral rootles (**C2r – C2**); dentate ligament (**dl**).

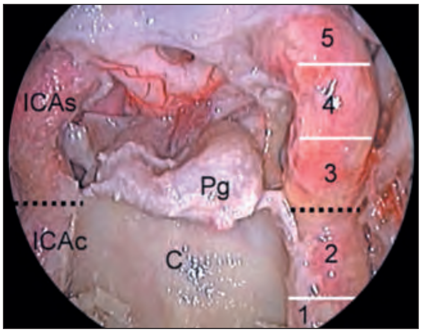

Fig. 95 Exposure of the carotid protuberance. Schematic subdivision of the various segments and portions of the intracavernous carotid artery. Parasellar segment of the intracavernous internal carotid artery (**ICAs**); paraclival segment of the internal carotid artery (**ICAc**); clivus (**C**); pituitary gland (**Pg**); lacerum segment (**1**); trigeminal segment (**2**); inferior horizontal segment (**3**); vertical segment (**4**); superior horizontal segment (**5**).

By lateralizing the intracavernous carotid, it is possible to view, behind the latter and the pituitary gland, the meningohypophyseal trunk and its branches, the dorsal meningeal, inferior hypophyseal and tentorial arteries (Fig. 96). On the other hand, passing laterally to the carotid artery, the inferolateral trunk, i.e. the artery of the inferior cavernous sinus, with its branches to the intracavernous cranial nerves, can be identified along the lateral wall of the cavernous sinus (Fig. 97). Furthermore, the oculomotor, abducent and maxillary nerves can be visualized lying on a closer plane as compared to that occupied by the trochlear and the ophthalmic nerves (Figs. 98, 99).

As visualized through the endoscope from below, the oculomotor nerve superiorly and the abducent inferiorly define a triangular area, the base of which is formed by the lateral loop of the carotid artery. The outer surface of this area contains the fourth cranial nerve and a portion of the V1 branch of the trigeminal nerve. The abducent nerve superiorly and V2 inferiorly enclose a quadrangular area, laterally demarcated by the bone surface of the lateral sphenoid sinus wall, extending from the superior orbital fissure to the foramen rotundum, and medially by the carotid artery. The ophthalmic branch of the trigeminal nerve and arteries to the inferior cavernous sinus pass through this area. Finally, particularly in the case of a well-pneumatized sinus, an inferior quadrangular area can be identified (Fig. 100). It is delineated superiorly by V2 and inferiorly by the vidian nerve. This quadrangular area is of great clinical relevance because it appear s to be the safest entry to the lateral compartment of the cavernous sinus when it is involved by the lesion.

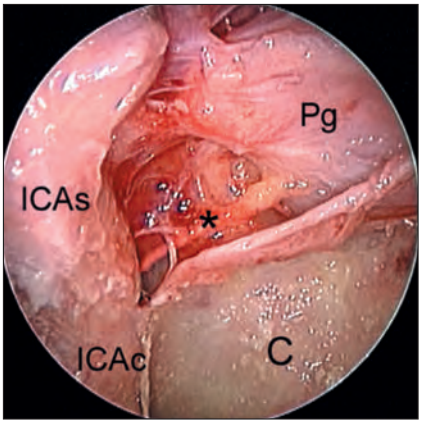

Fig. 96 Exposure of the right carotid protuberance. Lateralization of the intracavernous carotid artery and exposure of the right inferior hypophyseal artery (✱). Parasellar segment of the intracavernous internal carotid artery (**ICAs**); paraclival segment of the internal carotid artery (**ICAc**); clivus (**C**); pituitary gland (**Pg**).

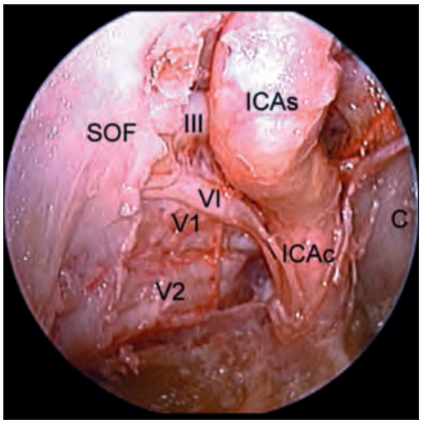

Fig. 97

Fig. 97 Opening the right carotid protuberance. Removal of the lateral sphenoid wall and exposure of the neurovascular structures of the right cavernous sinus. Superior orbital fissure (**SOF**); parasellar segment of the intracavernous internal carotid artery (**ICAs**); paraclival segment of the internal carotid artery (**ICAc**); clivus (**C**); oculomotor nerve (**III**); first branch of the trigeminal nerve (**V1**); second branch of the trigeminal nerve (**V2**); abducent nerve (**VI**).

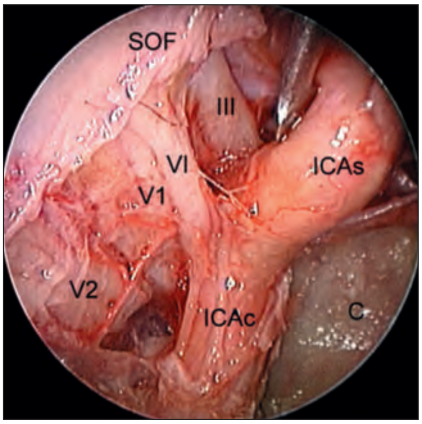

Fig. 98 Opening of the carotid protuberance. Medialization of the carotid artery and exposure of the neurovascular structures of the right cavernous sinus. Superior orbital fissure (**SOF**); parasellar segment of the intracavernous internal carotid artery (**ICAs**); paraclival segment of the internal carotid artery (**ICAc**); clivus (**C**); oculomotor nerve (**III**); first branch of the trigeminal nerve (**V1**); second branch of the trigeminal nerve (**V2**); abducent nerve (**VI**).

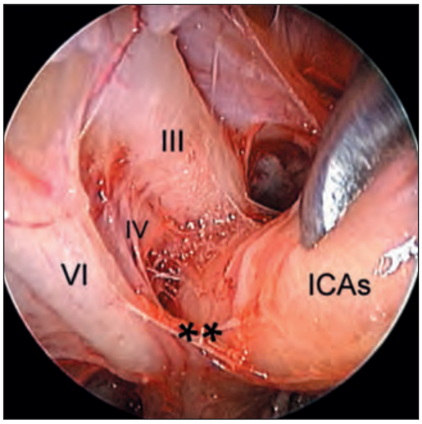

Fig. 99 Opening of the carotid protuberance. Medialization of the intracavernous carotid artery and exposure of the neurovascular structures of the right cavernous sinus. Parasellar segment of the intracavernous internal carotid artery (**ICAs**); oculomotor nerve (**III**); trochlear nerve (**IV**); abducent nerve (**VI**); inferior hypophyseal artery (✱).

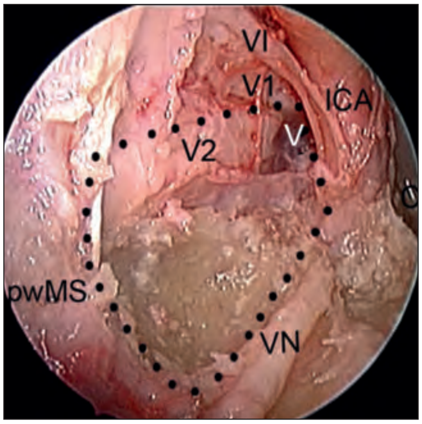

Fig. 100 The boundary of the inferior quadrangular area is demarcated by the **dotted line**. Internal carotid artery (**ICA**); first branch of the trigeminal nerve (**V1**); second branch of the trigeminal nerve (**V2**); abducent nerve (**VI**); vidian nerve (**VN**); clivus (**C**); posterior wall of the maxillary sinus (**pwMS**).

7 Extended Endoscopic Endonasal Approaches to the Skull Base

7.1. Operating Room Set-up

The use of some additional tools has been shown to make the endoscopic endonasal trans-sphenoidal procedures safer and more effective, particularly in case of extended approaches.

A detailed, complete preoperative planning – even with the integrated 3D reconstruction of MRI and/or CT scans, post-processed and displayed by use of open source software (e.g., OsiriX, MRIcro) – is essential to assess the size and position of the skull base opening in relation to the 3D volume of the lesion.

Image-guided surgery systems (neuronavigation) are very useful for intra-operative identification of the boundaries of the lesion providing relevant information concerning the midline and trajectory, and offering enhanced precision in defining the bony delineations and neurovascular spatial relationships.

Finally, it is extremely important to use dedicated instruments, such as **high-speed low-profile microdrills, micro-Doppler probes,** and **coagulating instruments,** including a dedicated bipolar forceps with angled tips, either in sagittal and in coronal plane. The use of a low-profile ultrasonic aspirator can be very helpful in lesion debulking.

Nevertheless, as in the standard approach, the endoscopic equipment and neuronavigation system are positioned behind the head of the patient and in front of the surgeon. Both the screens of the neuronavigation and endoscopic equipment have to be positioned side by side in an ergonomic way. The surgeons are on the right side (the first) and on the left (the second), respectively. Again, the anesthesiologist is positioned with his/her equipment at the left side of the patient at the level of the head and the nurse is positioned at the level of the patient's legs.

As with the standard transsphenoidal approach, rigid HOPKINS® 0°, 30°, and 45° telescopes (length 18 cm, diameter 4 mm) are the only optical devices used to visualize the surgical field during an extended transsphenoidal procedure. At times, it can be helpful, particularly during the intradural stage of the procedure, to additionally use a scope, 18 cm in length and 2.7 mm in diameter.

7.2. Patient Positioning

Depending on the surgical target area, the head is extended about 10–20 degrees to achieve a more anterior trajectory (as for planum sphenoidale or olfactory groove approach) or flexed (as for clival approach), to obtain a posterior trajectory. In both cases, impinging the thorax of the patient with either the scope and/or the surgical instruments must be avoided.

7.3. Approach to the Suprasellar Area

After the preliminary stage, to expose the suprasellar area using an endoscopic endonasal approach, additional bone removal from the cranial base is required, i.e. the tuberculum sellae and planum sphenoidale *(transtuberculum-transplanum approach).*

Bone removal begins with drilling (using a 2-mm burr) of the upper half of the sella and the tuberculum sellae, extending laterally up to both medial opto-carotid recesses, and ensuingly opening the planum sphenoidale with a Kerrison rongeur. Above the medial opto-carotid recesses, bone removal can be extended more laterally, so that the opening resembles an "upside down trapezoid" This particular shape is due to the fact that the inferior part of the osteodural opening is narrowed by the parasellar portion of both the intracavernous carotid arteries and the optic nerves at their entrance in the optic canals. In its superior half, bone removal can be extended laterally because the optic nerves diverge towards the orbits.

In order to better define the limits of bone removal, it is advisable to make use of a neuronavigation system. During bone removal, bleeding from the superior intercavernous sinus can occur. This can be controlled with different hemostatic agents, and with temporary gentle compression with cottonoids. Nevertheless, before opening the dura mater, the sinus should be coagulated with bipolar forceps.

The dura mater is incised horizontally a few millimeters above and below the superior intercavernous, so that the sinus can be coagulated between the two tips of the bipolar forceps (Figs. 101–104); it is then incised with microscissors, and the two resulting dural flaps are again coagulated, to obtain further retraction.

The strategy for dissection and removal of the lesion is tailored to each individual lesion following the same principles as in transcranial microsurgery.

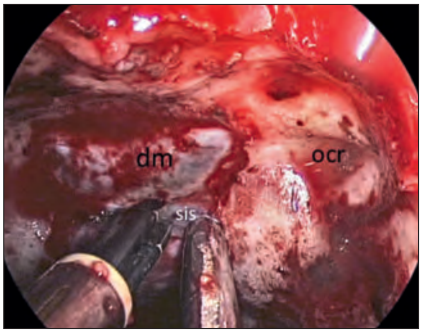

Fig. 101 Coagulation of the superior intercavernous sinus. Opto-carotid recess (**ocr**); dura mater (**dm**); superior intercavernous sinus (**sis**).

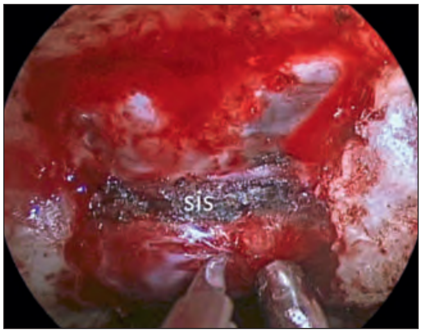

Fig. 102 Opening of the dura mater below the superior intercavernous sinus. Superior intercavernous sinus (**sis**).

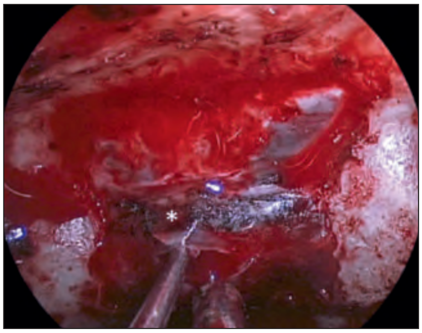

Fig. 103 Dissection of the superior intercavernous sinus. Superior intercavernous sinus (✱) elevated by the dissector.

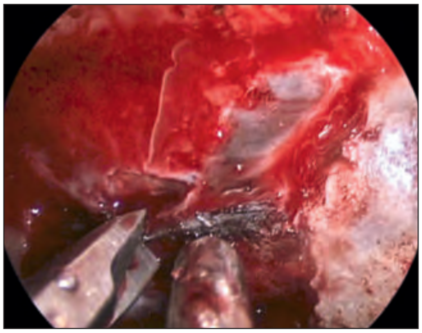

Fig. 104 Cutting of the superior intercavernous sinus..

Craniopharyngiomas

Suprasellar craniopharyngiomas are readily seen upon creation of the dural opening in the prechiasmatic space, anterior to the pituitary stalk, whereas intraventricular craniopharyngiomas, posterior to the stalk, must be approached by passing on each side of the stalk. The stalk and infundibular recess can be enlarged by the craniopharyngioma, thus allowing the removal of the lesion through it. Tumor removal can be performed observing the same principles as in microsurgery, i.e. internal debulking of the solid component and/or cystic evacuation and careful dissection of the tumor capsule from the major neurovascular structures (Figs. 105–108).

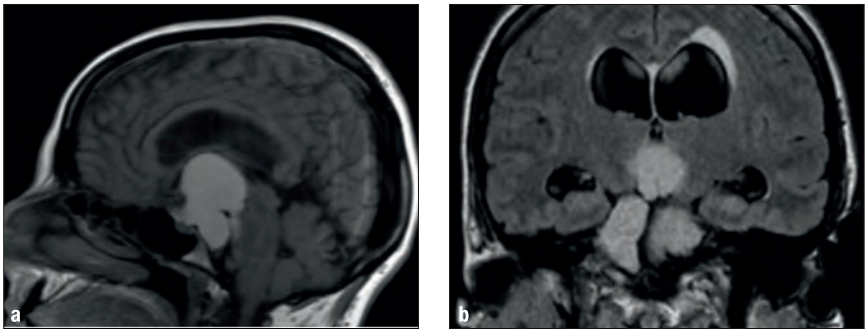

Fig. 105 Preoperative MRI scans (**a, b**) showing a case of suprasellar, retrosellar and intraventricular craniopharyngioma.

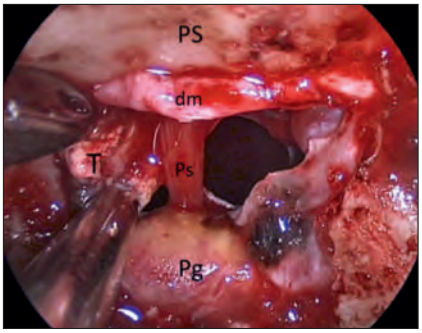

Fig. 106 The lesion is removed through a corridor lateral to the pituitary stalk followed by piecemeal removal. Dura mater (**dm**); planum sphenoidale (**PS**); pituitary stalk (**Ps**); tumor (**T**); pituitary gland (**Pg**).

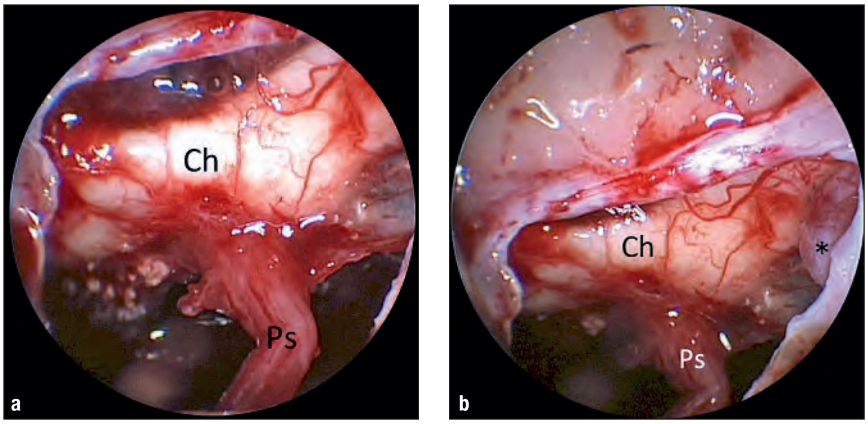

Fig. 107 Exploration of the suprasellar infrachiasmatic area with a 30°-scope (**a, b**). Internal carotid artery (✱). Optic chiasm (**Ch**); pituitary stalk (**Ps**).

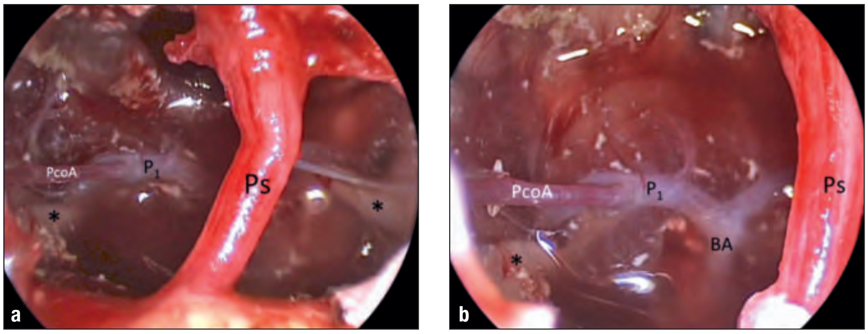

Fig. 108 Panoramic view after removal of the craniopharyngioma. The entire retrosellar area can be inspected (**a, b**). Basilar artery (**BA**); posterior communicating artery (**PcoA**); third cranial nerves (✱); posterior cerebral artery (**P1**); pituitary stalk (**Ps**).

Meningiomas of the Tuberculum Sellae and Planum Sphenoidale

The removal of such lesions is preceded by coagulation of the dural attachment so that early tumor devascularisation is achieved. The tumor is therefore debulked safely and its capsule finally dissected from the surrounding microvascular structures via the extraarachnoidal route. In this particular case, the main advantage of the endoscopic endonasal technique comes from the early devascularization and from the dissection of the tumor with or without minimal manipulation of the optic pathways (Figs. 109–113).

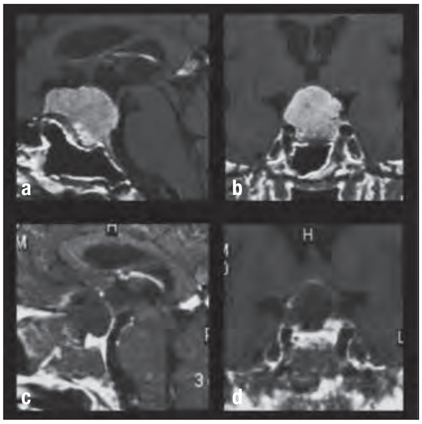

Fig. 109 Preoperative MRI scan showing the case of a tuberculum sellae meningioma (**a**). Postoperative MRI scan demonstrating total removal of the lesion (**b**).

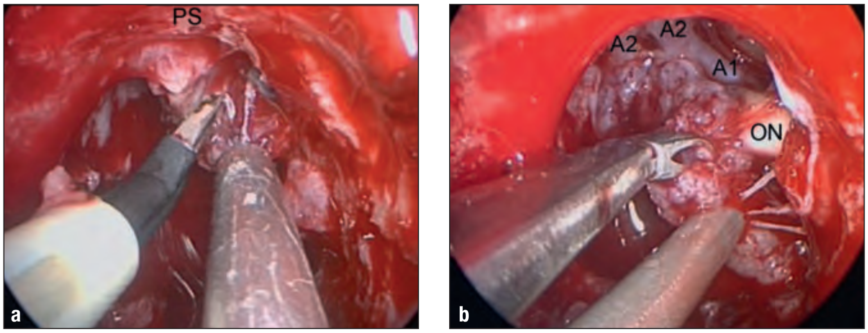

Fig. 110 After early devascularization and internal debulking, the arachnoidal plane is delineated (**a**). The tumor is dissected off the left optic nerve (**b**). Pituitary stalk (**Ps**); optic nerve (**ON**); pre-communicating segment of the anterior cerebral artery (**A1**); post-communicating segment of the anterior cerebral artery (**A2**).

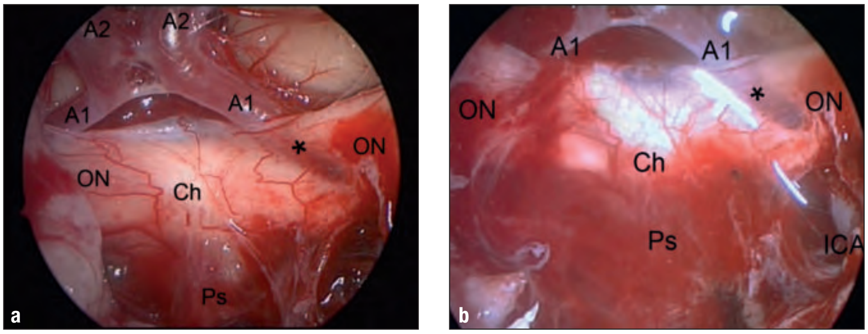

Fig. 111 Note the neurovascular conflict between the left optic nerve and A1 (**a**). Panoramic view after tumor removal (**b**). Pituitary stalk (**Ps**); optic nerve (**ON**); pre-communicating segment of the anterior cerebral artery (**A1**); post-communicating segment of the anterior cerebral artery (**A2**); chiasm (**Ch**); neurovascular conflict (**✱**); internal carotid artery (**ICA**).

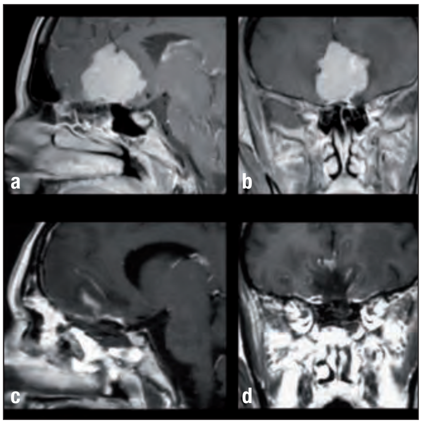

Fig. 112 Preoperative MRI scan showing the case of a meningioma of the spheno-ethmoidal planum (**a, b**). Postoperative MRI scan demonstrating total removal of the lesion and multilayer reconstruction over the osteodural defect (**c, d**).

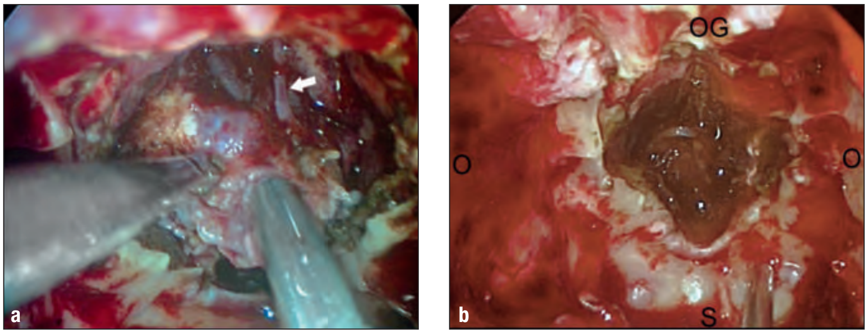

Fig. 113 During extracapsular dissection an artery is identified and preserved (**white arrow**) (**a**). Panoramic view after tumor removal (**b**). Olfactory groove (**OG**); orbit (**O**); sella (**S**).

7.4. Approach to the Olfactory Groove

Such an approach is currently used for the management of many different lesions such as CSF leaks, meningoencephaloceles and esthesioneuroblastomas arising from or involving this area. Therefore, bone removal and exposure of the target area can be tailored to each case according to lesion extension. In case of olfactory groove meningiomas, middle turbinectomy is performed bilaterally, followed by a radical anterior and posterior ethmoidectomy, and removal of the superior half of the nasal septum. The bone of the anterior skull base enclosed between the two orbits is removed, thus creating a wide surgical corridor, which can be extended laterally between the two medial orbital walls, and anteroposteriorly from the frontal sinus to the sella, according to tumor extension. Once the dura has been opened, the lesion can be removed following the steps described previously. The endoscopic approach again allows coagulation of the dural attachment and early devascularization of the tumor (Figs. 114–118).

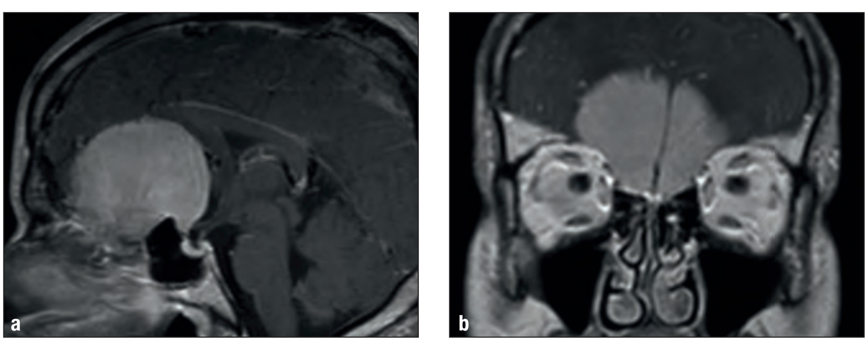

Fig. 114 Preoperative MRI scans (**a, b**) showing the case of an olfactory groove meningioma.

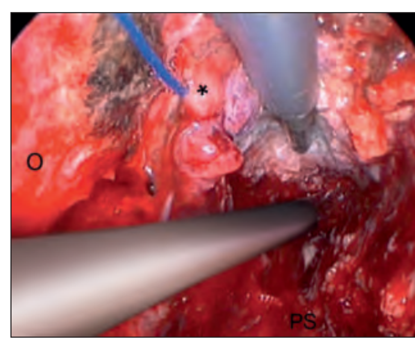

Fig. 115 Intracapsular debulking with an ultrasonic aspirator. Orbit (**O**); pledget interposed between the tumor and the brain (*****); planum sphenoidale (**PS**).

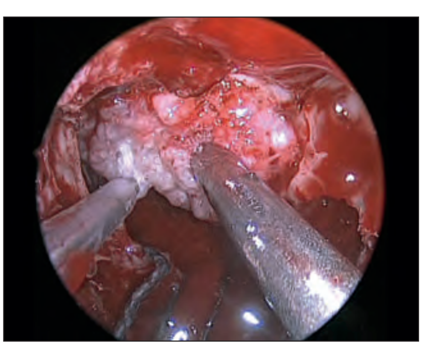

Fig. 116 Intracapsular debulking using an ultrasonic surgical aspirator.

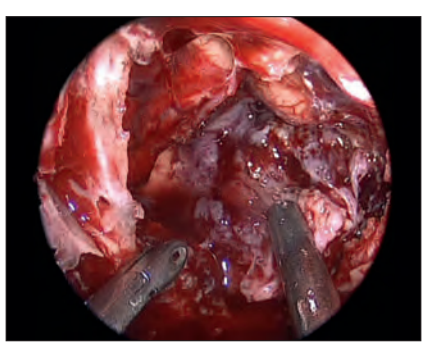

Fig. 117 Extracapsular dissection.

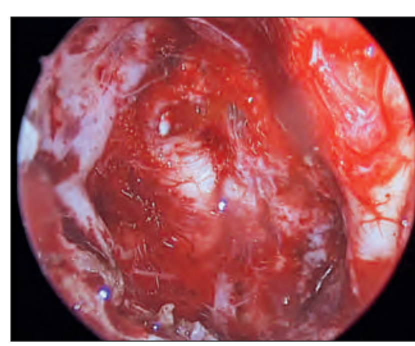

Fig. 118 Operative field after complete tumor removal.

7.5. Approach to the Clivus

Access to the clivus takes a lower trajectory compared with the one used to reach the sellar and suprasellar region. After the preliminary steps common to the extended procedures, the nasal mucosa is detached from the vomer, along the inferior wall of the sphenoid sinus, and bilaterally up to identify the vidian nerves, that represent the lateral boundaries of the surgical corridor. Hence, staying medial to the vidian nerve, damage to the intrapetrous carotid artery can be avoided. The vomer and floor of the sphenoid sinus are completely removed, obtaining access to the junction between the sphenoidal and the rhinopharyngeal parts of the clivus. Depending on the extent of the lesion, the bone of the clivus is more or less extensively removed. The clivus contains the basilar plexus, which is the most extensive series of intercavernous venous connections across the midline, joined by the superior and inferior petrosal sinuses. The abducens nerve enters the cavernous sinus passing through the basilar sinus close to the paraclival tract of the intracavernous carotid artery. Therefore, particular attention must be paid during bone removal in this area. The most frequent lesions arising from this area are usually located extradurally, i.e. chordomas, which is why the dura is opened only upon its infiltration. Nevertheless, even intradural lesions such as clival and/or petroclival tumors may also be removed using this approach (Figs. 119–121).

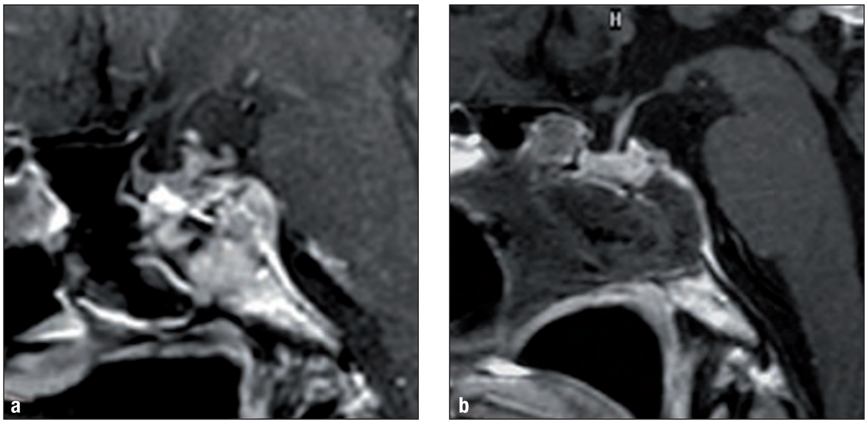

Fig. 119 Preoperative (**a**) and postoperative (**b**) MRI scans showing a case of clivus chordoma.

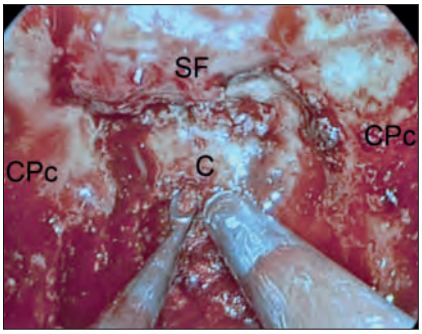

Fig. 120 Clival bone removal. Sellar floor (**SF**); clivus (**C**); paraclival segment of the internal carotid artery (**CPc**); parasellar segment of the internal carotid artery (**CPs**).

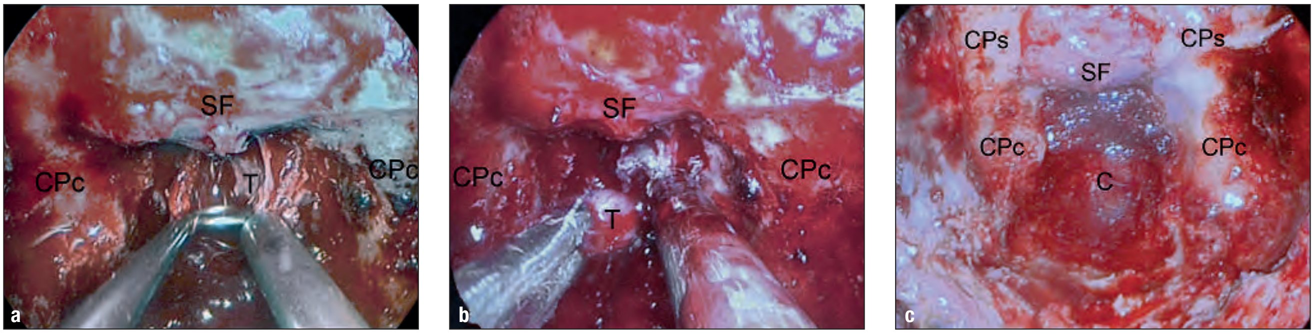

Fig. 121 Tumor dissection (**a**). Piecemeal tumor removal (**b**). Close-up view of the tumor bed (**c**). Sellar floor (**SF**); tumor (**T**); paraclival segment of the internal carotid artery (**CPc**); parasellar segment of the internal carotid artery (**CPs**).

7.6. Approach to the Cavernous Sinus

Multiple endoscopic endonasal surgical corridors have been described to get into the cavernous sinus. The corridors can give access to the medial and lateral cavernous sinus compartments, with respect to the position of the intracavernous ICA. One of the approaches allows the cavernous sinus compartment to be entered medially to the ICA, and a second provides exposure of the lateral compartment. As a general rule, the surgical corridor to the medial compartment can be created more easily through the contralateral nostril, whereas the corridor to access the lateral compartment can be established through the ipsilateral nostril via a transethmoidal route. In order to facilitate and improve exposure of the lateral compartment, the anterior sphenoidotomy must be extended more laterally on the same side of tumor invasion. The superior and supreme turbinates together with the posterior ethmoidal cells must be removed and the medial pterygoid process has to be drilled out to identify the vidian canal, medially, and the foramen rotundum, laterally. In this way, a quadrangular area is created, bounded superiorly by V2, inferiorly by the vidian nerve, and posteriorly by the intrapetrous and paraclival segment of the internal carotid artery. Through such a corridor, the tumor portion extending lateral to the carotid as well as toward the middle cranial fossa can be managed.

7.7. Reconstruction of the Skull Base in Extended Approaches

During an extended transsphenoidal approach, especially to the suprasellar area, a large osteodural opening has to be created, and the cisternal space is often widely dissected. A conspicuous intraoperative CSF leak should therefore be anticipated. An effective watertight closure, however, is mandatory to prevent postoperative CSF leaks.

In our department, we use the “sandwich technique”: in the first instance, the cistern is covered with a layer of collagen sponge coated with fibrinogen and thrombin, and the surgical cavity is filled with fat graft sutured to the inner layer of three layers of fascia lata or dural substitute. The first layer is then positioned intradurally, the second between the dura and the bone, and the third is applied to cover the bone. In order to support the materials used for reconstruction at the level of the skull base defect, a vascular flap of septal mucosa is created by cutting the septal mucosa along the inferior edge of the septum, from the choana to the cartilage portion of the septum, and superiorly to the level of the rostral portion of the middle turbinate. Following mucosal dissection from the septal bone, the flap is pedicled laterally around the sphenopalatine foramen and positioned in the choana during the operation. At the end of the procedure, the flap is used to cover the posterior wall of the sphenoid sinus. An inflated Foley balloon catheter, filled with 7 to 8 ml of saline solution, is then placed in the sphenoid sinus to support the reconstruction (Figs. 122–125).

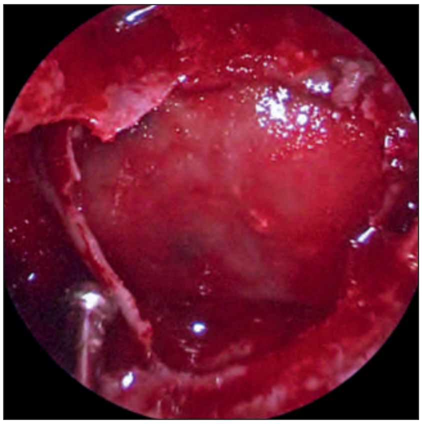

Fig. 122 Reconstruction technique. Dural substitute is placed intradurally.

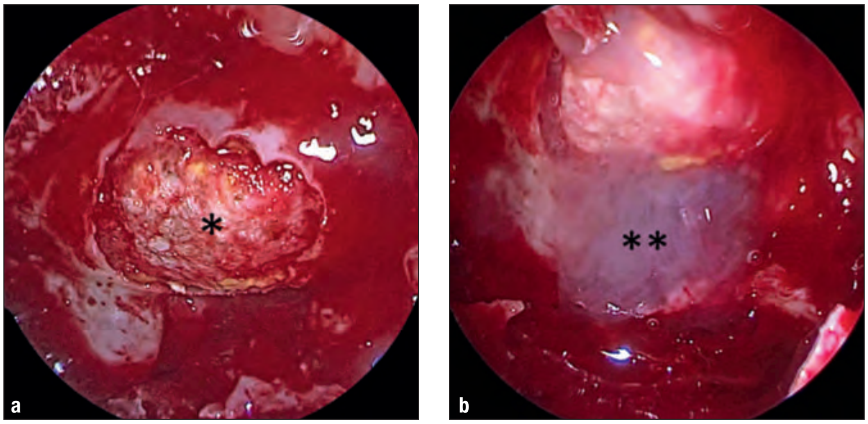

Fig. 123 The dural substitute is encased in the extradural space and covered by fibrin glue (**a, b**). Tachosil® (*); fibrin glue (**).

It must be kept in mind, however, that an effective and watertight reconstruction requires the following goals to be met, ranked in order of relevance:

1. intradural sealing of the arachnoid;
2. watertight closure of the osteodural skull base defect;
3. packing of the sphenoid.

Finally, as adjunct postoperative measures, we also advise our patients to have:

- Bed rest for 3–5 days, depending also on the grade of pneumoencephalus. This can be relevant, particularly in case of third ventricle craniopharyngiomas

Medical therapy with:

- acetazolamide;
- stool softeners;
- broad-spectrum antibiotics.

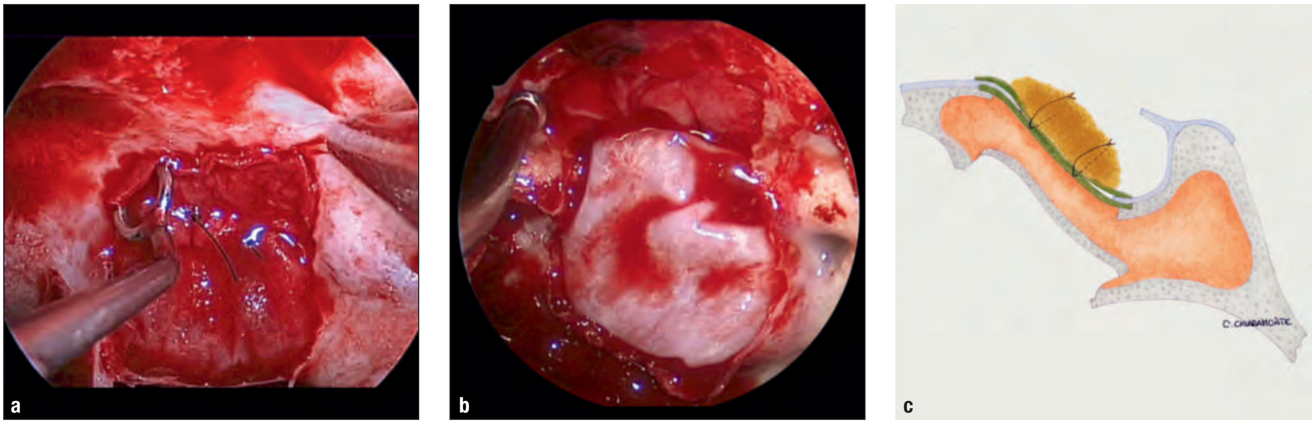

Fig. 124 Reconstruction technique. Multilayer technique (**a, b**). Schematic drawing of the multilayer reconstruction (**c**).

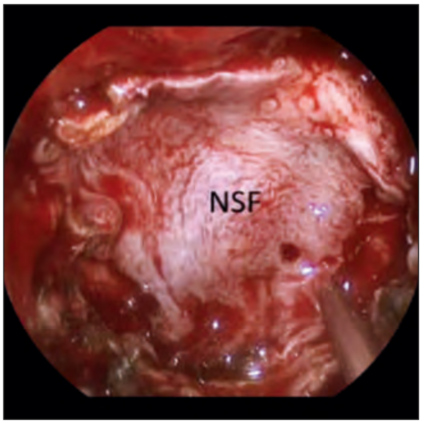

Fig. 125 The naso-septal flap is used to cover the skull base defect. Naso-septal flap (**NSF**).

References

1. AFIERI A, JHO HD. Endoscopic endonasal approaches to he cavernous sinus: surgical approaches. Neurosurgery. 2001;49(2):354–360; discussion 360–352.
2. ALFIERI A, JHO HD. Endoscopic endonasal cavernous sinus surgery: an anatomic study. Neurosurgery. 2001;48(4):827–836; discussion 836–827.
3. ALFIERI A, JHO HD, SCHETTINO R, TSCHABITSCHER M. Endoscopic endonasal approach to the pterygopalatine fossa: anatomic study. Neurosurgery. 2003;52(2):374–378; discussion 378–380.
4. ALFIERI A, JHO HD, TSCHABITSCHER M. Endoscopic endonasal approach to the ventral cranio-cervical junction: anatomical study. Acta Neurochir (Wien). 2002;144(3):219–225; discussion 225.
5. ANAND VK, SCHWARTZ TH. Practical endoscopic skull base surgery. San Diego, Oxford, Brisbane: Plural Publishing Inc.; 2007.
6. CAPPABIANCA P, ALFIERI A, DE DIVITIIS E. Endoscopic endonasal transsphenoidal approach to the sella: towards functional endoscopic pituitary surgery (FEPS). Minim Invasive Neurosurg. 1998;41(2):66–73.
7. CAPPABIANCA P, ALFIERI A, THERMES S, BUONAMASSA S, DE DIVITIIS E. Instruments for endoscopic endonasal transsphenoidal surgery. Neurosurgery. 1999;45(2):392–395; discussion 395–396.
8. CAPPABIANCA P, CAVALLO LM, COLAO A, DE DIVITIIS E. Surgical complications associated with the endoscopic endonasal transsphenoidal approach for pituitary adenomas. J Neurosurg. 2002;97(2):293–298.
9. CAPPABIANCA P, CAVALLO LM, DE DIVITIIS E. Endoscopic endonasal transsphenoidal surgery. Neurosurgery. 2004;55(4):933–940; discussion 940–931.
10. CAPPABIANCA P, CAVALLO LM, ESPOSITO F, DE DIVITIIS O, MESSINA A. Extended endoscopic endonasal approach to the midline skull base: the evolving role of transsphenoidal surgery. In: Pickard JD, Akalan N, Di Rocco C, et al., editors. Advances and Technical Standards in Neurosurgery. Wien – New York: Springer Verlag; 2008. p. 152–199.
11. CAPPABIANCA P, CAVALLO LM, ESPOSITO F, DE DIVITIIS O, MESSINA A, DE DIVITIIS E. Extended endoscopic endonasal approach to the midline skull base: the evolving role of transsphenoidal surgery. Adv Tech Stand Neurosurg. 2008;33: 151–199.
12. CAPPABIANCA P, CAVALLO LM, ESPOSITO F, VALENTE V, DE DIVITIIS E. Sellar repair in endoscopic endonasal transsphenoidal surgery: results of 170 cases. Neurosurgery. 2002;51(6):1365–1371; discussion 1371–1362.
13. CAPPABIANCA P, CAVALLO LM, SOLARI D, DE DIVITIIS O, CHIARAMONTE C, ESPOSITO F. Size does not matter. The intrigue of giant adenomas: a true surgical challenge. Acta Neurochir (Wien). 2014;156(12):2217–2220.
14. CAPPABIANCA P, DE DIVITIIS E. Endoscopy and transsphenoidal surgery. Neurosurgery. 2004;54(5):1043–1048; discussions 1048–1050.
15. CARRAU RL, JHO HD, KO Y. Transnasal-transsphenoidal endoscopic surgery of the pituitary gland. Laryngoscope. 1996;106(7):914–918.
16. CASTELNUOVO P, BATTAGLIA P, TURRI-ZANONI M, TOMEI G, LOCATELLI D, BIGNAMI M, VILLARET AB, NICOLAI P. Endoscopic endonasal surgery for malignancies of the anterior cranial base. World Neurosurg. 2014;82(6 Suppl):S22–31.
17. CASTELNUOVO P, DALLAN I, TSCHABITSCHER M. Surgical Anatomy of the Internal Carotid Artery – An Atlas for Skull Base Surgeons. Berlin Heidelberg: Springer-Verlag; 2013. XV, 162 p.
18. CASTELNUOVO P, LOCATELLI D, MAURI S. Extended endoscopic approaches to the skull base. Anterior cranial base CSF leaks. In: De Divitiis E, Cappabianca P, editors. Endoscopic endonasal trans-sphenoidal surgery. Wien – New York: Springer; 2003. p.137–158.
19. CASTELNUOVO P, PISTOCHINI A, LOCATELLI D. Different surgical approaches to the sellar region: focusing on the "two nostrils four hands technique". Rhinology. 2006;44(1):2–7.
20. CAVALLO LM, CAPPABIANCA P, GALZIO R, IACONETTA G, DE DIVITIIS E, TSCHABITSCHER M. Endoscopic transnasal approach to the cavernous sinus versus transcranial route: anatomic study. Neurosurgery. 2005;56(2 Suppl):379–389; discussion 379–389.
21. CAVALLO LM, DAL FABBRO M, JALALOD'DIN H, MESSINA A, ESPOSITO I, ESPOSITO F, DE DIVITIIS E, CAPPABIANCA P. Endoscopic endonasal transsphenoidal surgery. Before scrubbing in: tips and tricks. Surg Neurol. 2007;67(4):342–347.
22. CAVALLO LM, DE DIVITIIS O, AYDIN S, MESSINA A, ESPOSITO F, IACONETTA G, TALAT K, CAPPABIANCA P, TSCHABITSCHER M. Extended endoscopic endonasal transsphenoidal approach to the suprasellar area: anatomic considerations – part 1. Neurosurgery. 2007;61(3 Suppl):24–33; discussion 33–24.
23. CAVALLO LM, FRANK G, CAPPABIANCA P, SOLARI D, MAZZATENTA D, VILLA A, ZOLI M, D'ENZA AI, ESPOSITO F, PASQUINI E. The endoscopic endonasal approach for the management of craniopharyngiomas: a series of 103 patients. J Neurosurg. 2014;121(1):100–113.
24. CAVALLO LM, MESSINA A, CAPPABIANCA P, ESPOSITO F, DE DIVITIIS E, GARDNER P, TSCHABITSCHER M. Endoscopic endonasal surgery of the midline skull base: anatomical study and clinical considerations. Neurosurg Focus. 2005;19(1):E2.
25. CAVALLO LM, MESSINA A, ESPOSITO F, DE DIVITIIS O, DAL FABBRO M, DE DIVITIIS E, CAPPABIANCA P. Skull base reconstruction in the extended endoscopic transsphenoidal approach for suprasellar lesions. J Neurosurg. 2007;107(4): 713–720.
26. CAVALLO LM, MESSINA A, GARDNER P, ESPOSITO F, KASSAM AB, CAPPABIANCA P, DE DIVITIIS E, TSCHABITSCHER M. Extended endoscopic endonasal approach to the pterygopalatine fossa: anatomical study and clinical considerations. Neurosurg Focus. 2005;19(1):E5.
27. CAVALLO LM, PREVEDELLO DM, SOLARI D, GARDNER PA, ESPOSITO F, SNYDERMAN CH, CARRAU RL, KASSAM AB, CAPPABIANCA P. Extended endoscopic endonasal transsphenoidal approach for residual or recurrent craniopharyngiomas. J Neurosurg. 2009;111(3):578–589.
28. CAVALLO LM, SOLARI D, ESPOSITO F, CAPPABIANCA P. The endoscopic endonasal approach for the management of craniopharyngiomas involving the third ventricle. Neurosurg Rev. 2013;36(1):27–37; discussion 38.
29. CEBULA H, KURBANOV A, ZIMMER LA, POCZOS P, LEACH JL, DE BATTISTA JC, FROELICH S, THEODOSOPOULOS PV, KELLER JT. Endoscopic, endonasal variability in the anatomy of the internal carotid artery. World Neurosurg. 2014;82(6):e759–764.
30. CEYLAN S, KOC K, ANIK I. Extended endoscopic approaches for midline skull-base lesions. Neurosurg Rev. 2009;32(3):309–319; discussion 318–309.
31. CHIBBARO S, CORNELIUS JF, FROELICH S, TIGAN L, KEHRLI P, DEBRY C, ROMANO A, HERMAN P, GEORGE B, BRESSON D. Endoscopic endonasal approach in the management of skull base chordomas – clinical experience on a large series, technique, outcome, and pitfalls. Neurosurg Rev. 2014;37(2):217–224; discussion 224–215.

32. DE DIVITIIS E, CAPPABIANCA P. Endoscopic Endonasal Transsphenoidal Surgery. In: Pickard JD, Dolenc VV, Antunes JL, et al., editors. Advances and Technical Standards in Neurosurgery. 27. Springer Vienna; 2002. p. 137–177.

33. DE DIVITIIS E, CAPPABIANCA P, CAVALLO LM. Endoscopic transsphenoidal approach: adaptability of the procedure to different sellar lesions. Neurosurgery. 2002;51(3):699–705; discussion 705–697.

34. DE DIVITIIS E, CAPPABIANCA P, CAVALLO LM, ESPOSITO F, DE DIVITIIS O, MESSINA A. Extended endoscopic transsphenoidal approach for extrasellar craniopharyngiomas. Neurosurgery. 2007;61(5 Suppl 2):219–227; discussion 228.

35. DE DIVITIIS E, CAVALLO LM, CAPPABIANCA P, ESPOSITO F. Extended endoscopic endonasal transsphenoidal approach for the removal of suprasellar tumors: Part 2. Neurosurgery. 2007;60(1):46–58; discussion 58–49.

36. DE DIVITIIS E, ESPOSITO F, CAPPABIANCA P, CAVALLO LM, DE DIVITIIS O. Tuberculum sellae meningiomas: high route or low route? A series of 51 consecutive cases. Neurosurgery. 2008;62(3):556–563; discussion 556–563.

37. DE NOTARIS M, CAVALLO LM, PRATS-GALINO A, ESPOSITO I, BENET A, POBLETE J, VALENTE V, GONZALEZ JB, FERRER E, CAPPABIANCA P. Endoscopic endonasal transclival approach and retrosigmoid approach to the clival and petroclival regions. Neurosurgery. 2009;65(6 Suppl):42–50; discussion 50–42.

38. DE NOTARIS M, PALMA K, SERRA L, ENSENAT J, ALOBID I, POBLETE J, GONZALEZ JB, SOLARI D, FERRER E, PRATS-GALINO A. A three-dimensional computer-based perspective of the skull base. World Neurosurg. 2014;82(6 Suppl):S41–48.

39. DE NOTARIS M, PRATS-GALINO A. Surgical freedom: a challenging topic in endoscopic endonasal approaches. World Neurosurg. 2014;82(1–2):e387–388.

40. DE NOTARIS M, PRATS-GALINO A, ENSENAT J, TOPCZEWSKI T, FERRER E, CAVALLO LM, CAPPABIANCA P, SOLARI D. Quantitative analysis of progressive removal of nasal structures during endoscopic suprasellar approach. Laryngoscope. 2014;124(10):2231–2237.

41. DE NOTARIS M, SOLARI D, CAVALLO LM, D'ENZA AI, ENSENAT J, BERENGUER J, FERRER E, PRATS-GALINO A, CAPPABIANCA P. The "suprasellar notch," or the tuberculum sellae as seen from below: definition, features, and clinical implications from an endoscopic endonasal perspective. J Neurosurg. 2012;116(3):622–629.

42. DE PAIVA NETO MA, VANDERGRIFT A, FATEMI N, GORGULHO AA, DESALLES AA, COHAN P, WANG C, SWERDLOFF R, KELLY DF. Endonasal transsphenoidal surgery and multimodality treatment for giant pituitary adenomas. Clin Endocrinol (Oxf). 2010;72(4): 512–519.

43. DEHDASHTI AR, GANNA A, WITTERICK I, GENTILI F. Expanded endoscopic endonasal approach for anterior cranial base and suprasellar lesions: indications and limitations. Neurosurgery. 2009;64(4):677–687; discussion 687–679.

44. DI MAIO S, CAVALLO LM, ESPOSITO F, STAGNO V, CORRIERO OV, CAPPABIANCA P. Extended endoscopic endonasal approach for selected pituitary adenomas: early experience. J Neurosurg. 2011;114(2):345–353.

45. DUSICK JR, ESPOSITO F, MALKASIAN D, KELLY DF. Avoidance of carotid artery injuries in transsphenoidal surgery with the Doppler probe and micro-hook blades. Neurosurgery. 2007;60 (4 Suppl 2):322–328; discussion 328–329.

46. ESPOSITO F, DUSICK JR, FATEMI N, KELLY DF. Graded repair of cranial base defects and cerebrospinal fluid leaks in transsphenoidal surgery. Neurosurgery. 2007;60(4 Suppl 2): 295–303; discussion 303–294.

47. FORTES FS, SENNES LU, CARRAU RL, BRITO R, RIBAS GC, YASUDA A, RODRIGUES AJ, JR., SNYDERMAN CH, KASSAM AB. Endoscopic anatomy of the pterygopalatine fossa and the transpterygoid approach: development of a surgical instruction model. Laryngoscope. 2008;118(1):44–49.

48. FRANK G, PASQUINI E. Approach to the cavernous sinus. In: de Divitiis E, Cappabianca P, editors. Endoscopic Endonasal Transsphenoidal Surgery. Springer Vienna; 2003. p. 159–175.

49. FRANK G, PASQUINI E, DOGLIETTO F, MAZZATENTA D, SCIARRETTA V, FARNETI G, CALBUCCI F. The endoscopic extended transsphenoidal approach for craniopharyngiomas. Neurosurgery. 2006;59(1 Suppl 1):ONS75–83; discussion ONS75–83.

50. GUIOT J, ROUGERIE J, FOURESTIER M, FOURNIER A, COMOY C, VULMIERE J, GROUX R. [Intracranial endoscopic explorations]. Presse Med. 1963;71:1225–1228.

51. HADAD G, BASSAGASTEGUY L, CARRAU RL, MATAZA JC, KASSAM A, SNYDERMAN CH, MINTZ A. A novel reconstructive technique after endoscopic expanded endonasal approaches: vascular pedicle nasoseptal flap. Laryngoscope. 2006;116(10):1882–1886.

52. JHO HD, CARRAU RI, KO Y. Endoscopic Pituitary Surgery. In: Jho HD, Carrau RI, Ko Y, editors. Neurosurgical Operative Atlas. Park Ridge, IL: American Association of Neurological Surgeons; 1996. p. 1–12.

53. JHO HD, HA HG. Endoscopic endonasal skull base surgery: Part 1 – The midline anterior fossa skull base. Minim Invasive Neurosurg. 2004;47(1):1–8.

54. JHO HD, HA HG. Endoscopic endonasal skull base surgery: Part 2 – The cavernous sinus. Minim Invasive Neurosurg. 2004;47(1):9–15.

55. JHO HD, HA HG. Endoscopic endonasal skull base surgery: Part 3 – The clivus and posterior fossa. Minim Invasive Neurosurg. 2004;47(1):16–23.

56. JOUANNEAU E, SIMON E, JACQUESSON T, SINDOU M, TRINGALI S, MESSERER M, BERHOUMA M. The endoscopic endonasal approach to the Meckel's cave tumors: surgical technique and indications. World N eurosurg. 2014;82(6 Suppl):S155–161.

57. JURASCHKA K, KHAN OH, GODOY BL, MONSALVES E, KILIAN A, KRISCHEK B, GHARE A, VESCAN A, GENTILI F, ZADEH G. Endoscopic endonasal transsphenoidal approach to large and giant pituitary adenomas: institutional experience and predictors of extent of resection. J Neurosurg. 2014;121(1):75–83.

58. KAPTAIN GJ, VINCENT DA, SHEEHAN JP, LAWS ER, JR. Transsphenoidal approaches for the extracapsular resection of midline suprasellar and anterior cranial base lesions. Neurosurgery. 2001;49(1):94–100; discussion 100–101.

59. KASSAM A, CARRAU RL, SNYDERMAN CH, GARDNER P, MINTZ A. Evolution of reconstructive techniques following endoscopic expanded endonasal approaches. Neurosurg Focus. 2005;19(1):E8.

60. KASSAM A, SNYDERMAN CH, MINTZ A, GARDNER P, CARRAU RL. Expanded endonasal approach: the rostrocaudal axis. Part I. Crista galli to the sella turcica. Neurosurg Focus. 2005;19(1):E3.

61. KASSAM A, SNYDERMAN CH, MINTZ A, GARDNER P, CARRAU RL. Expanded endonasal approach: the rostrocaudal axis. Part II. Posterior clinoids to the foramen magnum. Neurosurg Focus. 2005;19(1):E4.

62. KASSAM AB, GARDNER P, SNYDERMAN C, MINTZ A, CARRAU R. Expanded endonasal approach: fully endoscopic, completely transnasal approach to the middle third of the clivus, petrous bone, middle cranial fossa, and infratemporal fossa. Neurosurg Focus. 2005;19(1):E6.

63. KASSAM AB, GARDNER PA, SNYDERMAN CH, CARRAU RL, MINTZ AH, PREVEDELLO DM. Expanded endonasal approach, a fully endoscopic transnasal approach for the resection of midline suprasellar craniopharyngiomas: a new classification based on the infundibulum. J Neurosurg. 2008;108(4):715–728.

64. KASSAM AB, PREVEDELLO DM, CARRAU RL, SNYDERMAN CH, GARDNER P, OSAWA S, SEKER A, RHOTON AL, JR. The front door to meckel's cave: an anteromedial corridor via expanded endoscopic endonasal approach – technical considerations and clinical series. Neurosurgery. 2009;64(3 Suppl):ons71–82; discussion ons82–73

65. KASSAM AB, PREVEDELLO DM, CARRAU RL, SNYDERMAN CH, THOMAS A, GARDNER P, ZANATION A, DUZ B, STEFKO ST, BYERS K, HOROWITZ MB. Endoscopic endonasal skull base surgery: analysis of complications in the authors' initial 800 patients. J Neurosurg. 2011;114(6):1544–1568.

66. KASSAM AB, PREVEDELLO DM, THOMAS A, GARDNER P, MINTZ A, SNYDERMAN C, CARRAU R. Endoscopic endonasal pituitary transposition for a transdorsum sellae approach to the interpeduncular cistern. Neurosurgery. 2008;62(3 Suppl 1):57–72; discussion 72–54.

67. KASSAM AB, SNYDERMAN C, GARDNER P, CARRAU R, SPIRO R. The expanded endonasal approach: a fully endoscopic transnasal approach and resection of the odontoid process: technical case report. Neurosurgery. 2005;57(1 Suppl):E213; discussion E213.

68. KASSAM AB, THOMAS A, CARRAU RL, SNYDERMAN CH, VESCAN A, PREVEDELLO D, MINTZ A, GARDNER P. Endoscopic reconstruction of the cranial base using a pedicled nasoseptal flap. Neurosurgery. 2008;63(1 Suppl 1):ONS44–52; discussion ONS52–43.

69. KASSAM AB, VESCAN AD, CARRAU RL, PREVEDELLO DM, GARDNER P, MINTZ AH, SNYDERMAN CH, RHOTON AL. Expanded endonasal approach: vidian canal as a landmark to the petrous internal carotid artery. J Neurosurg. 2008;108(1):177–183.

70. KOMOTAR RJ, STARKE RM, RAPER DM, ANAND VK, SCHWARTZ TH. Endoscopic endonasal compared with microscopic transsphenoidal and open transcranial resection of craniopharyngiomas. World Neurosurg. 2012;77(2):329–341.

71. KOUTOUROUSIOU M, FERNANDEZ-MIRANDA JC, STEFKO ST, WANG EW, SNYDERMAN CH, GARDNER PA. Endoscopic endonasal surgery for suprasellar meningiomas: experience with 75 patients. J Neurosurg. 2014;120(6):1326–1339.

72. KOUTOUROUSIOU M, FERNANDEZ-MIRANDA JC, WANG EW, SNYDERMAN CH, GARDNER PA. Endoscopic endonasal surgery for olfactory groove meningiomas: outcomes and limitations in 50 patients. Neurosurg Focus. 2014;37(4):E8.

73. KOUTOUROUSIOU M, GARDNER PA, FERNANDEZ-MIRANDA JC, PALUZZI A, WANG EW, SNYDERMAN CH. Endoscopic endonasal surgery for giant pituitary adenomas: advantages and limitations. J Neurosurg. 2013;118(3):621–631.

74. LAUFER I, ANAND VK, SCHWARTZ TH. Endoscopic, endonasal extended transsphenoidal, transplanum transtuberculum approach for resection of suprasellar lesions. J Neurosurg. 2007;106(3):400–406.

75. LAWS ER, KANTER AS, JANE JA, JR., DUMONT AS. Extended transsphenoidal approach. J Neurosurg. 2005;102(5):825–827; discussion 827–828.

76. LOCATELLI M, BERTANI G, CARRABBA G, RAMPINI P, ZAVANONE M, CAROLI M, SALA E, FERRANTE E, GAINI SM, SPADA A, MANTOVANI G, LANIA A. The trans-sphenoidal resection of pituitary adenomas in elderly patients and surgical risk. Pituitary. 2013;16(2):146–151.

77. LOCATELLI D, RAMPA F, ACCHIARDI I, BIGNAMI M, DE BERNARDI F, CASTELNUOVO P. Endoscopic endonasal approaches for repair of cerebrospinal fluid leaks: nine-year experience. Neurosurgery. 2006;58(4 Suppl 2):ONS-246–256; discussion ONS-256–247.

78. MAGRO F, SOLARI D, CAVALLO LM, SAMII A, CAPPABIANCA P, PATERNO V, LUDEMANN WO, DE DIVITIIS E, SAMII M. The endoscopic endonasal approach to the lateral recess of the sphenoid sinus via the pterygopalatine fossa: comparison of endoscopic and radiological landmarks. Neurosurgery. 2006;59 (4 Suppl 2):ONS237–242; discussion ONS242–233.

79. MESSINA A, BRUNO MC, DECQ P, COSTE A, CAVALLO LM, DE DIVITTIS E, CAPPABIANCA P, TSCHABITSCHER M. Pure endoscopic endonasal odontoidectomy: anatomical study. Neurosurg Rev. 2007;30(3):189–194; discussion 194.

80. PREVEDELLO DM, DITZEL FILHO LF, SOLARI D, CARRAU RL, KASSAM AB. Expanded endonasal approaches to middle cranial fossa and posterior fossa tumors. Neurosurg Clin N Am. 2010;21(4):621–635, vi.

81. PREVEDELLO DM, EBNER FH, DE LARA D, DITZEL FILHO L, OTTO BA, CARRAU RL. Extracapsular dissection technique with the cotton swab for pituitary adenomas through an endoscopic endonasal approach – how I do it. Acta Neurochir (Wien). 2013;155(9): 1629–1632.

82. PREVEDELLO DM, KASSAM AB, SNYDERMAN C, CARRAU RL, MINTZ AH, THOMAS A, GARDNER P, HOROWITZ M. Endoscopic cranial base surgery: ready for prime time? Clin Neurosurg. 2007;54:48–57.

83. SNYDERMAN C, KASSAM A, CARRAU R, MINTZ A, GARDNER P, PREVEDELLO DM. Acquisition of surgical skills for endonasal skull base surgery: a training program. Laryngoscope. 2007;117(4): 699–705.

84. SOLARI D, MAGRO F, CAPPABIANCA P, CAVALLO LM, SAMII A, ESPOSITO F, PATERNO V, DE DIVITIIS E, SAMII M. Anatomical study of the pterygopalatine fossa using an endoscopic endonasal approach: spatial relations and distances between surgical landmarks. J Neurosurg. 2007;106(1):157–163.

85. TSCHABITSCHER M, GALZIO RJ. Endoscopic Anatomy Along the Transnasal Approach to the Pituitary Gland and the Surrounding Structures. In: de Divitiis E, Cappabianca P, editors. Endoscopic Endonasal Transsphenoidal Surgery. Springer Vienna; 2003. p. 21–39.

86. ZADA G, AGARWALLA PK, MUKUNDAN S, JR., DUNN I, GOLBY AJ, LAWS ER, JR. The neurosurgical anatomy of the sphenoid sinus and sellar floor in endoscopic transsphenoidal surgery. J Neurosurg. 2011;114(5):1319–1330.

87. ZADA G, WOODMANSEE WW, RAMKISSOON S, AMADIO J, NOSE V, LAWS ER, JR. Atypical pituitary adenomas: incidence, clinical characteristics, and implications. J Neurosurg. 2011;114(2): 336–344.

88. ZHAO B, WEI YK, LI GL, LI YN, YAO Y, KANG J, MA WB, YANG Y, WANG RZ. Extended transsphenoidal approach for pituitary adenomas invading the anterior cranial base, cavernous sinus, and clivus: a single-center experience with 126 consecutive cases. J Neurosurg. 2010;112(1):108–117.

Recommended Set for Endoscopic Pituitary and Skull Base Surgery

Endoscopic Pituitary and Skull Base Surgery

Recommended Sets acc. to CAPPABIANCA-de DIVITIIS

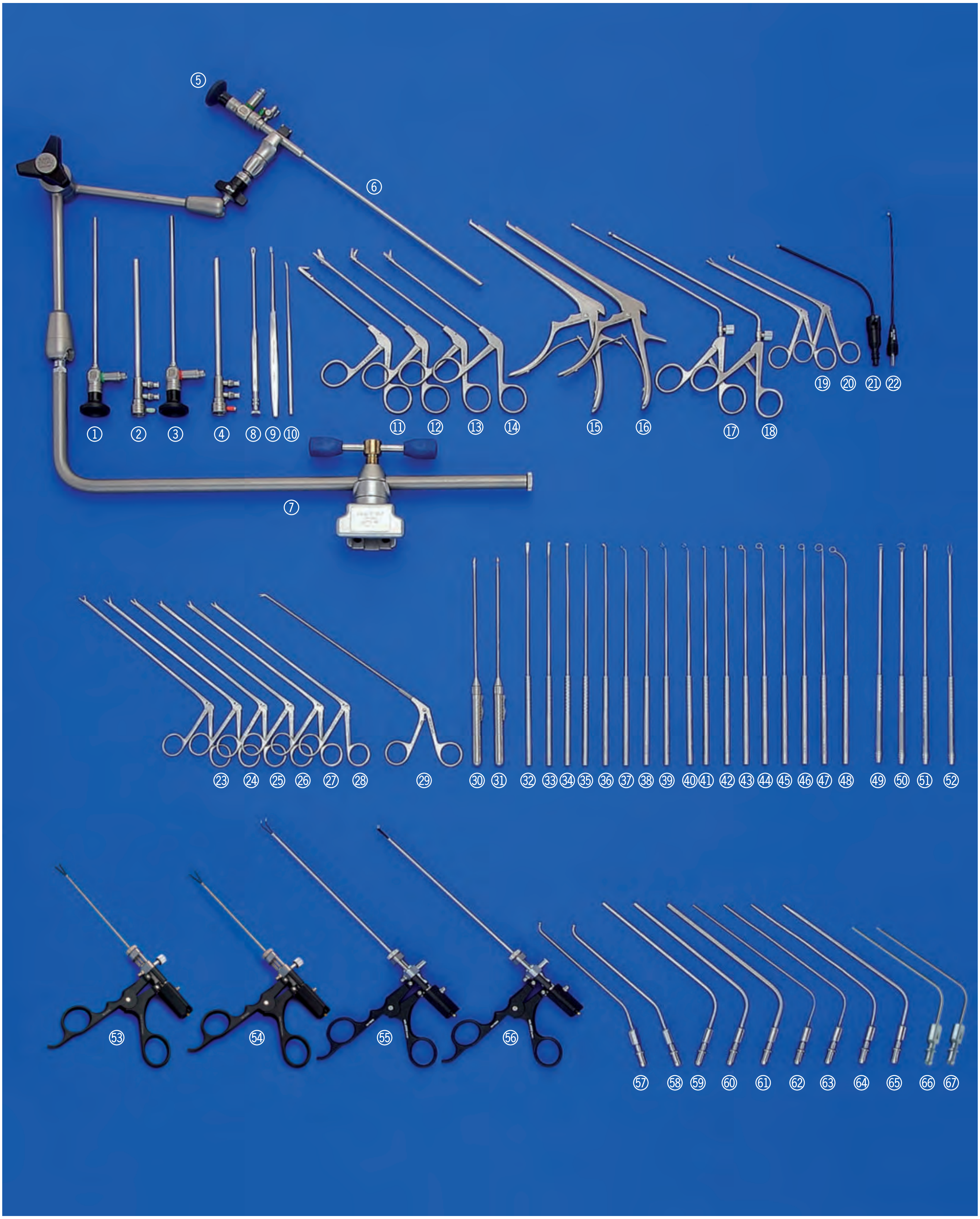

Endoscopic Pituitary and Skull Base Surgery

Recommended Sets acc. to CAPPABIANCA-de DIVITIIS

Endoscopic Visualization

①	28132 AA	**HOPKINS® Straight Forward Telescope 0°,** enlarged view, diameter 4 mm, length 18 cm, **autoclavable**
②	7230 AS	**Irrigation Sheath,** outer diameter 5 mm, working length 14 cm, for use with HOPKINS® Telescope 28132 AA and KARL STORZ lens irrigation system CLEARVISION® II
③	28132 BA	**HOPKINS® Forward-Oblique Telescope 30°,** enlarged view, diameter 4 mm, length 18 cm, **autoclavable**
④	7230 BS	**Irrigation Sheath,** outer diameter 5 mm, working length 14 cm, for use with HOPKINS® Telescope 28132 BA and KARL STORZ lens irrigation system CLEARVISION® II
⑤	28164 AA	**HOPKINS® Straight Forward Telescope 0°,** enlarged view, diameter 4 mm, length 30 cm, **autoclavable**
⑥	28164 ASA	**Irrigation Sheath,** outer diameter 5.0 mm, working length 16 cm, for use with HOPKINS® Telescopes 28164 AA
⑦	28272 RKB	**Holding System, autoclavable**

optional

	28132 FA	**HOPKINS® Forward-Oblique Telescope 45°,** enlarged view, diameter 4 mm, length 18 cm, **autoclavable** (not illustrated)
	7230 FS	**Irrigation Sheath,** outer diameter 5 mm, working length 14 cm, for use with HOPKINS® Telescope 28132 FA/FVA and KARL STORZ lens irrigation system CLEARVISION® II (not illustrated)
	7229 AA	**HOPKINS® Straight Forward Telescope 0°,** enlarged view, diameter 2.7 mm, length 18 cm, **autoclavable** (not illustrated)
	28164 CAA	**Irrigation Sheath,** outer diameter 3.8 mm, working length 15 cm, for use with HOPKINS® Telescopes 7229 AA (not illustrated)

Nasal and Sphenoid Stage

⑧	474001	FREER **Suction Elevator,** with stylet, length 21 cm
⑨	628702	**Antrum Curette,** oblong small size, length 19 cm
⑩	660500	**Sickle Knife,** length 18 cm
⑪	459010	STAMMBERGER **RHINOFORCE® II Antrum Punch,** upside backward cutting, length 10 cm
⑫	449211	**RHINOFORCE® II Nasal Scissors,** working length 13 cm, straight
⑬	452501 B	MACKAY-GRÜNWALD **RHINOFORCE® II Nasal Forceps,** through-cutting, tissue sparing, delicate, upturned 45°, size 1.8 x 3 mm, working length 13 cm
⑭	452001 B	MACKAY-GRÜNWALD **RHINOFORCE® II Nasal Forceps,** through-cutting, tissue sparing, delicate, straight, size 1.8 x 3 mm, working length 13 cm
⑮	28164 MKB	KERRISON **Punch,** upbiting 40° forward, size 2 mm, working length 17 cm
⑯	28164 MKC	KERRISON **Punch,** upbiting 40° forward, size 3 mm, working length 17 cm
⑰	651050	STAMMBERGER **Punch,** circular cutting for sphenoid, ethmoid and choanal atresia, working length 18 cm, diameter 4.5 mm
⑱	651055	STAMMBERGER **Punch**, circular cutting, for sphenoid, ethmoid and choanal atresia
⑲	634824	STRÜMPEL **Forceps,** with oval, fenestrated cupped jaws, working length 12.5 cm
⑳	634825 A	STRÜMPEL **Forceps,** with oval, fenestrated, cupped jaws, 45° upturned, working length 12.5 cm
㉑	839310 N	**Unipolar Suction-Coagulation Tube,** insulated, with connector pin for unipolar coagulation, diameter 3 mm, working length 10 cm
	28164 ED	**Coagulation Ball Electrode,** diameter 2 mm, laterally curved, working length 13 cm (not illustrated)
㉒	28164 EF	**Coagulation Ball Electrode,** diameter 4 mm, laterally curved, working length 13 cm

Sellar Stage

㉓	663231	**Forceps,** with round spoon, diameter 2.5 mm, straight, working length 18 cm
㉔	663239	**Forceps,** with oval, fenestrated, cupped jaws, 2.5 mm wide, straight, working length 18 cm
㉕	663301	**Scissors,** straight, delicate, working length 18 cm
㉖	663304	**Scissors,** curved right, delicate, working length 18 cm
㉗	663305	**Scissors,** curved left, delicate, working length 18 cm
㉘	663307	**Scissors,** 45° upturned, delicate, working length 18 cm
㉙	28164 SAD	**Scissors,** curved up 45°, delicate, sheath 360° rotatable, working length 18 cm
㉚	28164 KK	de DIVITIIS-CAPPABIANCA **Scalpel,** with telescopic blade, including: **Handle** **Outer Tube** **Micro-Knife,** sickle-shaped
㉛	28164 M	de DIVITIIS-CAPPABIANCA **Scalpel**, with telescopic blade, including: **Handle** **Outer Tube** **Micro Knife,** pointed

It is recommended to check the suitability of the product for the intended procedure prior to use.

Endoscopic Pituitary and Skull Base Surgery

Recommended Sets acc. to CAPPABIANCA-de DIVITIIS

32	28164 DM	**Elevator,** sharp, slightly curved spatula, size 2 mm, with round handle, length 25 cm
33	28164 DS	**Elevator,** sharp, slightly curved spatula, size 3 mm, with round handle, length 25 cm
34	28164 DB	**Dissector,** sharp, round spatula, tip angled 45°, size 3 mm, with round handle, length 25 cm
35	28164 H	CASTELNUOVO **Hook,** 90°, blunt, length 25 cm, with round handle
36	28164 KB	**Curette,** round spoon, tip slightly angled, with round handle, length 25 cm
37	28164 RN	CAPPABIANCA-de DIVITIIS **Ring Curette,** round wire, inner diameter 3 mm, tip angled 45°, with round handle, length 25 cm
38	28164 RE	**Same,** malleable
39	28164 RO	CAPPABIANCA-de DIVITIIS **Ring Curette,** round wire, inner diameter 5 mm, tip angled 45°, with round handle, length 25 cm
40	28164 RJ	**Same,** malleable
41	28164 RI	De DIVITIIS-CAPPABIANCA **Ring Curette,** round wire, inner diameter 3 mm, tip angled 90°, with round handle, length 25 cm
42	28164 RG	**Same,** inner diameter 5 mm
43	28164 RB	de DIVITIIS-CAPPABIANCA **Ring Curette,** round wire, inner diameter 3 mm, distally curved shaft, with round handle, length 25 cm
44	28164 RA	**Same,** inner diameter 5 mm
45	28164 RV	CAPPABIANCA-de DIVITIIS **Ring-Curette,** round wire, inner diameter 3 mm, tip laterally angled 90°, with round handle, length 25 cm
46	28164 RD	**Same,** inner diameter 5 mm
47	28164 RW	**Same,** inner diameter 7 mm
48	28164 RF	CAPPABIANCA-de DIVITIIS **Ring Curette,** round wire, vertical, inner diameter 5mm, tip angled 45°, with round handle, length 25 cm
49	28164 RSB	de DIVITIIS-CAPPABIANCA **Suction-Curette,** with round wire, inner diameter 5 mm, tip angled 45°, LUER, length 25 cm
50	28164 RSC	**Same,** inner diameter 7 mm
51	28164 RT	CAPPABIANCA-de DIVITIIS **Suction Curette,** with basket, round, size 5 mm, rotatable tube, LUER, length 25 cm
52	28164 RU	**Same,** size 6.5 mm
53	28164 BDB	**TAKE-APART® Bipolar Forceps,** short, rounded tip, width 2 mm, outer diameter 3.4 mm, working length 14 cm, including: **Bipolar Ring Handle** **Outer Sheath** **Inner Sheath** **Forceps Insert**
54	28164 BDC	**TAKE-APART® Bipolar Forceps,** width 2 mm, outer diameter 3.4 mm, working length 14 cm, including: **Handle** **Outer Sheath** **Inner Sheath** **Bipolar Insert**
55	28164 BDL	**TAKE-APART® Bipolar Forceps,** width 1 mm, delicate jaws, distally angled 45°, vertical closing, outer diameter 3.4 mm, working length 20 cm, including: **Handle** **Outer Tube** **Inner Tube** **Bipolar Insert**
56	28164 BDM	**TAKE-APART® Bipolar Forceps**, width 1 mm, delicate jaws, distally angled 45°, horizontal closing, outer diameter 3.4 mm, working length 20 cm, including: **Handle** **Outer Tube** **Inner Tube** **Bipolar Insert**
	28164 MI	**Lesion Meter,** to determine the size of transnasal lesions, with wheel handle and scale, width 2 mm, working length 19 cm (not illustrated)
57	662882	FRANK-PASQUINI **Suction Tube,** angular, outer diameter 2.4 mm, tip curved upwards, ball end, with grip plate and cut-off hole, LUER, working length 13 cm
58	662885	FRANK-PASQUINI **Suction Tube**, angular, outer diameter 3 mm, tip curved upwards, ball end, with grip plate and cut-off hole, LUER, working length 13 cm
59	649183	FERGUSON **Suction Tube,** with cut-off hole and stylet, LUER, 10 Fr., working length 15 cm
60	649184	**Same,** 12 Fr.
61	649185	**Same,** 15 Fr.
62	649179 B	**Suction Tube**, malleable, with elongated cut-off hole and stylet, LUER, 4 Fr., working length 15 cm
63	649180 B	**Same,** 6 Fr.
64	649182 B	**Same,** 8 Fr.
65	649183 B	**Same,** 10 Fr.
66	28164 XA	**Suction Tube,** with cut-off hole, drop-shaped, with distance markings, LUER, conical distal end, 8 Fr., working length 15 cm
67	28164 XB	**Same,** 6 Fr.

HOPKINS® Telescopes – autoclavable
diameter 4 mm, length 18 cm

28132 AA/BA/FA

28132 AA **HOPKINS® Straight Forward Telescope 0°,**
enlarged view, diameter 4 mm, length 18 cm,
autoclavable,
fiber optic light transmission incorporated,
color code: green

28132 BA **HOPKINS® Forward-Oblique Telescope 30°,**
enlarged view, diameter 4 mm, length 18 cm,
autoclavable,
fiber optic light transmission incorporated,
color code: red

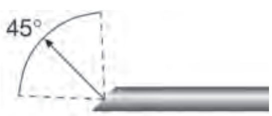

28132 FA **HOPKINS® Forward-Oblique Telescope 45°,**
enlarged view, diameter 4 mm, length 18 cm,
autoclavable,
fiber optic light transmission incorporated,
color code: black

7230 AS/BS/FS

7230 AS **Irrigation Sheath,** outer diameter 5 mm,
working length 14 cm, for use with
HOPKINS® Telescope 28132 AA and
KARL STORZ lens irrigation system CLEARVISION® II

7230 BS **Irrigation Sheath,** outer diameter 5 mm,
working length 14 cm, for use with
HOPKINS® Telescope 28132 BA and
KARL STORZ lens irrigation system CLEARVISION® II

7230 FS **Irrigation Sheath,** outer diameter 5 mm,
working length 14 cm, for use with
HOPKINS® Telescope 28132 FA/FVA and
KARL STORZ lens irrigation system CLEARVISION® II

723750 B

723750 B **Protection Tube,**
for use with HOPKINS® Telescopes with length 18 cm

HOPKINS® Telescopes – autoclavable
diameter 4 mm, length 30 cm

28164 AA

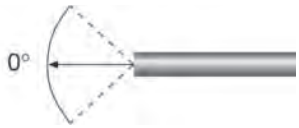

28164 AA **HOPKINS® Straight Forward Telescope 0°,**
enlarged view, diameter 4 mm, length 30 cm,
autoclavable,
fiber optic light transmission incorporated,
color code: green

Irrigation Sheath
for use with KARL STORZ CLEARVISION® II System

28164 ASA

28164 ASA **Irrigation Sheath,** outer diameter 5 mm,
working length 24 cm, for use with
HOPKINS® Telescope 28164 AA and
KARL STORZ Lens Irrigation System CLEARVISION® II

723750 E **Protection Tube,**
for HOPKINS® telescope with length 30 cm

HOPKINS® Telescopes – autoclavable

diameter 2.7 mm, length 18 cm

7229 AA

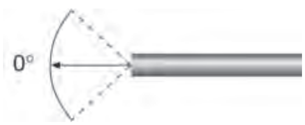

7229 AA **HOPKINS® Straight Forward Telescope 0°,**
enlarged view, diameter 2.7 mm, length 18 cm,
autoclavable,
fiber optic light transmission incorporated,
color code: green

28164 CAA

28164 CAA **Irrigation Sheath,** outer diameter 3.8 mm,
working length 15 cm, for use with
HOPKINS® Telescope 7229 AA,
compatible to **KARL STORZ**
Lens Irrigation System CLEARVISION® II

723750 B

723750 B **Protection Tube,**
for use with HOPKINS® Telescopes with length 18 cm

KARL STORZ CLEARVISION® II System

for intra-operative rinsing of the telescope lens

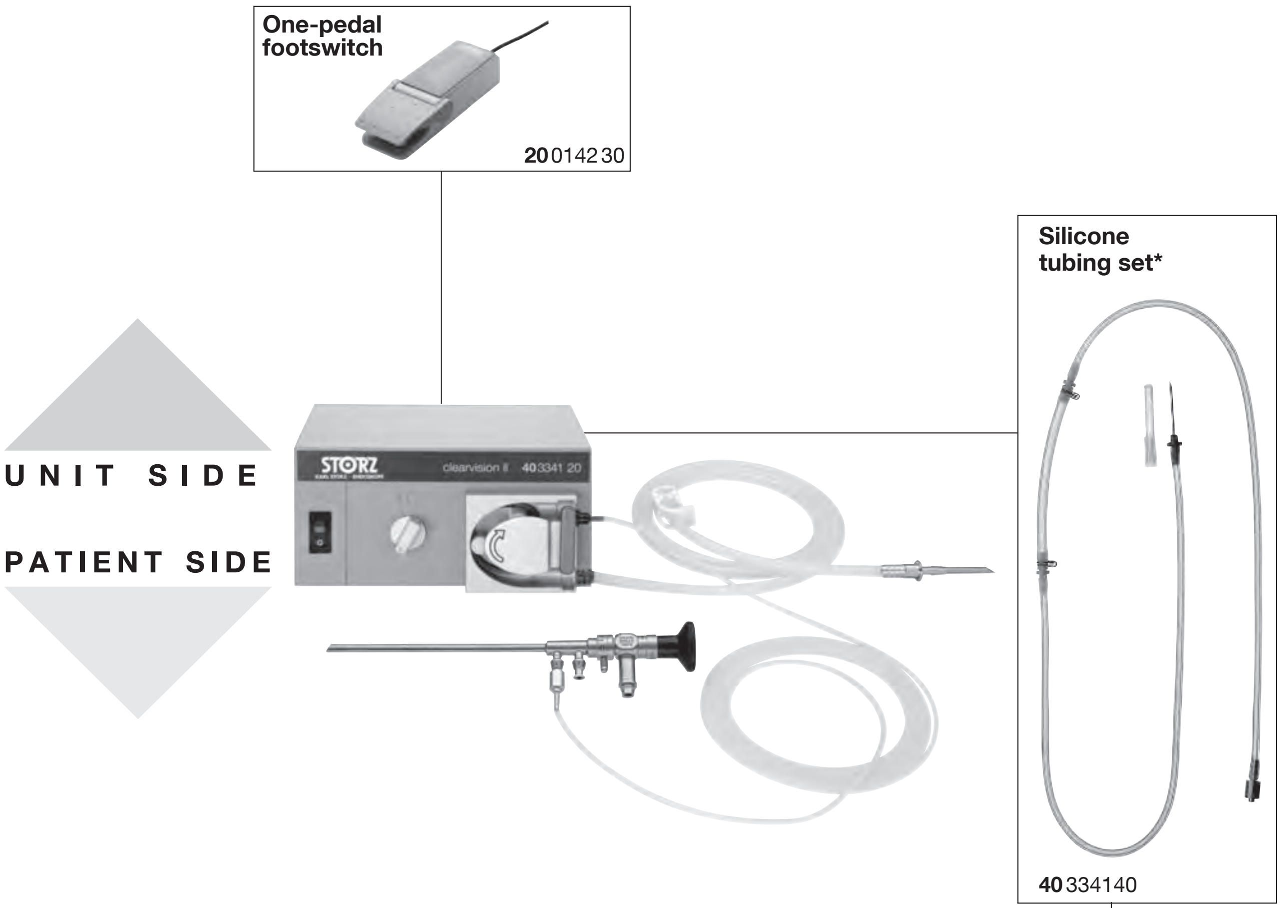

40 3341 01 **CLEARVISION® II,** irrigation pump
for irrigation of the front lens,
power supply 100 – 240 VAC, 50/60 Hz
including:

CLEARVISION® II

Mains Cord

One-Pedal Footswitch, two-stage

Silicone Tubing Set, for irrigation, sterilizable

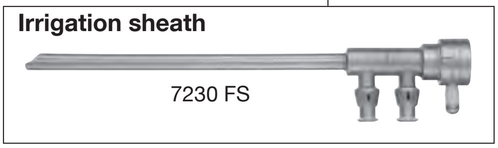

)*Optional Accessories:

MTP 031229-10 Single-use tubing set.
For use with Karl Storz CLEARVISION® II. Sterile,
10 per pack

Submit your order to:

*mtp medical technical promotion gmbh,
Take-Off GewerbePark 46, 78579 Neuhausen ob Eck, Germany

KARL STORZ CLEARVISION® II System
Irrigation Sheath for use with CLEARVISION® II System

Irrigation Sheath, proximally reinforced for use with Adjustable Holder 28272 RKB 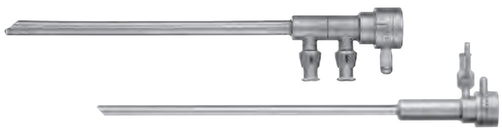				**Compatible HOPKINS® Telescopes** 			
Detail	**Order No.**	**Outer Diameter**	**Working length**	**Order No.**	**View**	**Outer Diameter**	**Working length**
	7230 AS	4.8 × 6.0	14 cm	7230 AA 28132 AA	0°	4 mm	18 cm
	7230 BS	4.8 × 6.0	14 cm	7230 BA 28132 BA	30°	4 mm	18 cm
	7230 FS	4.8 × 6.0	14 cm	7230 FA 28132 FA	45°	4 mm	18 cm
	7230 CS	4.8 × 6.0	14 cm	7230 CA 28132 CA	70°	4 mm	18 cm
	28164 CAA	3.8	15 cm	7229 AA	0°	2.7 mm	18 cm
	28164 CAB	3.8	15 cm	7229 BA	30°	2.7 mm	18 cm
	28164 CAF	3.8	15 cm	7229 FA	45°	2.7 mm	18 cm
	28164 ASA	5	24 cm	28164 AA	0°	4 mm	30 cm
	28164 BSA	5	24 cm	28164 BA	30°	4 mm	30 cm

Holder

for use with rigid KARL STORZ telescopes attached to CLEARVISION® II irrigation sheaths

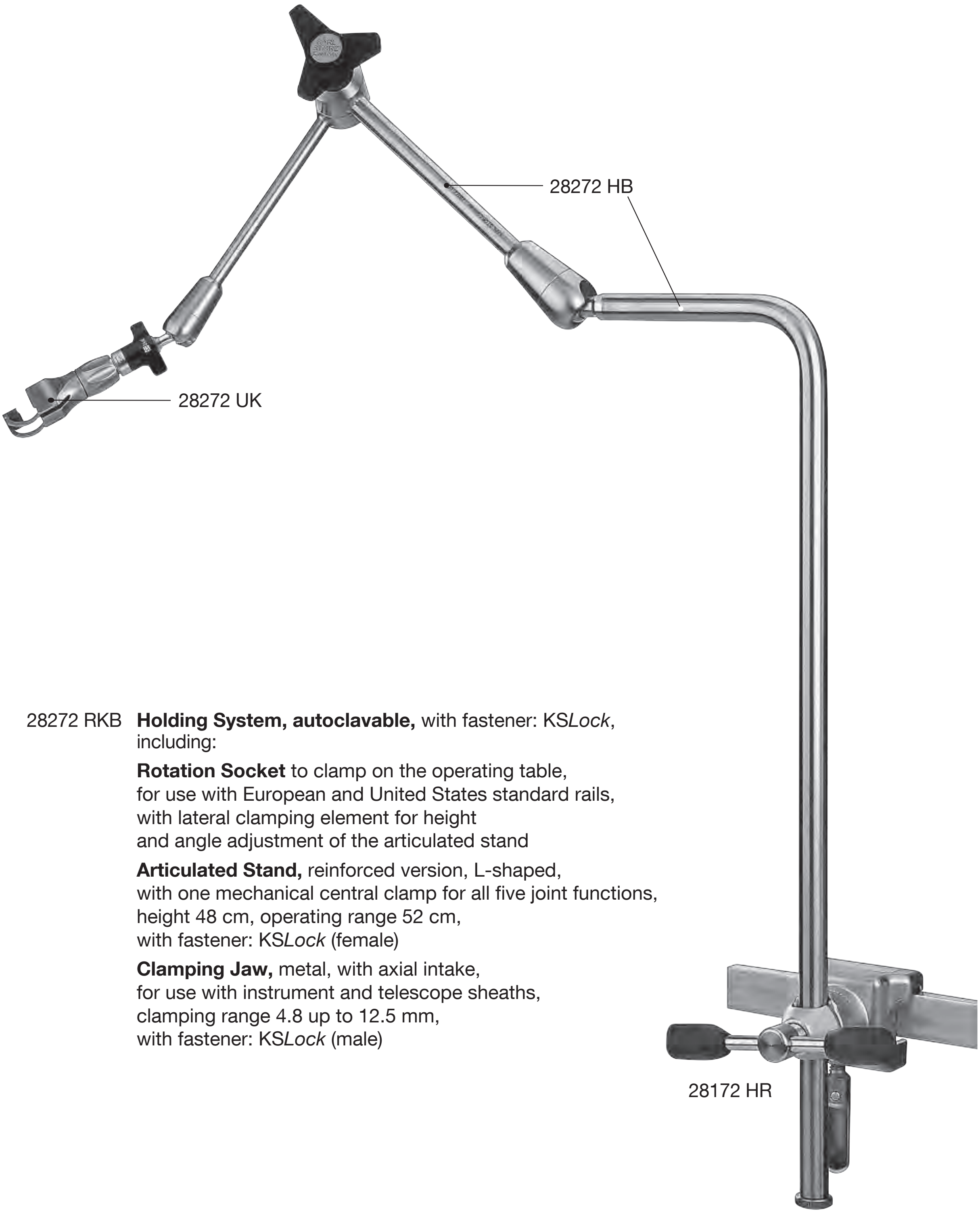

28272 RKB **Holding System, autoclavable,** with fastener: KS*Lock*, including:

Rotation Socket to clamp on the operating table, for use with European and United States standard rails, with lateral clamping element for height and angle adjustment of the articulated stand

Articulated Stand, reinforced version, L-shaped, with one mechanical central clamp for all five joint functions, height 48 cm, operating range 52 cm, with fastener: KS*Lock* (female)

Clamping Jaw, metal, with axial intake, for use with instrument and telescope sheaths, clamping range 4.8 up to 12.5 mm, with fastener: KS*Lock* (male)

Nasal Stage
Basic Instrumentation

474001	FREER **Suction Elevator,** with stylet, length 19 cm
628702	**Antrum Curette,** oblong small size, length 19 cm
660500	**Sickle Knife,** slightly curved, pointed, length 18 cm

Nasal Stage
RHINOFORCE® II Nasal Scissors

449211 **RHINOFORCE® II**, **Nasal Scissors,** straight, small model, length of cut 10 mm, with cleaning connector, working length 13 cm

Nasal Stage

STAMMBERGER **RHINOFORCE® Antrum Punch and**
MACKAY-GRÜNWALD **RHINOFORCE® II Nasal Forceps**

459010

459010 STAMMBERGER **RHINOFORCE® II Antrum Punch, upside backward cutting,** with cleaning connector, working length 10 cm

452001 B

Size 1

452001 B MACKAY-GRÜNWALD **RHINOFORCE® II Nasal Forceps,** through-cutting, straight, delicate, tissue-sparing, 8 x 3 mm, size 1, with cleaning connector, working length 13 cm

Size 1

452501 B MACKAY-GRÜNWALD **RHINOFORCE® II Nasal Forceps,** 45° upturned, through-cutting, tissue-sparing, extra delicate, 8 x 3 mm, size 1, with cleaning connector, working length 13 cm

Sphenoid Stage

STRÜMPEL **Nasal Forceps**

634824
634825 A

	634824	STRÜMPEL **Forceps,** with oval, fenestrated cupped jaws, straight, width 2.5 mm, working length 12.5 cm
	634825 A	**Same,** 45° upturned

Nasal and Sphenoid Stages

Punches

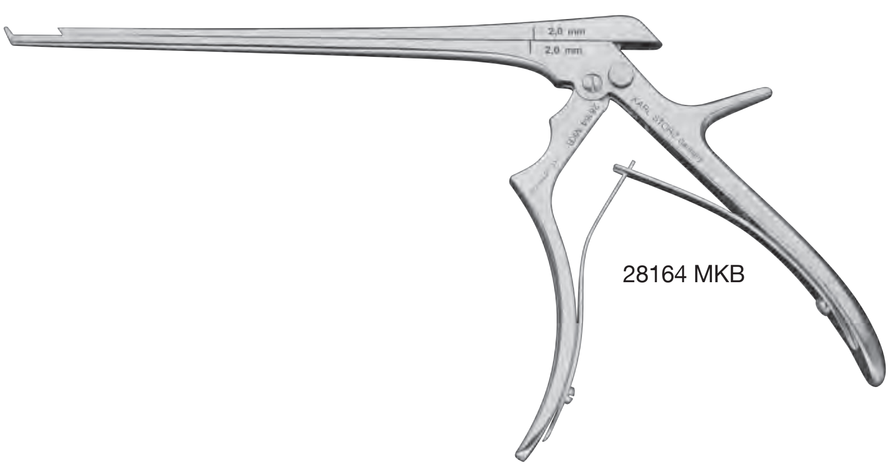

28164 MKB

	28164 MKB	**Punch,** upbiting 60° forward, size 2 mm, working length 17 cm
	28164 MKC	**Same,** size 3 mm

Sphenoid Stage

STAMMBERGER **Circular Cutting Punches**

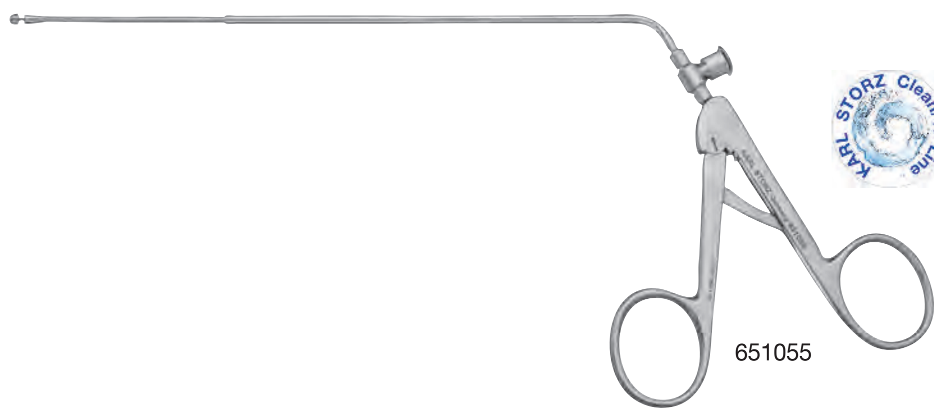

651055

651055 STAMMBERGER **Punch**, circular cutting, for sphenoid, ethmoid and choanal atresia, diameter 3.5 mm, with cleaning connector, working length 18 cm

651050 **Same,** diameter 4.5 mm

Sphenoid and Sellar Stages

Grasping Forceps

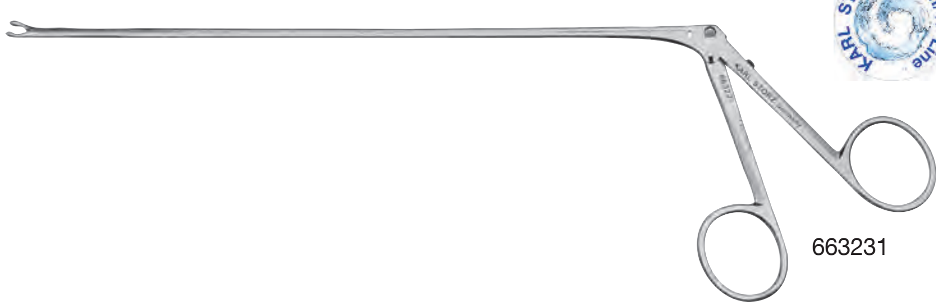

663231

663231 **Forceps,** straight, with round cupped jaws, diameter 2.5 mm, working length 18 cm

Sphenoid and Sellar Stages

Delicate Dissectors

28164 DB

28164 DB **Dissector,** sharp, tip angled 45°, round spatula, with round handle, size 3 mm, length 25 cm

28164 DS **Dissector,** sharp, tip angled 15°, slightly curved spatula, with round handle, size 2 mm, length 25 cm

28164 DM **Dissector,** sharp, straight tip, slightly curved spatula, with round handle, size 3 mm, length 25 cm

Sellar Stage

Scalpel, Very Delicate Scissors

28164 M

28164 M de DIVITIIS-CAPPABIANCA **Scalpel,** with retractable blade, including:
Handle
Outer Sheath
Micro Knife, pointed

28164 KK **Same,** including:
Handle
Outer Sheath
Micro Knife, sickle-shaped

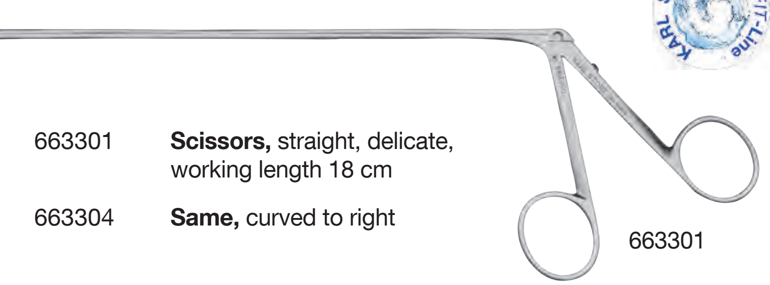

663301

663301 **Scissors,** straight, delicate, working length 18 cm

663304 **Same,** curved to right

663305 **Same,** curved to left

663307 **Same,** 45° curved up

28164 SAD **Scissors,** 45° upwards curve, delicate, shaft 360° rotatable, working length 18 cm

Sellar Stage
Forceps

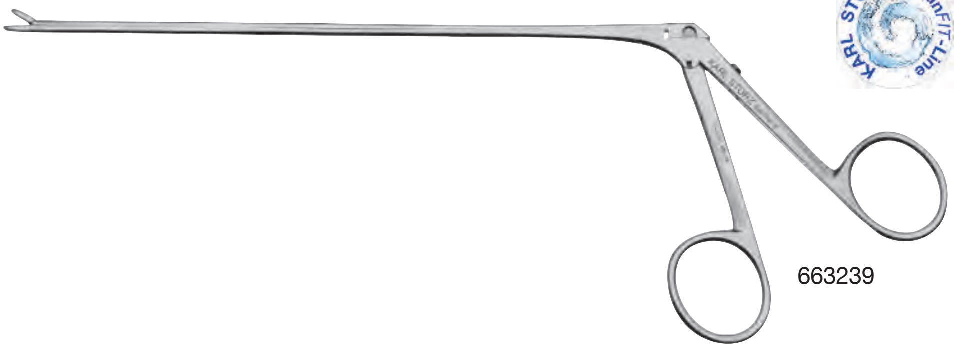

663239

663239 **Forceps,** straight, not through-cutting,
with oval, fenestrated spoon, width 2.5 mm,
working length 18 cm

Sellar Stage
Hooks, Curettes, round spoon

28164 H

28164 H CASTELNUOVO **Hook,** 90°, blunt,
with round handle, length 25 cm

28164 KB

28164 KB **Curette,** round spoon, tip slightly angled,
size 2 mm, with round handle, length 25 cm

Sellar Stage
Curettes

28164 RO

Inner diameter in mm:

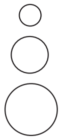

28164 RN CAPPABIANCA-de DIVITIIS **Ring Curette,** round wire, inner diameter 3 mm, tip angled 45°, with round handle, length 25 cm

28164 RE **Same,** malleable

28164 RO CAPPABIANCA-de DIVITIIS **Ring Curette,** round wire, inner diameter 5 mm, tip angled 45°, with round handle, length 25 cm

28164 RJ **Same,** malleable

28164 RI De DIVITIIS-CAPPABIANCA **Ring Curette,** round wire, inner diameter 3 mm, tip angled 90°, with round handle, length 25 cm

28164 RG **Same,** inner diameter 5 mm

28164 RB de DIVITIIS-CAPPABIANCA **Ring Curette,** round wire, inner diameter 3 mm, distally curved shaft, with round handle, length 25 cm

28164 RA **Same,** inner diameter 5 mm

28164 RV CAPPABIANCA-de DIVITIIS **Ring-Curette,** round wire, inner diameter 3 mm, tip laterally angled 90°, with round handle, length 25 cm

28164 RD **Same,** inner diameter 5 mm

28164 RW **Same,** inner diameter 7 mm

28164 RF

28164 RF CAPPABIANCA-de DIVITIIS **Ring Curette,** round wire, vertical, inner diameter 5 mm, tip angled 45°, with round handle, length 25 cm

Sellar Stage

CAPPABIANCA-de DIVITIIS **Suction Curettes, round wire – basket-shaped**

28164 RSB

28164 RSB de DIVITIIS-CAPPABIANCA **Suction-Curette,** with round wire, inner diameter 5 mm, tip angled 45°, LUER, length 25 cm

28164 RSC **Same,** inner diameter 7 mm

28164 RT CAPPABIANCA-de DIVITIIS **Suction Curette,** with basket, round, size 5 mm, rotatable tube, LUER, length 25 cm

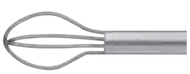

28164 RU **Same,** size 6.5 mm

Lesion Meter

28164 MI

28164 MI **Lesion Meter,** to determine the size of transnasal lesions, with wheel handle and scale, width 2 mm, working length 19 cm

Suction Tubes

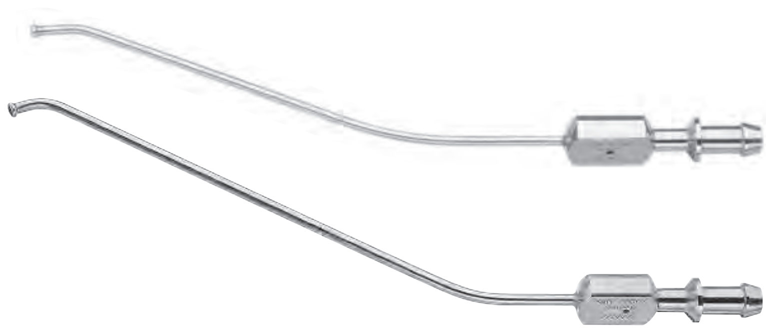

662882

662885

662882 FRANK-PASQUINI **Suction Tube,** knee bent, tip curved upwards, ball end, with grip plate and cut-off hole, LUER, diameter 2.4 mm, working length 13 cm

662885 FRANK-PASQUINI **Suction Tube,** knee bent, tip curved upwards, ball end, with grip plate and cut-off hole, LUER, diameter 3 mm, working length 13 cm

Suction Tubes

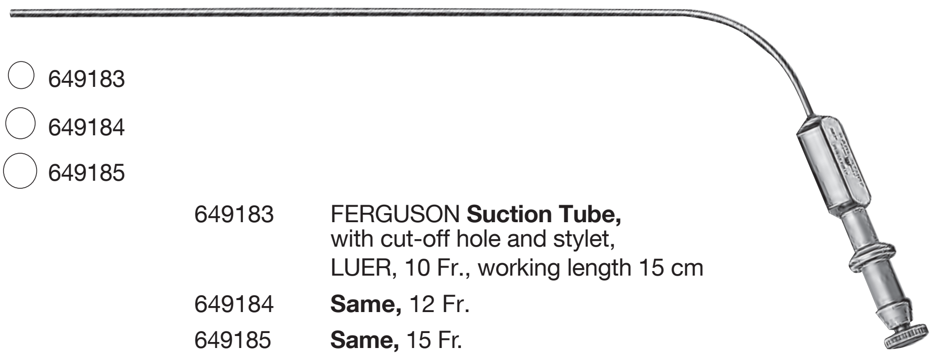

649183
649184
649185

649183	FERGUSON **Suction Tube,** with cut-off hole and stylet, LUER, 10 Fr., working length 15 cm
649184	**Same,** 12 Fr.
649185	**Same,** 15 Fr.

649183

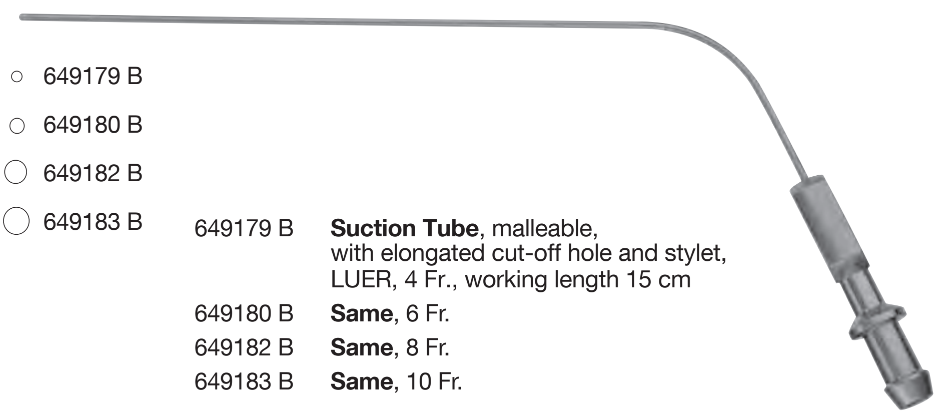

649179 B
649180 B
649182 B
649183 B

649179 B	**Suction Tube**, malleable, with elongated cut-off hole and stylet, LUER, 4 Fr., working length 15 cm
649180 B	**Same**, 6 Fr.
649182 B	**Same**, 8 Fr.
649183 B	**Same**, 10 Fr.

649179 B

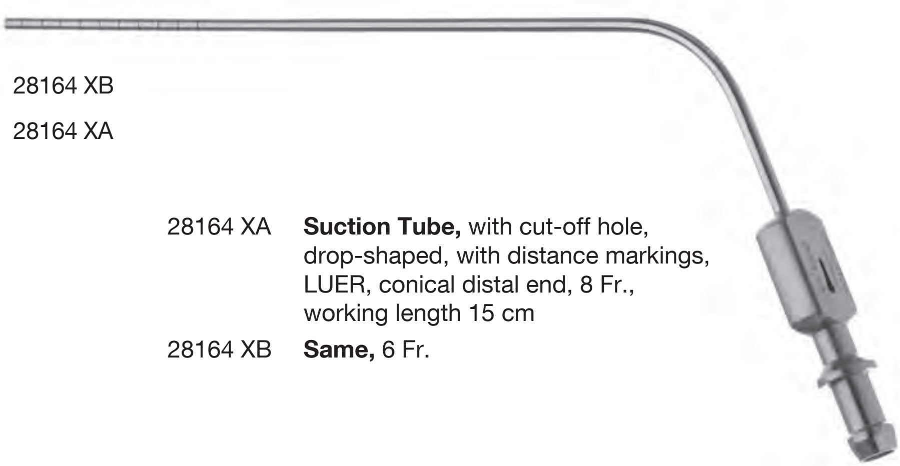

28164 XB
28164 XA

28164 XA	**Suction Tube,** with cut-off hole, drop-shaped, with distance markings, LUER, conical distal end, 8 Fr., working length 15 cm
28164 XB	**Same,** 6 Fr.

28164 XA

Basic Instrumentation for Extended Approaches

Micro Instruments

28164 PBA

28164 PBA **Micro Scissors,** bayonet-shaped, 0.5 mm, smooth, working length 10 cm

28164 PBB **Micro Scissors,** bayonet-shaped, spoon, 2 mm, working length 10 cm

28164 SBA **Micro Scissors,** horizontal, bayonet-shaped, sharp/sharp, straight, working length 10 cm

28164 SBB **Micro Scissors,** bayonet-shaped, sharp/sharp, left curved, working length 10 cm

28164 ZBA

28164 ZBA **Micro Applying Forceps,** Yasargil-Clips, working length 10 cm

28164 ZBB **Micro Applying Forceps,** Yasargil-Mini Clips, working length 10 cm

Instruments for Coagulation

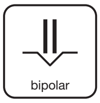

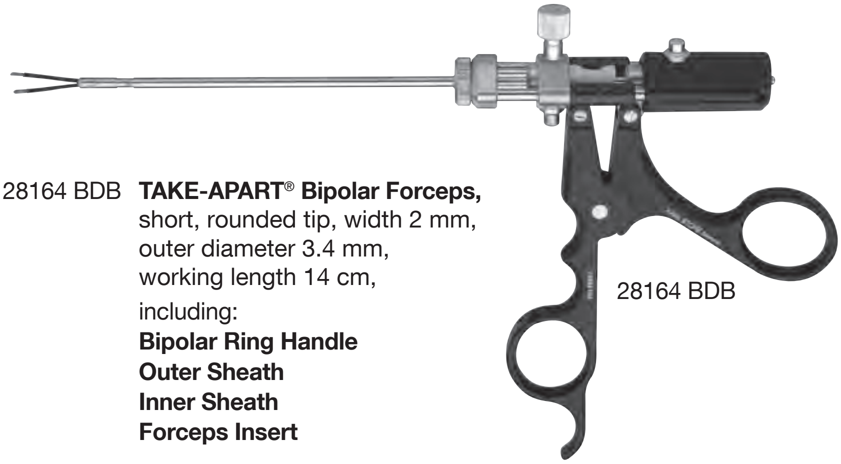

28164 BDB **TAKE-APART® Bipolar Forceps,**
short, rounded tip, width 2 mm,
outer diameter 3.4 mm,
working length 14 cm,
including:
Bipolar Ring Handle
Outer Sheath
Inner Sheath
Forceps Insert

28164 BDB

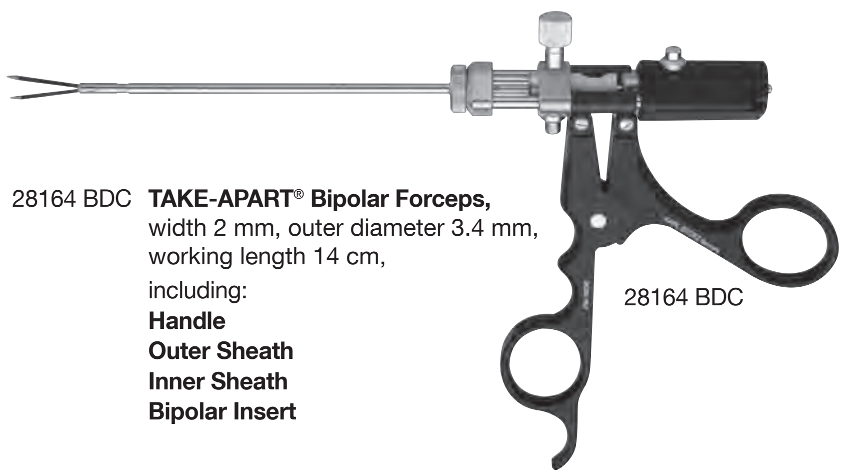

28164 BDC **TAKE-APART® Bipolar Forceps,**
width 2 mm, outer diameter 3.4 mm,
working length 14 cm,
including:
Handle
Outer Sheath
Inner Sheath
Bipolar Insert

28164 BDC

Instruments for Coagulation

bipolar

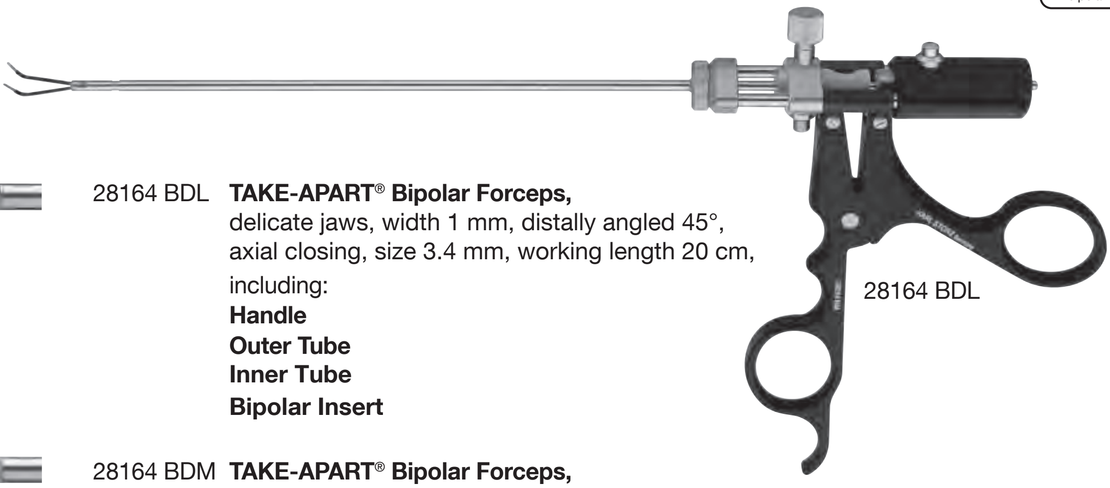

28164 BDL

28164 BDL **TAKE-APART® Bipolar Forceps,**
delicate jaws, width 1 mm, distally angled 45°, axial closing, size 3.4 mm, working length 20 cm, including:
Handle
Outer Tube
Inner Tube
Bipolar Insert

28164 BDM **TAKE-APART® Bipolar Forceps,**
delicate jaws, width 1 mm, distally angled 45°, axial closing, size 3.4 mm, working length 20 cm including:
Handle
Outer Tube
Inner Tube
Bipolar Insert

839310 N

839310 N **Insulated Suction Cannula,** for nose, straight, outer diameter 3 mm, working length 10 cm

28164 ED

28164 ED **Coagulation Ball Electrode,** diameter 2 mm, laterally curved, working length 13 cm

28164 EF **Same,** diameter 4 mm

EndoCAMeleon® NEURO HOPKINS® Telescope

The ENDOCAMELEON® is the newest member of the HOPKINS® family of rod-lens telescopes – and the most versatile.

With a simple turn of the adjusting knob, ENDOCAMELEON® enables the user to select the direction of view between 15° and 90°. Consequently, the surgeon can quickly and easily select the desired direction of view for optimal orientation and control.

The ENDOCAMELEON® from KARL STORZ brings a new quality to endoscopy in the OR as it often enhances orientation during an operation without the time-consuming changeover of telescopes, thereby ensuring safe and smooth surgery.

The ENDOCAMELEON® combines the user comfort of the proven HOPKINS® endoscopes with unprecedented versatility – in the proven KARL STORZ high quality.

Special Features:

- Variable direction of view (15° to 90°)
- Easy-to-use adjusting knob selects the desired direction of view
- Lightweight construction and modern design
- HOPKINS® telescope with unique rod-lens system
- Diameter 4 mm, length 18 cm
- Standard eyepiece fits all camera heads

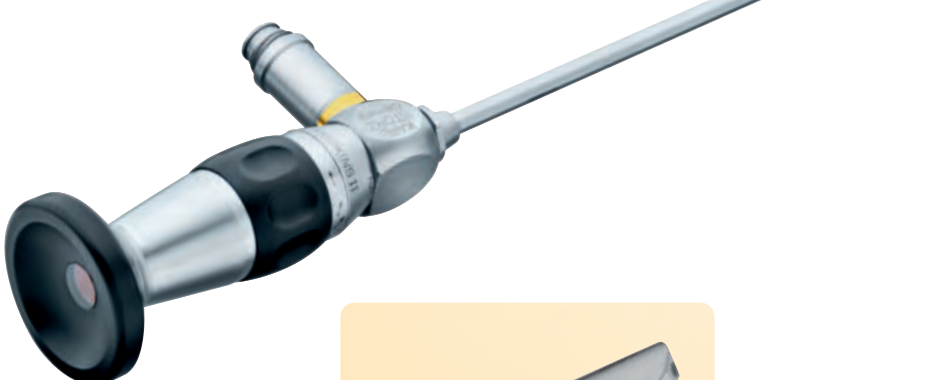

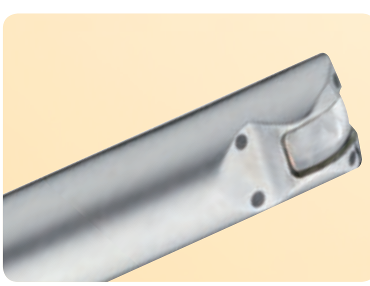

The familiar ergonomics and handling of conventional telescopes is enhanced with the additional convenience of a variable direction of view

The direction of view is adjusted by a mere turn of the adjusting knob at the proximal end of the ENDOCAMELEON®

Telescope

28132 AE **ENDOCAMELEON® HOPKINS® Telescope,**
diameter 4 mm**,** length 18 cm, **autoclavable,**
variable direction of view from 15° to 90°,
adjustment knob for selecting the desired direction of view,
fiber optic light transmission incorporated,
color code: gold

7230 AES **Irrigation and Suction Sheath,**
outer diameter 4.8 x 6 mm, working length 14 cm,
for use with ENDOCAMELEON® ENT HOPKINS® Telescope 7230 AE
and KARL STORZ lens irrigation system CLEARVISION® II

Accessories

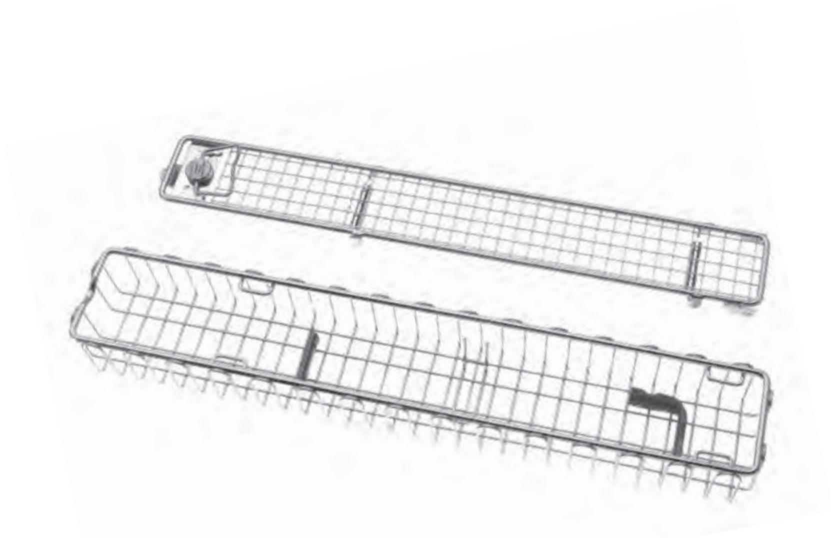

39501 A1 **Wire Tray for Cleaning, Sterilization and Storage**
of one rigid endoscope, including holder for light post adaptors,
silicone telescope holders and lid, external dimensions (w x d x h):
290 x 60 x 52 mm, for rigid endoscopes up to diameter 5 mm
and working length 20 cm

UNIDRIVE® S III NEURO SCB

Special Features

UNIDRIVE® S III NEURO SCB

Special Features:

Straightforward function selection and optimized user control via touch screen
Choice of user languages
Operating elements are single and clear to read due to color display
One unit – six functions: Neurosurgery: – Craniotomes – Perforators – High-Speed Handpieces 100,000 rpm – High-Speed Handpieces 60,000 rpm ENT: – Shaver system for surgery of the paranasal sinuses and anterior skull base – INTRA Drills – Sinus Shavers – Micro Saws – Dermatomes
Two motor outputs: Two motor outputs enable two motors to be connected simultaneously: for example, a high-speed handpiece and a shaver handpiece may be connected in parallel
Safe work due to rapid blade when the pedal is released
Integrated irrigation and coolant pump
Absolutely homogeneous, micro-processor controlled irrigation rate throughout the entire irrigation range. Quick and easy connection of the tubing set.
Easy program selection via automated motor recognition
Continuously variable revolution range
Maximum number of revolutions and motor torque: Microprocessor-controlled revolutions per minute. Therefore the preselected parameters are maintained all the time during drilling
Maximum number of evolutions can be preset
With connection possibilities to the KARL STORZ Communication Bus (KARL STORZ-SCB)
Irrigator rod included

UNIDRIVE® S III NEURO SCB

Recommended Standard Set Configurations

40 7017 01-1 **UNIDRIVE® S III NEURO SCB,** motor control unit with color display, touch screen, two motor outputs, integrated irrigation pump and integrated SCB module, power supply 100 – 240 VAC, 50/60 Hz

including:

Mains Cord

Irrigator Rod

Two-Pedal Footswitch, two-stage, with proportional function

Clip Set, for use with tubing set

SCB Connecting Cable, length 100 cm

Single Use Tubing Set*, sterile, package of 3

Specifications:

Touch Screen	6.4"/300 cd/m²
Available languages:	English, French, German, Spanish, Italian, Portuguese, Greek, Turkish, Polish, Russian
Power supply	100–240 VAC, 50/60 Hz

Dimensions w x h x d	300 x 165 x 265 mm
Weight	5.2 kg
Certified to:	IEC 601-1, CE acc. to MDD

*mtp medical technical promotion gmbh,
Take-Off GewerbePark 46, 78579 Neuhausen ob Eck, Germany

UNIDRIVE® S III NEURO SCB

High-Speed Micro Motor

Special Features:

- **Self-cooling and brushless high-speed micro motor**
- **Smallest possible dimensions**
- **Autoclavable**
- **Can be processed in a cleaning machine**
- **Maximum torque 6 Ncm**
- **Number of revolutions can be continuously adjusted from 1000 – 60,000 rpm**
- **Possible to adjust the number of revolutions to 100,000 rpm with the appropriate handle**

20 7120 33

20 7120 33 **High-Speed Micro-Motor,** max. speed 60,000 rpm, including connecting cable, for use with UNIDRIVE® S III ENT/NEURO

Accessories:

280053 **Universal Spray,** 6x 500 ml bottles – HAZARDOUS GOODS – UN 1950

including:

Spray Nozzle

031131-10* **Tubing Set,** for irrigation, for single use, sterile, package of 10

*mtp medical technical promotion gmbh,
Take-Off GewerbePark 46, 78579 Neuhausen ob Eck, Germany

UNIDRIVE® S III NEURO SCB

System Components

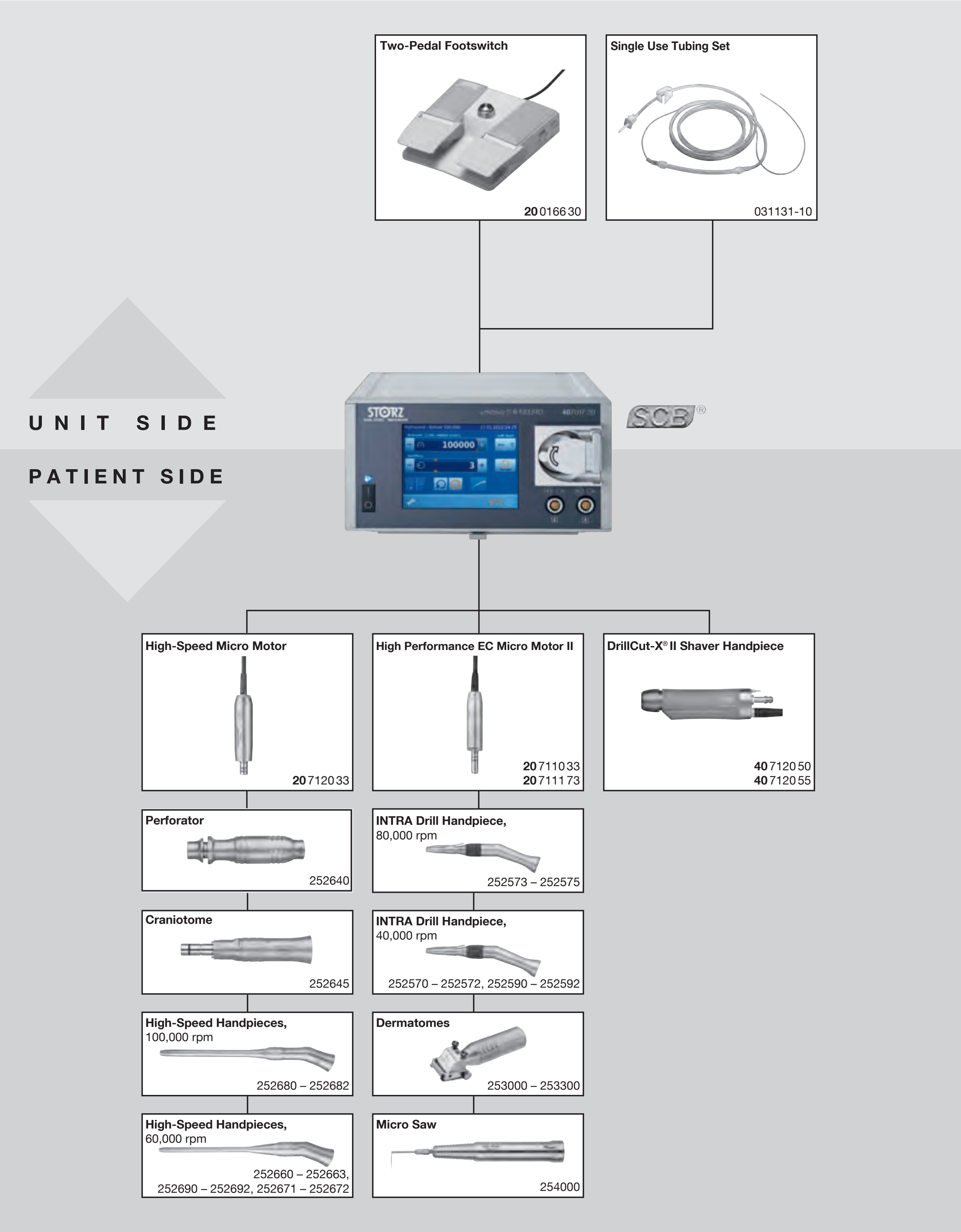

UNIDRIVE® S III NEURO SCB

High-Speed Handpieces, angled, 100,000 rpm

For use with drills with shaft diameter 3.17 mm

100,000 rpm
diameter 7.5 mm

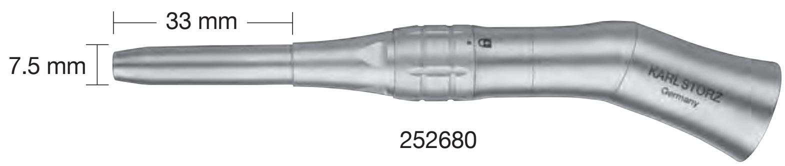

252680 **High-Speed Handpiece,** short, angled, 100,000 rpm,
for use with High-Speed Micro-Motor **20** 7120 33

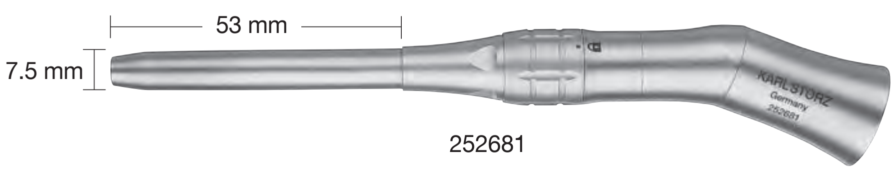

252681 **High-Speed Handpiece,** medium, angled, 100,000 rpm,
for use with High-Speed Micro-Motor **20** 7120 33

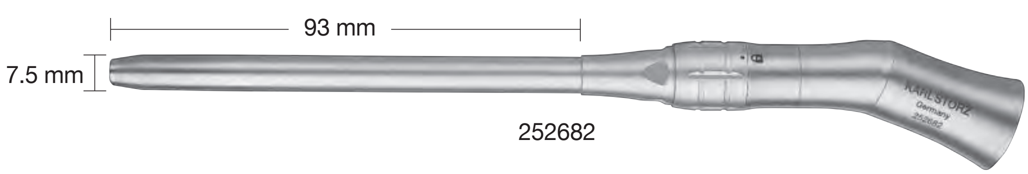

252682 **High-Speed Handpiece,** long, angled, 100,000 rpm,
for use with High-Speed Micro-Motor **20** 7120 33

UNIDRIVE® S III NEURO SCB

High-Speed Handpieces, angled, 60,000 rpm

For use with drills with shaft diameter 2.35 mm

60,000 rpm
diameter 5.5 mm

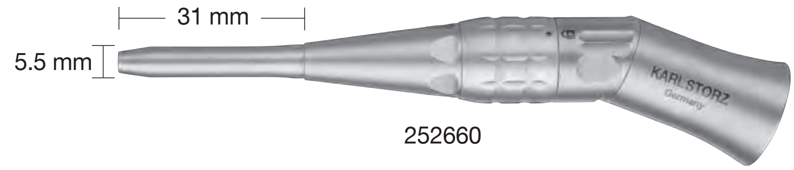

252660 **High-Speed Handpiece,** extra short, angled, 60,000 rpm, for use with High-Speed Micro-Motor **20** 7120 33

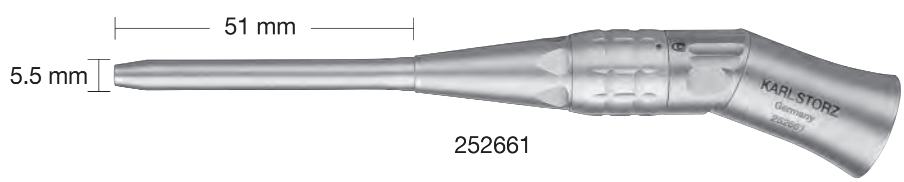

252661 **High-Speed Handpiece,** short, angled, 60,000 rpm, for use with High-Speed Micro-Motor **20** 7120 33

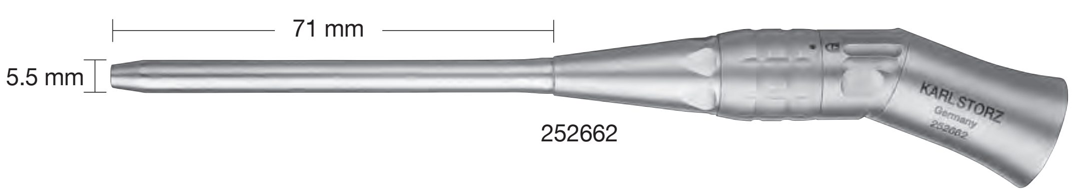

252662 **High-Speed Handpiece,** medium, angled, 60,000 rpm, for use with High-Speed Micro-Motor **20** 7120 33

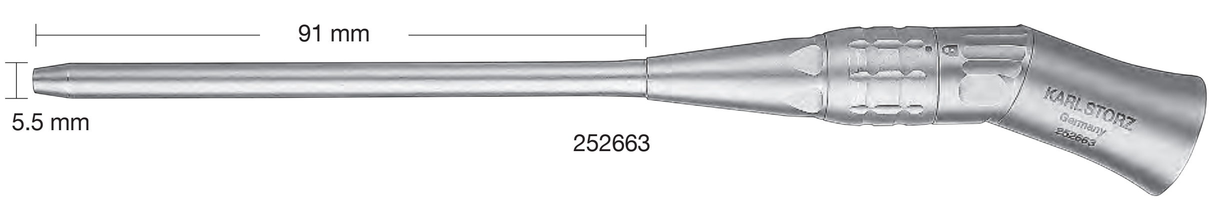

252663 **High-Speed Handpiece,** long, angled, 60,000 rpm, for use with High-Speed Micro-Motor **20** 7120 33

UNIDRIVE® S III NEURO SCB

High-Speed Handpieces, straight, 60,000 rpm

For use with drills with shaft diameter 2.35 mm

60,000 rpm
diameter 5.5 mm

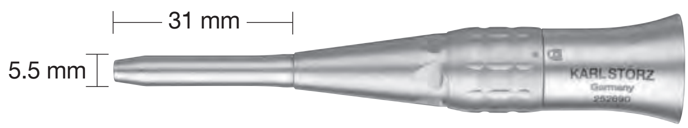

252690

252690 **High-Speed Handpiece,** extra short, straight, 60,000 rpm, for use with High-Speed Micro-Motor **20** 7120 33

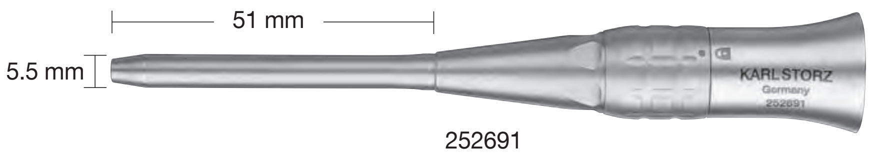

252691

252691 **High-Speed Handpiece,** short, straight, 60,000 rpm, for use with High-Speed Micro-Motor **20** 7120 33

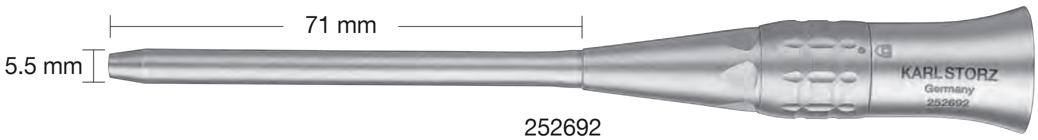

252692

252692 **High-Speed Handpiece,** medium, straight, 60,000 rpm, for use with High-Speed Micro-Motor **20** 7120 33

UNIDRIVE® S III NEURO SCB

High-Speed Handpieces, malleable, slim, angled, 60,000 rpm

For use with drills with shaft diameter 1 mm

60,000 rpm
diameter 4.7 mm

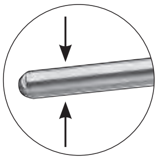

malleable

The handpieces have malleable shafts that can be bent up to 20° according to user requirements.

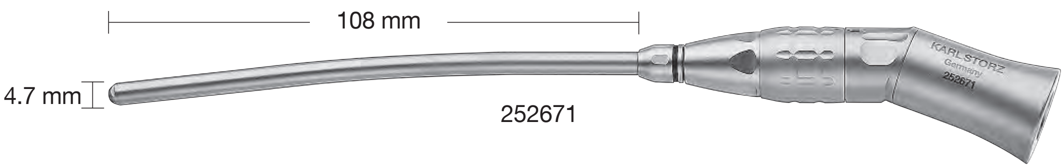

252671 **High-Speed Handpiece,** extra long, malleable, slim, angled, 60,000 rpm, for use with High-Speed Micro-Motor **20** 7120 33

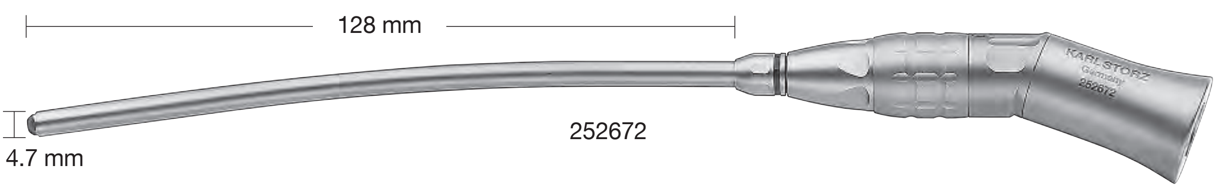

252672 **High-Speed Handpiece,** super long, malleable, slim, angled, 60,000 rpm, for use with High-Speed Micro-Motor **20** 7120 33

UNIDRIVE® S III NEURO SCB

For use with High-Speed Handpieces, 100,000 rpm

For use with High-Speed Handpieces, 100,000 rpm

100,000 rpm
diameter 7.5 mm


252680


252681


252682

High-Speed Standard Burrs, 100,000 rpm, for single use, sterile, package of 5

Diameter in mm	short	medium	long
1	350110 S	350110 M	–
2	350120 S	350120 M	350120 L
3	350130 S	350130 M	350130 L
4	350140 S	350140 M	350140 L
5	350150 S	350150 M	350150 L
6	350160 S	350160 M	350160 L
7	350170 S	350170 M	350170 L

High-Speed Diamond Burrs, 100,000 rpm, for single use, sterile, package of 5

Diameter in mm	short	medium	long
1	350210 S	350210 M	–
2	350220 S	350220 M	350220 L
3	350230 S	350230 M	350230 L
4	350240 S	350240 M	350240 L
5	350250 S	350250 M	350250 L
6	350260 S	350260 M	350260 L
7	350270 S	350270 M	350270 L

UNIDRIVE® S III NEURO SCB

High-Speed Coarse Diamond Burrs, High-Speed Acorns, High-Speed Barrel Burrs, High-Speed Neuro Fluted Burrs

For use with High-Speed Handpieces, 100,000 rpm

100,000 rpm
diameter 7.5 mm


252680


252681


252682

	**High-Speed Coarse Diamond Burrs, 100,000 rpm, for single use, sterile, package of 5**		
Diameter in mm	**short**	**medium**	**long**
3	350330 S	350330 M	350330 L
4	350340 S	350340 M	350340 L
5	350350 S	350350 M	350350 L
6	350360 S	350360 M	350360 L
7	350370 S	350370 M	350370 L

	**High-Speed Acorns, 100,000 rpm, for single use, sterile, package of 5**	
Diameter in mm	**short**	**medium**
7.5	350675 S	350675 M
9	350690 S	350690 M

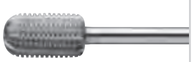	**High-Speed Barrel Burrs, 100,000 rpm, for single use, sterile, package of 5**	
Diameter in mm	**short**	**medium**
6	350960 S	350960 M
9.1	350991 S	350991 M

	**High-Speed Neuro Fluted Burrs, 100,000 rpm, for single use, sterile, package of 5**		
Diameter in mm	**short**	**medium**	**long**
1.8	350718 S	350718 M	350718 L
3	350730 S	350730 M	350730 L

UNIDRIVE® S III NEURO SCB

High-Speed Standard Burrs, High-Speed Diamond Burrs

For use with High-Speed Handpieces, 60,000 rpm

60,000 rpm
diameter 5.5 mm


252660


252661


252662


252663


252690


252691


252692

High-Speed Standard Burrs, 60,000 rpm, for single use, sterile, package of 5

Diameter in mm	extra short	short	medium	long
1	330110 ES	330110 S	330110 M	–
2	330120 ES	330120 S	330120 M	330120 L
3	330130 ES	330130 S	330130 M	330130 L
4	330140 ES	330140 S	330140 M	330140 L
5	330150 ES	330150 S	330150 M	330150 L
6	330160 ES	330160 S	330160 M	330160 L
7	330170 ES	330170 S	330170 M	330170 L

High-Speed Diamond Burrs, 60,000 rpm, for single use, sterile, package of 5

Diameter in mm	extra short	short	medium	long
0.6	330206 ES	330206 S	–	–
1	330210 ES	330210 S	330210 M	–
1.5	330215 ES	330215 S	–	–
2	330220 ES	330220 S	330220 M	330220 L
3	330230 ES	330230 S	330230 M	330230 L
4	330240 ES	330240 S	330240 M	330240 L
5	330250 ES	330250 S	330250 M	330250 L
6	330260 ES	330260 S	330260 M	330260 L
7	330270 ES	330270 S	330270 M	330270 L

UNIDRIVE® S III NEURO SCB

High-Speed Diamond Burrs, High-Speed Barrel Burrs,
LINDEMANN **High-Speed Fluted Burrs**

For use with High-Speed Handpieces, 60,000 rpm

60,000 rpm
diameter 5.5 mm


252660


252661


252662


252663


252690


252691


252692

High-Speed Coarse Diamond Burrs, 60,000 rpm, for single use, sterile, package of 5

Diameter in mm	extra short	short	medium	long
3	330330 ES	330330 S	330330 M	330330 L
4	330340 ES	330340 S	330340 M	330340 L
5	330350 ES	330350 S	330350 M	330350 L
6	330360 ES	330360 S	330360 M	330360 L
7	330370 ES	330370 S	330370 M	330370 L

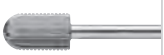

High-Speed Cylinder Burrs, 60,000 rpm, for single use, sterile, package of 5

Diameter in mm	extra short	short
4	330440 ES	330440 S
6	330460 ES	330460 S

LINDEMANN **High-Speed Fluted Burrs, 60,000 rpm, for single use, sterile, package of 5**

Diameter in mm (diameter x length)	extra short	short
Diameter 2.1/11	330511 ES	330511 S
Diameter 2.3/26	330526 ES	330526 S

UNIDRIVE® S III NEURO SCB

High-Speed Diamond Burrs

For use with High-Speed Handpieces, 60,000 rpm

60,000 rpm
diameter 4.7 mm

252671

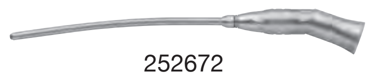

252672

	**High-Speed Diamond Burrs, 60,000 rpm, for single use, sterile, package of 5**	
Diameter in mm	**extra long**	**super long**
2	320220 EL	320220 SL
3	320230 EL	320230 SL
4	320240 EL	320240 SL

	**High-Speed Coarse Diamond Burrs, 60,000 rpm, for single use, sterile, package of 5**	
Diameter in mm	**extra long**	**super long**
2	320320 EL	320320 SL
3	320330 EL	320330 SL
4	320340 EL	320340 SL

Accessories for Burrs

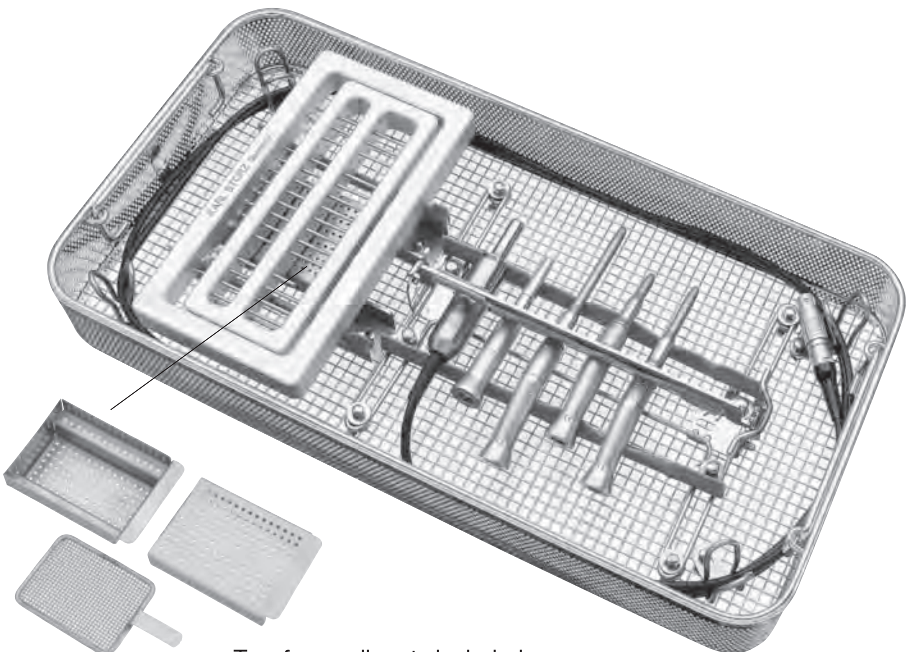

39552 B

Tray for small parts included

39552 A **Wire Tray,** provides safe storage of accessories for KARL STORZ drilling/grinding systems during cleaning and sterilization, includes tray for small parts, for use with Rack 280030, rack **not** included

for storage of:

– Up to 6 drill handpieces
– Connecting cable
– EC micro motor
– Small parts

39552 B **Wire Tray,** provides safe storage of accessories for KARL STORZ drilling/grinding systems during cleaning and sterilization, includes tray for small parts, for use with Rack 280030, rack **included**

for storage of:

– Up to 6 drill handpieces
– Connecting cable
– EC micro motor
– Up to 36 drill bits and burrs
– Small parts

Please note: The instruments displayed are not included in the sterilizing and storage tray.

IMAGE1 S Camera System NEW

Economical and future-proof

- **Modular concept for flexible, rigid and 3D endoscopy as well as new technologies**
- **Forward and backward compatibility with video endoscopes and FULL HD camera heads**
- **Sustainable investment**
- **Compatible with all light sources**

Innovative Design

- **Dashboard: Complete overview with intuitive menu guidance**
- **Live menu: User-friendly and customizable**
- **Intelligent icons: Graphic representation changes when settings of connected devices or the entire system are adjusted**
- **Automatic light source control**
- **Side-by-side view: Parallel display of standard image and the Visualization mode**
- **Multiple source control: IMAGE1 S allows the simultaneous display, processing and documentation of image information from two connected image sources, e.g., for hybrid operations**

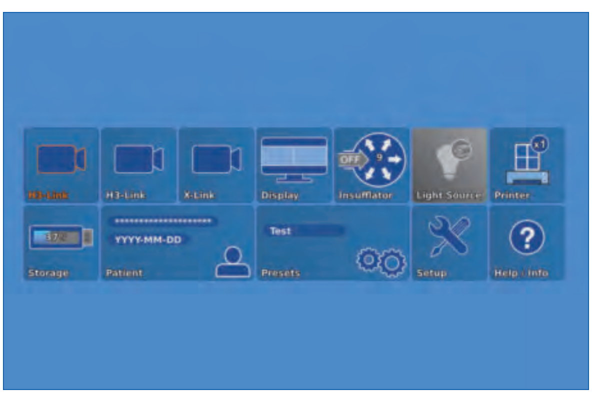

Dashboard

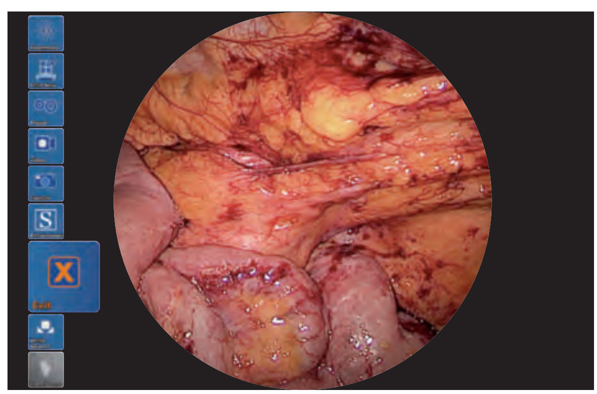

Live menu

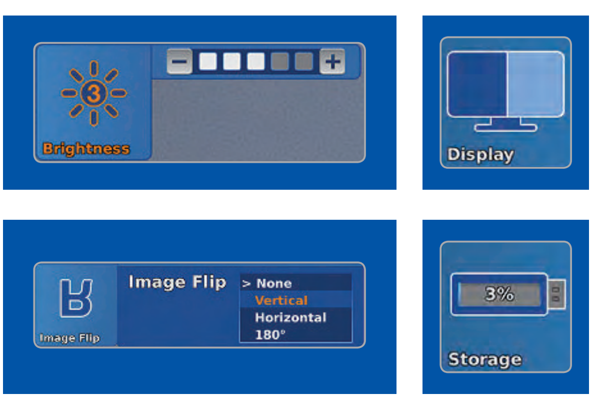

Intelligent icons

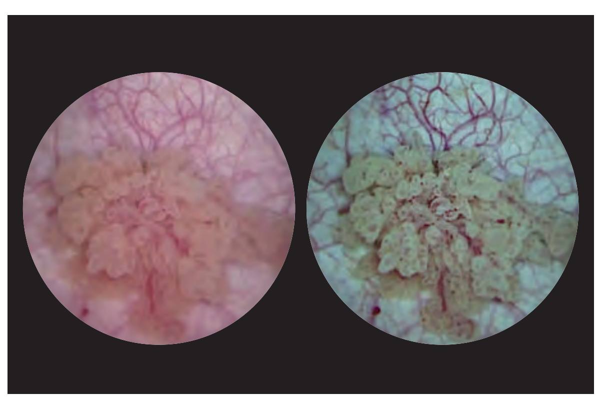

Side-by-side view: Parallel display of standard image and Visualization mode

IMAGE1 S Camera System NEW

Brilliant Imaging

- **Clear and razor-sharp endoscopic images in FULL HD**
- **Natural color rendition**
- **Reflection is minimized**
- **Multiple IMAGE1 S technologies for homogeneous illumination, contrast enhancement and color shifting**

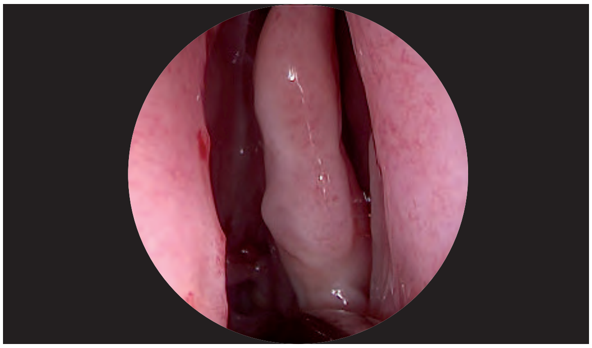

FULL HD image

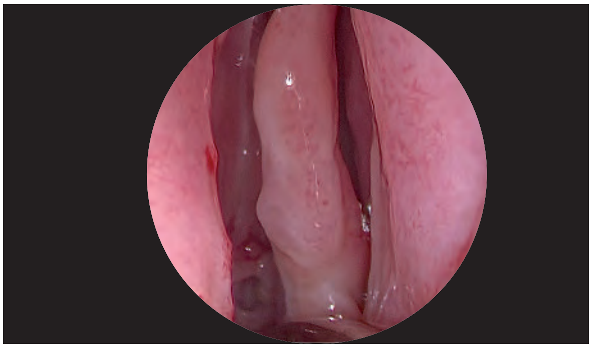

CLARA

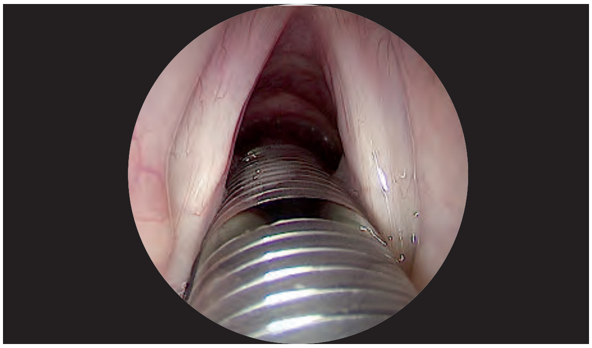

FULL HD image

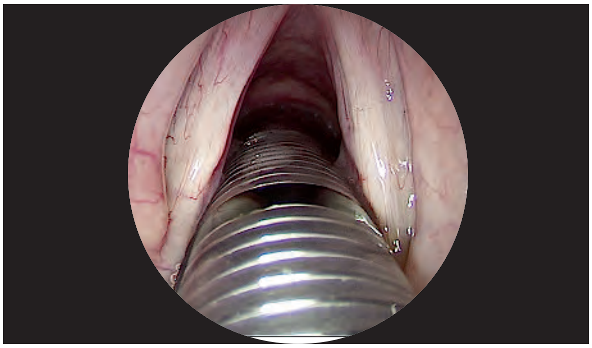

CHROMA

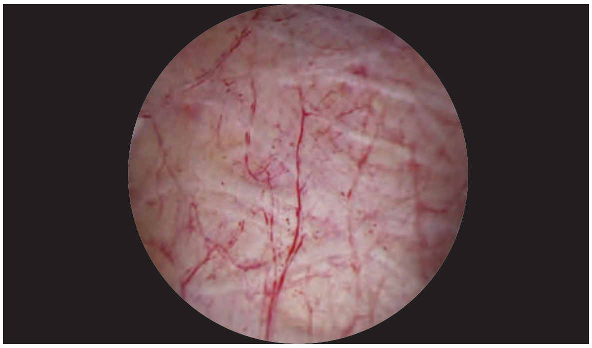

FULL HD image

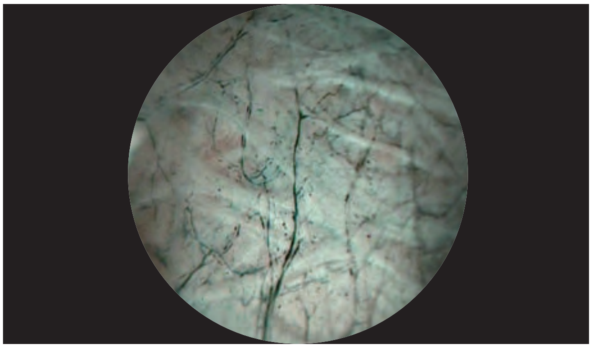

*SPECTRA A**

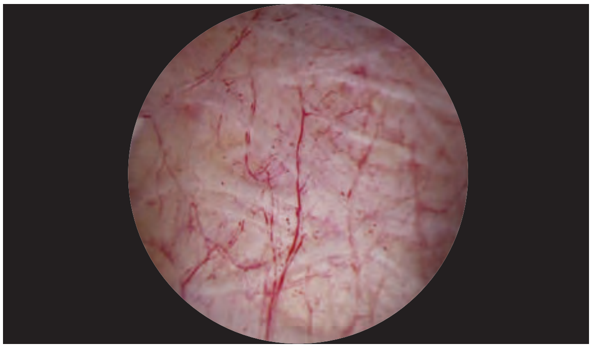

FULL HD image

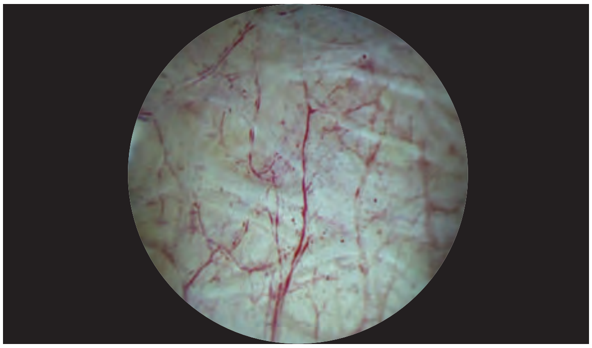

*SPECTRA B***

* *SPECTRA A:* **Not for sale in the U.S.**
** *SPECTRA B:* **Not for sale in the U.S.**

IMAGE1 S Camera System NEW

IMAGE1 S

TC 200EN

TC 200EN* **IMAGE1 S CONNECT**, connect module, for use with up to 3 link modules, resolution 1920 x 1080 pixels, with integrated KARL STORZ-SCB and digital Image Processing Module, power supply 100–120 VAC/200–240 VAC, 50/60 Hz
including:
Mains Cord, length 300 cm
DVI-D Connecting Cable, length 300 cm
SCB Connecting Cable, length 100 cm
USB Flash Drive, 32 GB, USB silicone keyboard, with touchpad, US

***Available in the following languages:** DE, ES, FR, IT, PT, RU

Specifications:

HD video outputs	- 2x DVI-D - 1x 3G-SDI
Format signal outputs	1920 x 1080p, 50/60 Hz
LINK video inputs	3x
USB interface SCB interface	4x USB, (2x front, 2x rear) 2x 6-pin mini-DIN

Power supply	100–120 VAC/200–240 VAC
Power frequency	50/60 Hz
Protection class	I, CF-Defib
Dimensions w x h x d	305 x 54 x 320 mm
Weight	2.1 kg

For use with IMAGE1 S
IMAGE1 S CONNECT Module TC 200EN

TC 300

TC 300 **IMAGE1 S H3-LINK,** link module, for use with IMAGE1 FULL HD three-chip camera heads, power supply 100–120 VAC/200–240 VAC, 50/60 Hz,
for use with IMAGE1 S CONNECT TC 200EN
including:
Mains Cord, length 300 cm
Link Cable, length 20 cm

Specifications:

Camera System	**TC 300 (H3-Link)**
Supported camera heads/video endoscopes	TH 100, TH 101, TH 102, TH 103, TH 104, TH 106 (fully compatible with IMAGE1 S) **22** 2200 55-3, **22** 2200 56-3, **22** 2200 53-3, **22** 2200 60-3, **22** 2200 61-3, **22** 2200 54-3, **22** 2200 85-3 (compatible without IMAGE1 S technologies CLARA, CHROMA, SPECTRA*)
LINK video outputs	1x
Power supply	100–120 VAC/200–240 VAC
Power frequency	50/60 Hz
Protection class	I, CF-Defib
Dimensions w x h x d	305 x 54 x 320 mm
Weight	1.86 kg

* *SPECTRA A:* **Not for sale in the U.S.**
** *SPECTRA B:* **Not for sale in the U.S.**

IMAGE1 S Camera Heads NEW

IMAGE1 S

For use with IMAGE1 S Camera System
IMAGE1 S CONNECT Module TC 200EN, IMAGE1 S H3-LINK Module TC 300
and with all IMAGE1 HUB™ HD Camera Control Units

TH 100

TH 100 **IMAGE1 S H3-Z Three-Chip FULL HD Camera Head,** 50/60 Hz, IMAGE1 S compatible, progressive scan, soakable, gas- and plasma-sterilizable, with integrated Parfocal Zoom Lens, focal length f = 15–31 mm (2x), 2 freely programmable camera head buttons, for use with IMAGE1 S and IMAGE1 HUB™ HD/HD

Specifications:

IMAGE1 FULL HD Camera Heads	**IMAGE1 S H3-Z**
Product no.	TH 100
Image sensor	3x 1/3" CCD chip
Dimensions w x h x d	39 x 49 x 114 mm
Weight	270 g
Optical interface	integrated Parfocal Zoom Lens, f = 15–31 mm (2x)
Min. sensitivity	F 1.4/1.17 Lux
Grip mechanism	standard eyepiece adaptor
Cable	non-detachable
Cable length	300 cm

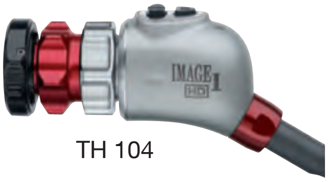

TH 104

TH 104 **IMAGE1 S H3-ZA Three-Chip FULL HD Camera Head,** 50/60 Hz, IMAGE1 S compatible, **autoclavable,** progressive scan, soakable, gas- and plasma-sterilizable, with integrated Parfocal Zoom Lens, focal length f = 15–31 mm (2x), 2 freely programmable camera head buttons, for use with IMAGE1 S and IMAGE1 HUB™ HD/HD

Specifications:

IMAGE1 FULL HD Camera Heads	**IMAGE1 S H3-ZA**
Product no.	TH 104
Image sensor	3x 1/3" CCD chip
Dimensions w x h x d	39 x 49 x 100 mm
Weight	299 g
Optical interface	integrated Parfocal Zoom Lens, f = 15–31 mm (2x)
Min. sensitivity	F 1.4/1.17 Lux
Grip mechanism	standard eyepiece adaptor
Cable	non-detachable
Cable length	300 cm

Monitors

9619 NB

9619 NB **19" HD Monitor,**
color systems **PAL/NTSC,** max. screen resolution 1280 x 1024, image format 4:3, power supply 100–240 VAC, 50/60 Hz, wall-mounted with VESA 100 adaption, including:
External 24 VDC Power Supply
Mains Cord

9826 NB

9826 NB **26" FULL HD Monitor,**
wall-mounted with VESA 100 adaption, color systems **PAL/NTSC,**
max. screen resolution 1920 x 1080, image format 16:9,
power supply 100–240 VAC, 50/60 Hz including:
External 24 VDC Power Supply
Mains Cord

Monitors

KARL STORZ HD and FULL HD Monitors	**19"**	**26"**
Wall-mounted with VESA 100 adaption	9619 NB	9826 NB
Inputs:		
DVI-D	●	●
Fibre Optic		
3G-SDI		●
RGBS (VGA)	●	●
S-Video	●	●
Composite/FBAS	●	●
Outputs:		
DVI-D	●	●
S-Video	●	
Composite/FBAS	●	●
RGBS (VGA)	●	
3G-SDI		●
Signal Format Display:		
4:3	●	●
5:4	●	●
16:9	●	●
Picture-in-Picture	●	●
PAL/NTSC compatible	●	●

Optional accessories:

9826 SF **Pedestal,** for monitor 9826 NB

9626 SF **Pedestal,** for monitor 9619 NB

Specifications:

KARL STORZ HD and FULL HD Monitors	**19"**	**26"**
Desktop with pedestal	optional	optional
Product no.	9619 NB	9826 NB
Brightness	200 cd/m² (type)	500 cd/m² (type)
Max. viewing angle	178° vertical	178° vertical
Pixel distance	0.29 mm	0.3 mm
Reaction time	5 ms	8 ms
Contrast ratio	700:1	1400:1
Mount	100 mm VESA	100 mm VESA
Weight	7.6 kg	7.7 kg
Rated power	28 W	72 W
Operating conditions	0–40°C	5–35°C
Storage	-20–60°C	-20–60°C
Rel. humidity	max. 85%	max. 85%
Dimensions w x h x d	469.5 x 416 x 75.5 mm	643 x 396 x 87 mm
Power supply	100–240 VAC	100–240 VAC
Certified to	EN 60601-1, protection class IPX0	EN 60601-1, UL 60601-1, MDD93/42/EEC, protection class IPX2

Accessories for Video Documentation

495 NL	**Fiber Optic Light Cable,** with straight connector, diameter 3.5 mm, length 180 cm
495 NA	**Same,** length 230 cm

Cold Light Fountain XENON NOVA® 175

20131501	**Cold Light Fountain XENON NOVA® 175,** power supply: 100–125 VAC/220–240 VAC, 50/60 Hz including: **Mains Cord**
20132026	**XENON Spare Lamp,** only, 175 watt, 15 volt

Cold Light Fountain XENON NOVA® 300

20134001	**Cold Light Fountain XENON NOVA® 300,** Lamp type: 300 W XENON power supply: 100–125 VAC/220–240 VAC, 50/60 Hz including: **Mains Cord**
20133028	**XENON Spare Lamp,** only, 300 watt, 15 volt

Cold Light Fountain XENON 300 SCB

20133101-1	**Cold Light Fountain XENON 300 SCB** with built-in antifog air-pump, and integrated KARL STORZ Communication Bus System SCB power supply: 100–125 VAC/220–240 VAC, 50/60 Hz including: **Mains Cord** **SCB Connecting Cable,** length 100 cm
20133027	**Spare Lamp Module XENON** with heat sink, 300 watt, 15 volt
20133028	**XENON Spare Lamp,** only, 300 watt, 15 volt

Data Management and Documentation

KARL STORZ AIDA® – Exceptional documentation

The name AIDA stands for the comprehensive implementation of all documentation requirements arising in surgical procedures: A tailored solution that flexibly adapts to the needs of every specialty and thereby allows for the greatest degree of customization.

This customization is achieved in accordance with existing clinical standards to guarantee a reliable and safe solution. Proven functionalities merge with the latest trends and developments in medicine to create a fully new documentation experience – AIDA.

AIDA seamlessly integrates into existing infrastructures and exchanges data with other systems using common standard interfaces.

WD 200-XX* **AIDA Documentation System,**
for recording still images and videos,
dual channel up to FULL HD, 2D/3D,
power supply 100-240 VAC, 50/60 Hz

including:

USB Silicone Keyboard, with touchpad
ACC Connecting Cable
DVI Connecting Cable, length 200 cm
HDMI-DVI Cable, length 200 cm
Mains Cord, length 300 cm

WD 250-XX* **AIDA Documentation System,**
for recording still images and videos,
dual channel up to FULL HD, 2D/3D,
including SMARTSCREEN® (touch screen),
power supply 100-240 VAC, 50/60 Hz

including:

USB Silicone Keyboard, with touchpad
ACC Connecting Cable
DVI Connecting Cable, length 200 cm
HDMI-DVI Cable, length 200 cm
Mains Cord, length 300 cm

*XX Please indicate the relevant country code
(DE, EN, ES, FR, IT, PT, RU) when placing your order.

Workflow-oriented use

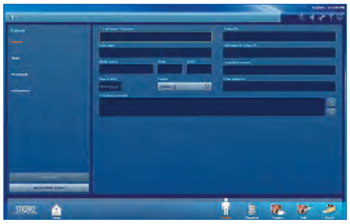

Patient

Entering patient data has never been this easy. AIDA seamlessly integrates into the existing infrastructure such as HIS and PACS. Data can be entered manually or via a DICOM worklist.
All important patient information is just a click away.

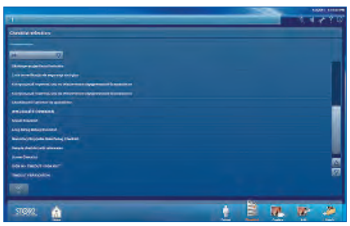

Checklist

Central administration and documentation of time-out. The checklist simplifies the documentation of all critical steps in accordance with clinical standards. All checklists can be adapted to individual needs for sustainably increasing patient safety.

Record

High-quality documentation, with still images and videos being recorded in FULL HD and 3D. The Dual Capture function allows for the parallel (synchronous or independent) recording of two sources. All recorded media can be marked for further processing with just one click.

Edit

With the Edit module, simple adjustments to recorded still images and videos can be very rapidly completed. Recordings can be quickly optimized and then directly placed in the report.
In addition, freeze frames can be cut out of videos and edited and saved. Existing markings from the Record module can be used for quick selection.

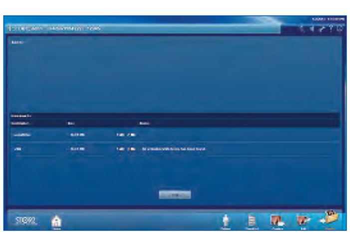

Complete

Completing a procedure has never been easier. AIDA offers a large selection of storage locations. The data exported to each storage location can be defined. The Intelligent Export Manager (IEM) then carries out the export in the background. To prevent data loss, the system keeps the data until they have been successfully exported.

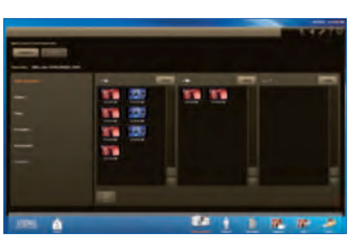

Reference

All important patient information is always available and easy to access. Completed procedures including all information, still images, videos, and the checklist report can be easily retrieved from the Reference module.

Equipment Cart

UG 220

UG 220

Equipment Cart
wide, high, rides on 4 antistatic dual wheels
equipped with locking brakes 3 shelves,
mains switch on top cover,
central beam with integrated electrical subdistributors
with 12 sockets, holder for power supplies,
potential earth connectors and cable winding
on the outside,

Dimensions:
Equipment cart: 830 x 1474 x 730 mm (w x h x d),
shelf: 630 x 510 mm (w x d),
caster diameter: 150 mm

including:

Base module equipment cart, wide
Cover equipment, equipment cart wide
Beam package equipment, equipment cart high
3x **Shelf,** wide
Drawer unit with lock, wide
2x **Equipment rail,** long
Camera holder

UG 540

UG 540

Monitor Swifel Arm,
height and side adjustable,
can be turned to the left or the right side,
swivel range 180°, overhang 780 mm,
overhang from centre 1170 mm,
load capacity max. 15 kg,
with monitor fixation VESA 5/100,
for usage with equipment carts UG xxx

Recommended Accessories for Equipment Cart

UG 310

UG 310 **Isolation Transformer,**
200 V–240 V; 2000 VA with 3 special mains socket,
expulsion fuses, 3 grounding plugs,
dimensions: 330 x 90 x 495 mm (w x h x d),
for usage with equipment carts UG xxx

UG 410

UG 410 **Earth Leakage Monitor,**
200 V–240 V, for mounting at equipment cart,
control panel dimensions: 44 x 80 x 29 mm (w x h x d),
for usage with isolation transformer UG 310

UG 510

UG 510 **Monitor Holding Arm,**
height adjustable, inclinable,
mountable on left or right,
turning radius approx. 320°, overhang 530 mm,
load capacity max. 15 kg,
monitor fixation VESA 75/100,
for usage with equipment carts UG xxx